UNIVERSIDADE FEDERAL DE PERNAMBUCO
CENTRO DE CIÊNCIAS BIOLÓGICAS
PROGRAMA DE PÓS-GRADUAÇÃO EM CIÊNCIAS BIOLÓGICAS
CURSO DE DOUTORADO

JANA MESSIAS SANDES

CARACTERIZAÇÃO MOLECULAR E ULTRAESTRUTURAL DO ESTRESSE DO RETÍCULO ENDOPLASMÁTICO DE *Trypanosoma cruzi*

Recife,
2016

JANA MESSIAS SANDES

CARACTERIZAÇÃO MOLECULAR E ULTRAESTRUTURAL DO ESTRESSE DO RETÍCULO ENDOPLASMÁTICO DE *Trypanosoma cruzi*

Tese apresentada ao Curso de Pós-graduação em Ciências Biológicas da Universidade Federal de Pernambuco, como requisito parcial à obtenção do título de Doutor em Ciências Biológicas.

Orientadora: Prof[a]. Dr[a]. Adriana Fontes

Co-Orientadora: Prof[a]. Dr[a]. Regina C. B. Q. Figueiredo

Recife,

2016

Catalogação na Fonte:
Bibliotecário Bruno Márcio Gouveia, CRB-4/1788

Sandes, Jana Messias
Caracterização molecular e ultraestrutural do estresse do retículo endoplasmático de *Trypanosoma cruzi* / Jana Messias Sandes. – Recife: O Autor, 2016.

127 f.: il.
Orientadores: Adriana Fontes, Regina C. B. Q. Figueiredo
Tese (doutorado) – Universidade Federal de Pernambuco. Centro de Ciências Biológicas. Programa de Pós-graduação em Ciências Biológicas, 2016.
Inclui referências e anexos

1. Protozoário 2. Trypanosoma cruzi 3. Citologia I. Fontes, Adriana (Orient.) II. Figueiredo, Regina C. B. Q. (Coorient.) III. Título

579.4 CDD (22.ed.) UFPE/CCB-2016-111

JANA MESSIAS SANDES

CARACTERIZAÇÃO MOLECULAR E ULTRAESTRUTURAL DO ESTRESSE DO RETÍCULO ENDOPLASMÁTICO DE *Trypanosoma cruzi*

Tese apresentada ao Curso de Pós-graduação em Ciências Biológicas da Universidade Federal de Pernambuco, como requisito parcial à obtenção do título de Doutor em Ciências Biológicas.

Aprovada em: ___/___/___

COMISSÃO EXAMINADORA:

_____

Dra. Adriana Fontes (Orientadora e Presidente da banca)

Universidade Federal de Pernambuco

_____

Dra. Maria Tereza dos Santos Correia (Examinadora Interna)

Universidade Federal de Pernambuco

_____

Dra. Janaina Viana de Melo (Examinadora Externa)

Centro de Tecnologias Estratégicas do Nordeste

_____

Dr. Bruno de Melo Carvalho (Examinador Externo)

Universidade de Pernambuco

_____

Dr. Luís Cláudio Nascimento da Silva (Examinador Externo)

University of Copenhagen

AGRADECIMENTOS

A Deus, por ter me sustentado e me dado força nos momentos mais difíceis de minha vida.

Aos meus pais, Paulo e Kátia, por sempre me apoiarem apesar da distância, por terem acreditado que eu era capaz de chegar até aqui e por terem incentivado o estudo e a busca por um futuro melhor.

Aos meus familiares, irmão, tios, primos, avós, sogros, sobrinhos e cunhados, por todo amor, apoio e carinho incondicionais.

Ao meu marido, Marcos, pela paciência, pelo amor, por ser o meu companheiro de todas as horas e por ter aguentado essa árdua jornada ao meu lado. Sem você não teria conseguido!

Às Dras. Regina Bressan e Adriana Fontes, pela orientação, pela paciência, pelo aprendizado e, acima de tudo, por acreditarem em mim e me incentivarem mesmo nos momentos em que eu mesma duvidava do meu potencial.

À Dra. Danielle Moura, por ter aceitado o desafio de me auxiliar a por em prática esse projeto e por sempre ter se mostrado disponível a tirar dúvidas, seja na bancada ou na escrita dos artigos.

À Dra. Milena Paiva e suas alunas Suênia e Cíntia, pelo carinho, pela troca de conhecimentos e pela paciência em tirar as minhas milhões de dúvidas sobre esse mundo novo da RT-qPCR.

À Moana, minha aluna de iniciação científica, que apesar de ter ficado relativamente pouco tempo comigo, foi essencial para que eu conseguisse dar início aos experimentos.

À Gustavo e Ada, pela disposição em me ajudar nos inúmeros Western blottings, mesmo quando faltava tempo para os próprios experimentos.

À Paulo Euzébio, pela ajuda com os dados da citometria de fluxo e pela paciência em repetir as inúmeras análises.

À Karla, Amanda, Steffany, Larissa e Taciana pela companhia até tarde da noite no CPqAM e por dividir as angústias desse difícil momento pré-defesa.

Aos colegas do LBCP, Ana Carla, Antonio, Andrezza, Carina, Cynarha, Danilo, Janaína, Karina, Karla, Keicy, Larissa, Mary, Moana, Rafaela e Taciana pela convivência diária, pela ajuda no cultivo das células, nos experimentos e na discussão dos resultados.

Aos demais colegas do Departamento de Microbiologia do CPqAM, pela ajuda na bancada, pelas doações de reagentes e discussões de resultados.

Aos colegas do LBCM, Alberon, Amanda, Ana Paula, Camila, Carmel, Catarina, Dyana, Duda, Elverson, Fernanda, Gabriel, Iany, Jefferson, Naironberg e Thiago, por terem me recebido com carinho e alegria.

Aos Drs. José Luiz, Luiz Carlos e Fábio Brayner, pelo apoio e compreensão em permitir que eu me dividisse entre o trabalho no LIKA e o doutorado.

Aos colegas do LIKA, em especial Olávio, Neyla, Rafael e Verinha, pelas risadas que tornam mais leve o trabalho diário.

Aos colegas de faculdade, em especial Amanda, Isabelle, Juliana, Lívia, Luís, Nina, Rafael, Renato, Steffany e Veridiana, pela boa e velha amizade, pelo ombro nas horas difíceis e pelos momentos de descontração e alegria.

Aos amigos de Recife, da Bahia e de outros tantos lugares, que de alguma maneira fizeram parte da minha vida e continuam torcendo por mim, em especial Lariza, Júlio, Poliana, Leandro, Fátima, Izabela, João, Lídia, Franklin, Aurora, Suellen, Lucas, Karla, Flávio, Fred, Matheus, Alessa, Monique S., Monique H., Josi e Murillo.

À todos que participaram direta ou indiretamente na construção desse trabalho, muito obrigada!

“Na vida, não vale tanto o que temos, nem tanto importa o que somos. Vale o que realizamos com aquilo que possuímos e, acima de tudo, importa o que fazemos de nós.”

Chico Xavier

RESUMO

O retículo endoplasmático (RE) é uma organela vital para as células eucarióticas, envolvido na síntese, modificação e enovelamento de proteínas, homeostase do cálcio e metabolismo de lipídios. Variações no nível de cálcio, inibição da glicosilação, estresse oxidativo, entre outros, podem levar o RE a uma condição de estresse, a qual dispara vias de sinalização específicas incluindo a *Unfolded Protein Response* (UPR). A UPR promove aumento na expressão de chaperonas, inibe a tradução de novas proteínas e aumenta a degradação de proteínas mal enoveladas. No entanto, quando o estresse é severo ou persistente, a UPR induz mecanismos de morte celular, principalmente por apoptose. Embora o RE possua papel fundamental na sobrevivência das células de mamíferos, estudos sobre a fisiologia desta organela em *Trypanosoma cruzi*, agente etiológico da Doença de Chagas, ainda são escassos. Dessa forma, o objetivo deste trabalho foi caracterizar molecular e morfologicamente a resposta de formas epimastigotas de *T. cruzi* ao estresse do RE induzido por ditiotreitol (DTT) ou tunicamicina (TM). As células tratadas com DTT apresentaram inibição do crescimento de maneira dose-dependente, com recuperação do crescimento após a retirada da droga. O tratamento com DTT não alterou os níveis proteicos de BiP (*binding protein*) mas reduziu significativamente os níveis de RNAm de BiP e calreticulina (CRT), sugerindo que o *T. cruzi* tenha uma resposta diferente da UPR de eucariotos superiores. O estresse persistente do RE induzido pelo DTT causou drásticas alterações morfológicas e fisiológicas compatíveis com morte celular por apoptose tardia/necrose, como observado pela dupla marcação com anexina-V e iodeto de propídeo, além da redução do tamanho do corpo celular, inchaço e desorganização das cristas mitocondriais, despolarização do potencial de membrana mitocondrial ($\triangle\psi m$) e aumento da produção (21 – 94%) de espécies reativas de oxigênio (ROS). No entanto, a presença de perfis do RE envolvendo porções do citoplasma sugere que a autofagia também esteja ocorrendo. Por outro lado, a TM apresentou um forte efeito tripanostático, sem crescimento celular independentemente da dose ou do tempo de incubação, inclusive após a retirada da droga. O tratamento com a TM também não foi capaz de alterar os níveis proteicos de BiP, porém induziu um aumento nos níveis de RNAm de BiP e CRT. A análise por citometria de fluxo demonstrou que o tratamento com TM induziu despolarização do $\triangle\psi m$ sem um aumento pronunciado na produção de ROS, e apenas cerca de 10% das células tratadas apresentaram fenótipos de apoptose. Alterações ultraestruturais também foram observadas nas células tratadas com TM, como o arredondamento do corpo celular, a presença de inclusões lipídicas e um grande número de perfis de RE ao redor de estruturas citoplasmáticas em processo de degradação. Dessa forma, nossos resultados sugerem que o tratamento com DTT compromete o funcionamento da célula de maneira geral mais do que atua como estressor do RE, devido ao seu forte efeito oxidativo, levando à morte da célula. Já a TM atua mais especificamente sobre o RE, desencadeando um processo de autofagia/RE-fagia na tentativa de reverter o estresse de RE sem induzir morte celular por apoptose.

Palavras-chave: *Trypanosoma cruzi*. Estresse do retículo endoplasmático. Ditiotreitol. Tunicamicina. Morte celular.

ABSTRACT

The endoplasmic reticulum (ER) is a vital organelle to eukaryotic cells, involved in the protein synthesis, folding and modification, calcium homeostasis and lipid metabolism. Changes in calcium levels, glycosylation inhibition, oxidative stress or others, can lead to an ER stress condition, which triggers specific signaling pathways including the Unfolded Protein Response (UPR). The UPR promotes an increase in the chaperone expression, inhibits the translation of new proteins and increases the degradation of unfolded proteins. However, when the stress is severe or persistent, the UPR induces cell death mechanisms, mainly by apoptosis. Although the ER has a pivotal role in the survival of mammalian cell, studies about the physiology of this organelle in *Trypanosoma cruzi*, the etiologic agent of Chagas disease, are still scarce. In this regard, the aim of this study was to characterize molecular and morphologically the response of epimastigote forms of *T. cruzi* to the ER stress induced by dithiothreitol (DTT) or tunicamycin (TM). DTT-treated cells showed a dose-dependent growth inhibition, with growth recovery after drug withdrawal. The DTT treatment did not alter the BiP (binding protein) protein levels but significantly reduced the mRNA levels of BiP and calreticulin (CRT), suggesting that *T. cruzi* has a different response from higher eukaryotes UPR. Persistent ER stress induced by DTT caused drastic morphological and physiological changes compatible with cell death by late apoptosis/necrosis, as observed by double staining with annexin-V and propidium iodide, reduction of cell body, swelling and disorganization of mitochondrial cristae, mitochondrial membrane potential ($\triangle\psi m$) depolarization and increasing of reactive oxygen species (ROS) production (21-94%). However, the presence of ER profiles involving cytoplasmic portions suggests that autophagy may also be occurring. On the other hand, the TM showed strong trypanostatic effect, with no cell growth observed independent of the dose and the time of incubation, even after drug withdrawal. The TM treatment was also unable to change the BiP protein levels, but induced an increase in BiP and CRT mRNA levels. The flow cytometry analysis showed that TM-treatment induced $\triangle\psi m$ depolarization without a pronounced increase in the ROS production (10 - 15%) and only about 10% of the treated cells exhibited apoptotic phenotypes. Ultrastructural changes were also observed in TM-treated cells, such as rounding of the cell body, the presence of lipid inclusions and a large number of ER profiles surrounding cytoplasmic structures in degradation process. Therefore, our results suggest that the DTT treatment compromises the whole cell function rather than acts as a specific inductor of ER stress, due to its strong oxidative effect, leading to cell death. The TM treatment acts more specifically on the ER, triggering an autophagy/ER-phagy process in an attempt to reverse the ER stress, without inducing cell death by apoptosis.

Key-words: *Trypanosoma cruzi*. Endoplasmic reticulum stress. Dithiothreitol. Tunicamycin. Cell death.

LISTA DE ILUSTRACÕES

Revisão de literatura:

Artigo 1:

Artigo 2:

LISTA DE TABELAS

Artigo 2:

Artigo 3:

LISTA DE ABREVIATURAS E SIGLAS

$\triangle\psi m$	Potencial de membrana mitocondrial (mitochondrial membrane potential)
ASK1	Cinase reguladora de sinais apoptóticos 1 (*Apoptosis signaling-regulating kinase 1*)
ATF4	Fator ativador da transcrição 4 (*Activating transcription factor 4*)
ATF6	Fator ativador da transcrição 6 (*Activating transcription factor 6*)
AV	Anexina-V
BAK	Proteína killer-antagonista homóloga a Bcl-2 (*Bcl-2 homologous antagonist/killer*)
BAX	Proteína X associada a Bcl-2 (*Bcl-2 associated X protein*)
Bcl-2	Proteína- 2 da leucemia/linfoma da célula B (*B-cell leukemia/lymphoma 2*)
BiP	Proteína de ligação (*binding protein*)
CHOP	Proteína homóloga C/EBP (*C/EBP-homologous protein*)
CLSM	Microscópio Confocal de Varredura a Laser *(Confocal Laser Scanning Microscope*)
CNX	Calnexina (*calnexin*)
CRT	Calreticulina (*calreticulin*)
DIC	Contraste de Interferência Diferencial (*Differential Interference Contrast*)
DMSO	Dimetilsulfóxido
DTT	Ditiotreitol
EIF2-α	Subunidade alfa do fator 2 de iniciação da tradução em eucariotos (*Eukaryotic translation initiation factor 2 alpha*)
EIF4A1	Fator de iniciação da tradução eucariótico 4A1 (*eukaryotic translation initiation factor 4A1*)
EN	Envelope nuclear
ER	Retículo endoplasmático (*Endoplasmic reticulum*)
ERAD	Degradação associada ao retículo endoplasmático (*Endoplasmic reticulum associated degradation*)
ERGIC	Compartimento intermediário RE-Golgi (*ER-Golgi Intermediate Compartment*)
FAZ	Zona de ligação do flagelo (*flagellar attachment zone*)
FBS	Soro Fetal Bovino (*Fetal Bovine Serum*)
GADD34	Proteína induzida por dano ao DNA e parada de crescimento (*Growth Arrest And*

	DNA-Damage Inducible Protein)
GPI	Glicosilfosfatidilinositol (*glycosylphosphatidylinositol*)
GRP-78	Proteína 78 regulada pela glicose (*78 kDa glucose-regulated protein*)
IP	Iodeto de Propídio
IRE1	Enzima 1 dependente de Inositol (Inositol-requiring enzyme 1)
IV	Índice de Variação (Index of variation)
JNK	Cinase c-Jun N-terminal (*c-jun N-terminal kinase*)
LIT	Infusão de fígado e triptose
MCP	Morte Celular Programada
MET	Microscopia Eletrônica de Transmissão
MEV	Microscopia Eletrônica de Varredura
OST	Oligossacariltransferase
PBS	Salina tamponada com fosfato
PCD	Morte Celular Programada (*Programmed cell death*)
PDI	Proteína dissulfeto isomerase (*protein disulfide isomerase*)
PERK	Proteína cinase tipo PKR residente no retículo endoplasmático (*protein kinase-related endoplasmic reticulum kinase*)
pH	Potencial hidrogeniônico
PI	*Propidium Iodide*
PKR	Proteína cinase dependente de RNA de fita dupla (*Double-stranded RNA dependent protein kinase*)
PS	Fosfatidilserina (*phosphatidylserine*)
RE	Retículo endoplasmático
REL	Retículo endoplasmático liso
RER	Retículo endoplasmático rugoso
RET	Retículo endoplasmático de transição
Rho 123	Rodamina 123
RIDD	Decaimento regulado do RNAm dependente de IRE1 (R*egulated IRE1-dependent mRNA decay)*
RT-PCR	Reação em cadeia da polimerase via transcriptase reversa (*Reverse transcription polymerase chain reaction*)
RT-qPCR	RT-PCR quantitativo em tempo real (*quantitative real-time RT-PCR*)
SDS-PAGE	Eletroforese em gel de poliacrilamida-dodecil sulfato de sódio

SEM	Microscopia eletrônica de varredura (*scanning electron microscopy*)
SFB	Soro fetal bovino
SL	Sequência Líder (*spliced-leader*)
SLS	Silenciamento do SL-RNA (*spliced-leader RNA silencing*)
TEM	Microscopia eletrônica de transmissão (*transmission electron microscopy*)
TG	Tapsigargina (*thapsigargin*)
TM	Tunicamicina (*tunicamycin*)
TRAF2	Fator 2 associado ao receptor de fator de necrose tumoral (*tumor necrosis factor receptor associated factor 2*)
t-SNAP	Proteína ativadora de snRNA (*small nuclear RNA-activating protein*)
UGGT	UDP-glicose: glicoproteína glicosiltransferase
UPR	Resposta a proteínas mal enoveladas (*Unfolded Protein Response)*
XBP1	Proteína 1 de ligação a X-box (*X-box binding protein 1*)

SUMÁRIO

1 INTRODUÇÃO

O retículo endoplasmático (RE) é considerado uma das principais organelas das células eucarióticas, envolvido na síntese, modificação e enovelamento de proteínas da via secretora e da membrana plasmática, a homeostase do cálcio e a síntese e metabolismo de lipídios. Para desempenhar suas funções o RE necessita de um ambiente oxidativo, que facilita a formação de ligações dissulfeto, um alto nível de Ca^{2+} e a presença de chaperonas como BiP (*binding protein*), calnexina, calreticulina, dissulfeto isomerases, entre outras. Essas chaperonas são responsáveis pelo dobramento e controle de qualidade das proteínas recém-sintetizadas do RE.

Situações adversas como a privação de nutrientes, variações no nível de cálcio, estresse oxidativo e inibição da glicosilação podem levar ao acúmulo de proteínas mal enoveladas no lúmen do RE. Este acúmulo pode induzir uma condição de estresse que, por sua vez, poderá ativar vias de transdução de sinal intracelulares na tentativa de manter a homeostase celular, conhecida como *Unfolded Protein Response* (UPR). Em eucariotos superiores, as principais proteínas sensoras de estresse do RE que estão envolvidas na indução da UPR são: IRE1 (*Inositol-requiring enzyme 1*), PERK (*PKR-like ER kinase*) e ATF6 (*activating transcription factor 6*). No estado basal, estas três proteínas estão inativadas pela associação com a chaperona BiP mas, durante o estresse de RE, BiP dissocia-se de seus ligantes para auxiliar no dobramento de proteínas, o que permite a ativação de IRE1, PERK e ATF6. A ativação dessas proteínas promove o aumento na expressão de chaperonas, para evitar a agregação e facilitar o correto dobramento das proteínas e, em paralelo, inibe a tradução de novas proteínas e aumenta a degradação das proteínas mal enoveladas por meio da degradação associada ao RE (ERAD, *Endoplasmic Reticulum Associated Degradation*). No entanto, quando o estresse se torna mais severo ou persistente, a UPR não consegue reestabelecer a homeostase da célula e pode ativar mecanismos de morte celular, principalmente por apoptose.

Os tripanossomatídeos, protozoários pertencentes à ordem Kinetoplastida, tais como o *Trypanosoma brucei, Trypanosoma cruzi* e *Leishmania* sp., possuem uma grande relevância médica e econômica, uma vez que são os agentes etiológicos de doenças infecciosas graves nos seres humanos e animais silvestres e domésticos. Como em outras células eucarióticas, o RE dos tripanossomatídeos possui importância fundamental para sua sobrevivência. Estudos utilizando agentes farmacológicos que levam ao estresse de RE como tunicamicina (TM), tapsigargina (TG), e ditiotreitol (DTT), demonstraram que a resposta ao estresse de RE nestes

parasitos difere da encontrada em eucariotos superiores. De fato, os tripanossomatídeos possuem um mecanismo de expressão gênica não convencional, em que a transcrição é feita de maneira policistrônica e a expressão dos genes é regulada pós-transcricionalmente pela taxa de degradação do RNAm e da taxa de tradução de proteínas. Além disso, algumas proteínas essenciais para a ativação da UPR como IRE1 e ATF6 não foram encontradas, indicando que os tripanossomatídeos podem possuir uma maquinaria da UPR menos elaborada ou que eles respondam ao estresse de RE por mecanismos diferentes. Realmente, para *T. brucei* o estresse inicial de RE parece induzir um aumento na estabilidade do RNAm de chaperonas e, sob estresse persistente, o silenciamento da sequência líder (SL). A SL é uma sequência espécie específica que é doada a todos os RNAm nascentes por *trans-splicing* e cujo silenciamento pode levar à morte celular programada (MCP) por apoptose. Essas características singulares de resposta ao estresse de RE fazem com que os tripanossomatídeos sejam um interessante modelo de estudo sob o ponto de visto biológico e pela possibilidade do RE ser um alvo potencial para o desenvolvimento de novos agentes quimioterápicos.

O *Trypanosoma cruzi* é o agente etiológico da doença de Chagas, uma doença negligenciada que afeta cerca de 6 a 7 milhões de pessoas principalmente na América Latina, onde é endêmica, mas também foi detectada nos Estados Unidos da América, Canadá, e muitos países europeus. Esta enfermidade é de difícil controle e os medicamentos disponíveis ainda são os mesmos que foram lançados há cinco décadas atrás, Benzonidazol e Nifurtimox, que apresentam baixa eficácia na fase crônica da doença e provoca graves efeitos colaterais. Alternativas como vacinas ou quimioterápicos mais eficientes dependem ainda de um maior conhecimento sobre os processos biológicos básicos deste parasito. A morfologia do RE de *T. cruzi* já foi previamente reportada, porém os aspectos do processamento de proteínas e da fisiologia do RE são pouco compreendidos e nenhum estudo sobre o estresse de RE neste parasito foi encontrado.

Dessa forma, o objetivo do presente estudo é avaliar o efeito do DTT e da TM sobre a viabilidade, a morfologia, a expressão de chaperonas e a indução de morte celular em formas epimastigotas de *T. cruzi* utilizando técnicas de biologia molecular aliadas a microscopia confocal a laser, citometria de fluxo e microscopia eletrônica de varredura e transmissão. Esperamos com a realização do presente estudo não só contribuir para o entendimento dos processos que medeiam os eventos de morte celular induzidos por estresse de RE neste parasito, como fornecer subsídio para o desenvolvimento de drogas mais eficientes contra a doença de Chagas.

2 OBJETIVOS

2.1 Objetivo Geral

- Caracterizar molecular e morfologicamente a resposta do *Trypanosoma cruzi* ao estresse do retículo endoplasmático.

2.2 Objetivos Específicos

- Avaliar o efeito dos estressores de retículo ditiotreitol e tunicamicina sobre a viabilidade de formas epimastigotas de *T. cruzi*;

- Avaliar a capacidade de recuperação do crescimento de formas epimastigotas de *T. cruzi* após exposição ao ditiotreitol e à tunicamicina;

- Analisar a expressão de BiP e Calreticulina na resposta ao estresse do retículo em *T. cruzi*;

- Avaliar o efeito do estresse persistente do retículo sobre a ultraestrutura de formas epimastigotas de *T. cruzi*;

- Avaliar o potencial do estresse persistente do retículo na indução de morte celular programada em *T. cruzi.*

3 REVISÃO DE LITERATURA

3.1 Retículo Endoplasmático de Células Eucarióticas Superiores

O retículo endoplasmático (RE) é uma organela encontrada nos organismos eucariotos e está envolvido em diversos processos dentro da célula como: síntese, enovelamento, glicosilação e transporte de proteínas; síntese e distribuição de fosfolipídios e esteróis; armazenamento e o controle da liberação de Ca^{2+} para o citoplasma (BRAVO et al., 2013). Em sua estrutura, o RE é formado por quatro subdomínios principais com diferentes funções (Figura 1), que incluem o envelope nuclear (EN), o RE rugoso (RER), o RE liso (REL) e o RE de transição (RET) (LAVOIE; PAIEMENT, 2008).

Figura 1 - Diferentes subcompartimentos do RE.

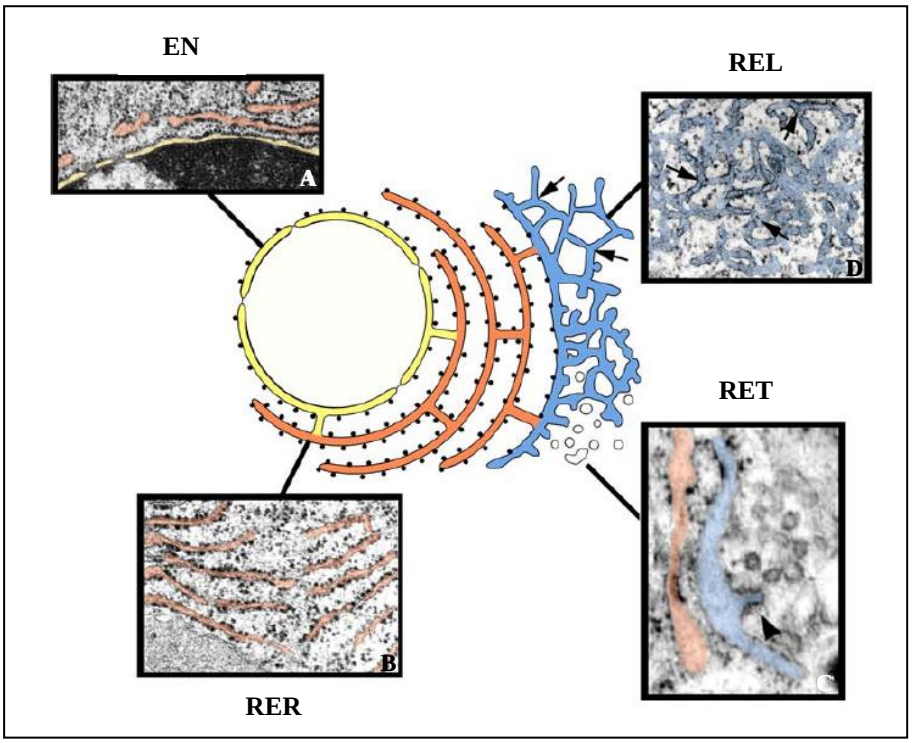

Fonte: Adaptado de Lavoie e Paiement (2008).
Legenda: A) Envelope nuclear (EN) com poros e ribossomos ligados à membrana externa. **B)** RE rugoso (RER) contínuo com o EN, consistindo de sáculos achatados empilhados, com membranas apresentando numerosas partículas ribossomais anexadas. **C)** RE de transição (RET) composto por RER e RE liso (REL) composto por vesículas em brotamento e túbulos (seta). **D)** REL composto por uma extensa rede de túbulos interconectados desprovidos de ribossomos associados.

O EN circunda o núcleo e consiste de sáculos achatados com ribossomos ligados à membrana externa os quais são contínuos ao RER e é responsável pela separação do material nuclear do citoplasma. Embebido no EN estão presentes os complexos do poro, permitindo o transporte altamente regulado de proteínas e RNA entre o nucleoplasma e o citoplasma nas células eucarióticas (KABACHINSKI, SCHWARTZ, 2015). O RER é o principal responsável pela síntese, enovelamento e transporte de uma grande variedade de proteínas essenciais para o crescimento e sobrevivência da célula (LAVOIE; PAIEMENT, 2008). O REL por sua vez é composto por túbulos interconectados sem ribossomos ligados e é o principal sítio de síntese de fosfolipídios e colesterol com função estrutural, assim como uma quantidade significativa de triacilglicerol e ésteres de colesterol não estruturais. O REL também participa de outras funções essenciais para a sobrevivência da célula como o armazenamento de cálcio, metabolização de drogas e detoxificação (PAGLIASSOTTI, 2012).

O RET é composto de dois domínios contínuos, mas distintos: um domínio caracterizado pela presença de ribossomos associados e um domínio liso, dando origem a brotamentos de membrana e túbulos. Um aglomerado de vesículas e túbulos é frequentemente observado em íntima associação com o RET e representa um compartimento intermediário, também chamado de compartimento intermediário RE-Golgi (*ER-Golgi Intermediate Compartment*, ERGIC), de "clusters" vesículo-tubular ou compartimento pré-Golgi. Os dois domínios do RET indicam uma função na formação de vesículas e túbulos que permitirão a saída de proteínas do RE e seu transporte para o Golgi (APPENZELLER-HERZOG; HAURI, 2006). Um tipo de RE altamente especializado, o retículo sarcoplasmático, é encontrado circundando os miofilamentos e mitocôndrias das células musculares e age como um sítio de rápida estocagem e liberação de Ca^{+2}, essencial para a contração e relaxamento muscular (SHIELS; GALLI, 2014).

Em eucariotos superiores, aproximadamente 20% das proteínas são direcionadas ao RE para fazer parte dos compartimentos endomembranares, da membrana plasmática ou para secreção. Isto representa um considerável fluxo de moléculas no RE, evidenciando o papel crucial desta organela para o equilíbrio celular (LAVOIE et al., 2011; SANO; REED, 2013). Para desempenhar tais funções o RE possui um ambiente altamente especializado e singular para o enovelamento, a formação de pontes dissulfeto e a glicosilação de proteínas. Este ambiente é mantido pelo alto nível de cálcio, um ambiente oxidativo e pela presença de chaperonas (ex: GRP-78/BiP, calnexina (CNX), calreticulina (CRT), proteína dissulfeto isomerase (PDI), dentre outras), as quais são responsáveis pelo dobramento e controle de qualidade das proteínas recém sintetizadas (CHEN et al., 2010; DUDEK et al., 2009).

Um dos primeiros controles de qualidade do RE sobre as proteínas nascentes é a N-glicosilação. Este processo contribui para o aumento da solubilidade proteica, reduz a agregação, torna disponível um sítio de ligação a CNX e CRT, facilita a interação de PDI e pode marcar glicoproteínas mal enoveladas para degradação (Figura 2) (BRODSKY; SKACH, 2011; IZQUIERDO et al., 2009). A glicosilação acontece assim que as proteínas entram no lúmen do RE, onde serão modificadas pela ação das seguintes enzimas: oligossacariltransferase (OST), que irá adicionar o oligossacarídeo $Glc_3Man_9GlcNAc_2$; as glicosidases I e II, que removem um resíduo externo de glicose; e a UDP-glicose: glicoproteína glicosiltransferase (UGGT), que adiciona um resíduo de glicose às glicoproteínas que foram mal enoveladas, permitindo que as glicoproteínas se liguem novamente às chaperonas. Portanto, a ação da UGGT é um componente chave do controle de qualidade (IZQUIERDO et al., 2009).

Figura 2 - Controle de qualidade da síntese proteica em eucariotos superiores.

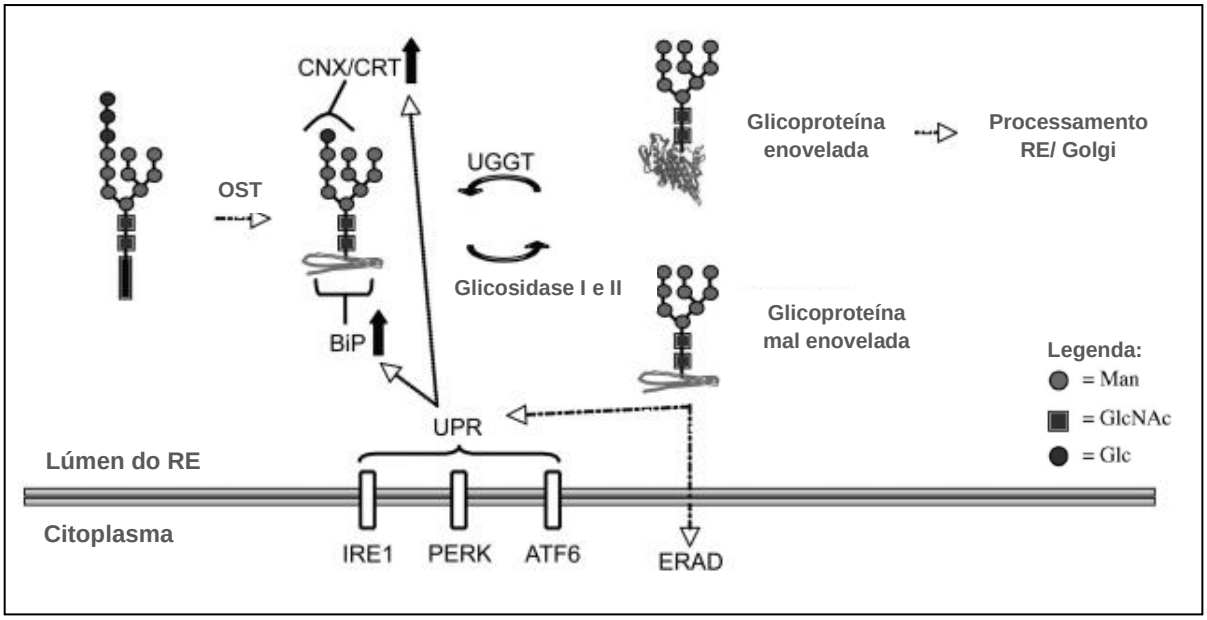

Fonte: Modificado de Izquierdo, et al. (2009).
Legenda: Fatores de controle de qualidade dependente de N-glicano em eucariotos superiores. OST, oligossacariltransferase; CNX, calnexina; CRT, calreticulina; ERAD, degradação associada ao RE; Man, manose; GlcNac, N-acetilglicosamina; Glc, glicose.

As lectinas residentes do RE, CNX e CRT, reconhecem e se ligam às glicoproteínas com apenas uma glicose terminal, ajudando a prevenir a agregação de proteínas além de auxiliar em seu enovelamento para que possam ser posteriormente liberadas e continuarem seu processamento no complexo de Golgi (ELLGAARD; FRICKEL, 2003). A chaperona BiP (*binding protein*) também se liga temporariamente às proteínas recém-sintetizadas que entram

no RE, evitando o enovelamento incorreto de seus segmentos ou a agregação. Além disso, a chaperona PDI também contribui para o correto enovelamento, já que catalisa a introdução de pontes dissulfeto intra e intermoleculares e rearranja as incorretas, estabilizando a estrutura terciária e quaternária de várias proteínas (WATANABE et al., 2014). No entanto, se mesmo assim a proteína não estiver corretamente enovelada, será exportada novamente para o citoplasma e degradada nos proteassomas em um processo chamado degradação associada ao RE (ERAD, *Endoplasmic Reticulum Associated Degradation*) (HEGDE; PLOEGH, 2010).

3.1.1 Estresse de RE e UPR

Variações no nível de cálcio, inibição da glicosilação, estresse oxidativo e exposição a agentes redutores podem levar o RE a uma condição de estresse, a qual dispara vias de sinalização específicas incluindo a *Unfolded Protein Response* (UPR) (DIEHL et al., 2011; RON; WALTER, 2007). As principais proteínas sensoras do RE que estão envolvidas na indução da UPR são: IRE1 (*Inositol-requiring enzyme 1*), PERK (*PKR-like ER kinase*) e ATF6 (*activating transcription factor 6*). No estado basal, estas três proteínas são mantidas inativadas pela associação com a chaperona BiP. Porém, durante o estresse de RE, o acúmulo de proteínas imaturas promove a dissociação de BiP dos seus ligantes, para auxiliar no dobramento das proteínas e, consequentemente, a ativação de PERK, IRE1 e ATF6 (Figura 3) (SZEGEZDI et al., 2006).

A ativação de PERK pode levar à indução da fosforilação do fator de transcrição NRF2, que induz a expressão de proteínas antioxidantes; e à fosforilação do fator de iniciação da tradução eIF2α (*α-subunit of the translation initiation factor eIF2*), que irá mediar a atenuação da tradução e a transcrição de genes específicos, como o fator de transcrição ATF4 (*activating transcription factor-4*) (PAGLIASSOTTI, 2012). O ATF4 ativado irá levar à indução de genes importantes para combater o estresse oxidativo, bem como à indução da expressão do fator de transcrição pró-apoptótico CHOP (*C/EBP-homologous protein*) e de GADD34, sendo este último responsável pela desfosforilação do eIF2α (WALTER; RON, 2011). O ATF6 ao ser liberado é clivado no Golgi e transportado ao núcleo para ativar a transcrição de chaperonas, tais como BiP, que irão auxiliar no enovelamento das proteínas acumuladas no RE, bem como a transcrição de CHOP e de XBP1 (*X-box protein*), que será processado posteriormente por IRE1 (LAI et al., 2007).

A IRE1 é uma proteína bi-funcional que funciona tanto como uma cinase como uma endonuclease. Uma vez ativada, a IRE1 sofre um processo de oligomerização, e os domínios

cinases presentes na porção citoplasmática são justapostos e autofosforilados, ativando a sua função endonucleásica no lúmen da cisterna reticular. A atividade de RNAse de IRE1 pode levar à degradação do RNA mensageiro (RNAm) para reduzir a síntese de proteínas, um processo conhecido como decaimento regulado do RNAm dependente de IRE1 (RIDD, R*egulated IRE1-dependent mRNA decay*) (IURLARO; MUÑOZ-PINEDO, 2015). No entanto, em condições de baixa ativação, sua atividade é específica, e está envolvida na regulação do RNAm de alguns genes, como o fator de transcrição XBP-1 que, ao ser processado por *splicing* (remoção de íntron), torna-se competente para se ligar ao promotor de genes essenciais da UPR (GARDNER; WALTER, 2011).

Juntos, esses fatores de transcrição (XBP-1, ATF4 e ATF6) promovem: a atenuação da taxa de tradução para reduzir a quantidade de proteínas que entram no RE; o aumento da transcrição de genes reguladores da homeostasia do RE (como as chaperonas); e a degradação de proteínas pelo sistema de degradação associado ao RE (ERAD) ou por autofagia (RASHID et al., 2015). Este último consiste numa via intracelular de degradação mediada por lisossomos para reciclagem e eliminação de proteínas, agregados ou organelas danificadas (KIEL, 2010).

Figura 3 - Vias de sinalização da UPR em células de mamíferos.

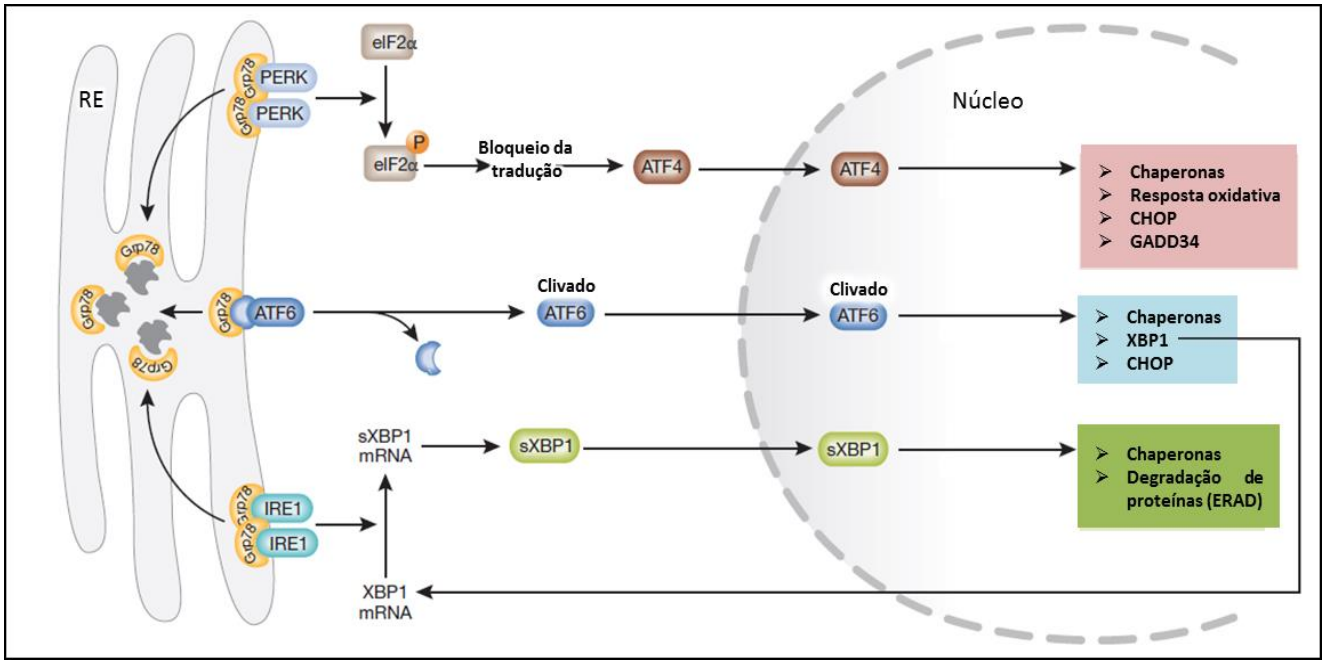

Fonte: Adaptado de Szegezdi et al. (2006).
Legenda: O acúmulo de proteínas mal enoveladas leva à dissociação da proteína GRP78/BiP e consequentemente ativação sequencial dos três receptores do RE: PERK, ATF6 e IRE1. A PERK ativada irá fosforilar eIF2α, que leva à atenuação da tradução global mas aumenta seletivamente a tradução do fator de transcrição ATF4, que é translocado para o núcleo onde irá induzir a transcrição

de genes envolvidos na restauração da homeostase do RE. O ATF6 é ativado por proteólise após ser translocado do RE para o complexo de Golgi. O ATF6 ativo também é um fator de transcrição que regula a expressão de chaperonas e XBP1, outro fator de transcrição. Para atingir sua forma ativa, XBP1 deve ser submetido ao *splicing* por IRE1 e depois é translocado para o núcleo, onde irá controlar a transcrição de chaperonas e genes envolvidos na degradação de proteínas. Por fim, a UPR visa restaurar a função do RE, bloqueando a síntese de novas proteínas, aumentando a capacidade de dobramento das proteínas acumuladas e levando à degradação dos agregados proteicos.

3.1.2 Estresse de RE e Morte Celular Programada

Quando os esforços em prol da manutenção da homeostase da célula se exaurem, o estresse persistente do RE desencadeia mecanismos de morte celular principalmente por apoptose, através da ativação de caspases via mitocôndria, a fim de eliminar células potencialmente defeituosas (DIEHL et al., 2011; RON; WALTER, 2007). As três proteínas sensoras da UPR descritas no tópico anterior também estão envolvidas na indução da morte celular em caso de estresse persistente do RE, principalmente pela via de ativação de PERK/ATF4/CHOP, embora outras vias também participem da regulação da sobrevivência celular (Figura 4) (IURLARO; MUÑOZ-PINEDO, 2015). De fato, tem sido sugerido que apesar de PERK apresentar um papel protetor durante a fase inicial do estresse de RE, a sua ativação persistente pode ser prejudicial, participando da ativação de mecanismos que irão promover apoptose e inflamação de tecidos (HOTAMISLIGIL, 2010).

Os mecanismos envolvidos na via de sinalização da UPR durante o estresse persistente de RE incluem: a indução de CHOP; a ativação mediada por IRE1 de TRAF2 (*tumor necrosis factor receptor associated factor 2*), o qual estimula a cascata das cinases ASK1 (*apoptotic-signaling kinase-1*)/ JNK (*Jun-N-terminal kinase*); e a liberação de Ca^{2+} pelo RE regulada por Bax/Bcl-2 (SANO; REED, 2013). O CHOP é um dos mediadores mais importantes da apoptose induzida pelo estresse de RE, uma vez que regula positivamente GADD34 (*growth arrest and DNA damage-inducible 34*), que leva à desfosforilação do eIF2α; além de regular a expressão de membros da família Bcl-2 (KIM et al., 2006). A PERK também regula a expressão de microRNAs, fornecendo mais um meio para modular a expressão de membros da família Bcl-2. A predominância dos membros pró-apoptóticos sobre os anti-apoptóticos leva à homo-oligomerização de Bax e Bak e posterior translocação para a mitocôndria, provocando a permeabilização da membrana externa mitocondrial, liberação de citocromo c, ativação de caspases e, finalmente, a morte da célula (IURLARO; MUÑOZ-PINEDO, 2015).

Enquanto a morte celular é associada com o aumento dos níveis de ATF4 e CHOP, a autofagia (que também pode ser regulada por esses dois fatores de transcrição) é reconhecida

como um dos principais mecanismos de sobrevivência da célula. No entanto, quando o estresse de RE é mais severo ou de longa duração, a autofagia também pode participar como um mecanismo de morte celular (SENFT; RONAI, 2015).

Figura 4 - Vias de sinalização da UPR durante o estresse persistente de RE.

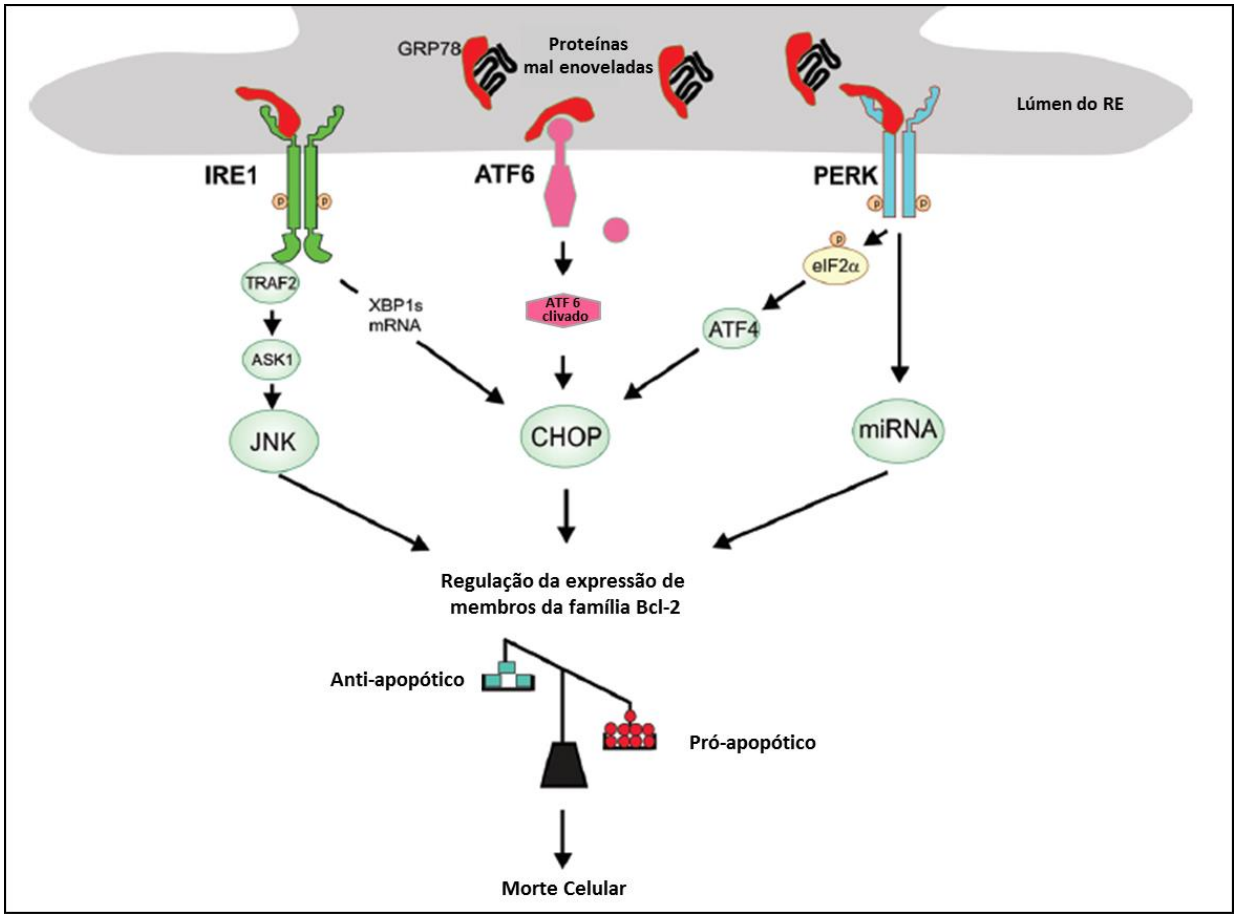

Fonte: Adaptado de Sovolyova et al. (2014)
Legenda: Após o estresse de RE prolongado ou excessivo, a UPR muda de uma resposta que leva predominantemente à sobrevivência para uma resposta que induz a morte celular. Todos os três ramos da UPR têm sido relacionados, de várias maneiras, para a regulação da expressão de membros da família Bcl-2 através de uma combinação de modificações transcricionais e pós-traducionais. Tem sido demonstrado que a IRE1 ativa desencadeia tanto um aumento na transcrição de membros da família Bcl-2 via CHOP, como também modula a atividade deles através de modificação pós-traducional mediada pelo recrutamento de TRAF2 e subsequente ativação de JNK. A sinalização de ATF6 pode ser ligada à expressão de membros da família Bcl-2 através da ativação do fator de transcrição pró-apoptótico CHOP. Da mesma forma, PERK pode desencadear a indução de CHOP, mas também regula a expressão de microRNA, fornecendo mais um meio para modular a expressão de membros da família Bcl-2. Todos os três braços da UPR agem em conjunto para fazer pender a balança a favor de membros pró-apoptóticos da família Bcl-2, levando à homo-oligomerização de Bax e Bak, inserção na membrana mitocondrial externa provocando a permeabilização da membrana mitocondrial externa, liberação de citocromo c, ativação de caspases e, finalmente, a morte celular.

3.2 Os Tripanossomatídeos

A família Trypanosomatidae compreende um vasto grupo de protozoários flagelados, separados em 12 gêneros, compreendendo parasitas monogenéticos (*Angomonas, Blastocrithidia, Crithidia, Herptomonas, Leptomonas, Rychoidomonasa* e *Wallaceina*) e digenéticos (*Endotrypanum, Leishmania, Phytomonas, Sauroleishmania* e *Trypanosoma*), os quais parasitam um grande número de hospedeiros incluindo animais, plantas e outros protistas. Entre os principais gêneros de importância médica e veterinária encontram-se o *Trypanosoma* e *Leishmania*. Estes organismos divergiram precocemente da linhagem evolutiva que deu origem aos demais eucariotos, tornando-se parasitos obrigatórios e provocando diferentes enfermidades de impacto mundial, tais como: a doença do sono, causada pelo *Trypanosoma brucei*; a doença de Chagas, causada pelo *Trypanosoma cruzi*; e os diferentes tipos de leishmanioses, causadas por *Leishmania* spp. Estas enfermidades são de difícil controle e alternativas como vacinas ou quimioterápicos mais eficientes dependem ainda de um maior conhecimento sobre os processos biológicos básicos destes agentes etiológicos (DUJARDIN et al., 2010; PALIWAL et al., 2011).

3.2.1 Biologia Celular dos Tripanossomatídeos

Os tripanossomatídeos possuem uma organização ultraestrutural eucariótica clássica com algumas organelas principais similares às encontradas nas células de mamíferos, tais como núcleo e complexo de Golgi, enquanto outras lhe são peculiares e estão ausentes em outros organismos eucariotos. Por exemplo, a mitocôndria é ramificada e contém uma região conhecida como o cinetoplasto, que abriga o DNA mitocondrial. Os parasitos também possuem uma camada de microtúbulos subpeliculares logo abaixo da membrana plasmática, que confere rigidez mecânica à célula, como é possível observar no esquema ilustrativo da organização intracelular do *T. cruzi* (forma epimastigota) na Figura 5. Algumas destas estruturas têm sido investigadas para determinar suas funções e identificar potenciais enzimas e vias metabólicas que possam servir como alvos para novos medicamentos, como será discutido nos tópicos a seguir.

Figura 5 - Representação da estrutura interna da forma epimastigota de *T. cruzi*.

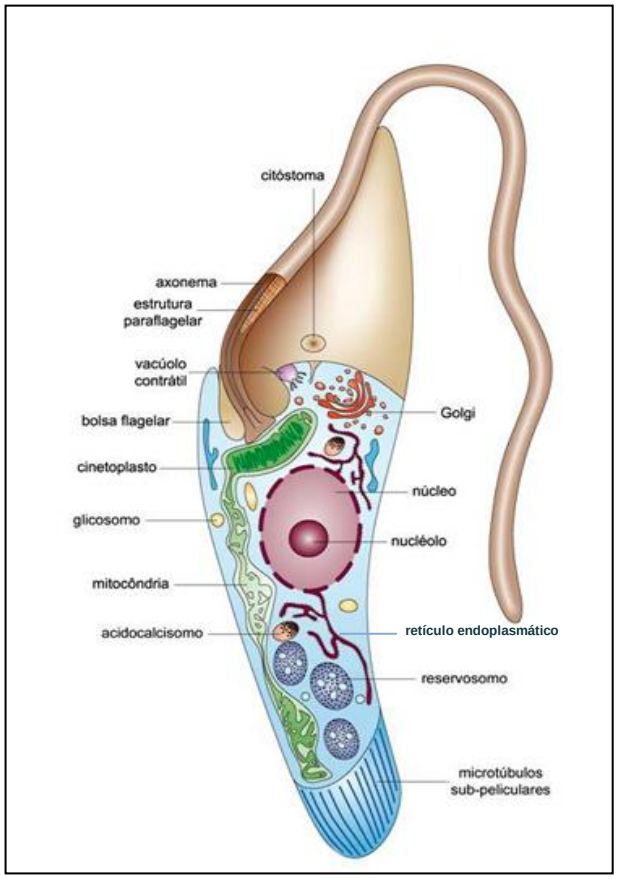

Fonte: Adaptado de DoCampo et al. (2005).
Legenda: Aspectos característicos das epimastigotas incluem um núcleo centralizado, o cinetoplasto anterior ao núcleo e a emergência lateral do flagelo fixado ao corpo celular na região anterior do protozoário.

3.2.1.1 Superfície Celular

Nos tripanossomatídeos a superfície da célula pode ser caracterizada pela presença de três componentes: a membrana plasmática, o glicocálice e os microtúbulos subpeliculares. A membrana plasmática do parasito varia em densidade e distribuição de proteínas integrais de membrana de acordo com sua forma evolutiva e também da região do corpo celular, podendo variar de constituição entre o corpo celular, o flagelo e a bolsa flagelar. Cada uma dessas estruturas possuem microdomínios específicos como, por exemplo, a zona de ligação do flagelo (FAZ, *flagellar attachment zone*) ao corpo da célula, em que um agrupamento linear de partículas intramembranares existem em ambas as faces da membrana flagelar que reveste a região de aderência; e a região do citóstoma, observada em formas epimastigotas e amastigotas de *T. cruzi*, que é uma invaginação da membrana plasmática seguido por alguns

microtúbulos especializados que penetram profundamente na célula podendo alcançar a região nuclear (SOUZA et al., 2009).

O glicocálice participa da interação entre as diferentes formas evolutivas e a superfície das células hospedeiras de mamífero e/ou células epiteliais intestinais dos insetos vetores. Para isso, o glicocálice é constituído por várias proteínas integrais e periféricas, glicoproteínas e glicolipídios, como as glicoproteínas ancoradas por GPI (glicosilfosfatidilinositol) de *T. brucei*; as mucinas de superfície de *T. cruzi*; e os glicofosfolipídios complexos de *Leishmania* sp. (RODRIGUES et al., 2014).

Os microtúbulos dos tripanossomatídeos estão organizados em arranjos citoplasmáticos paralelos, encontrados exclusivamente na parte periférica da célula. Análises por congelamento rápido, criofratura entre outras (HEUSER, 2001), mostraram que esses microtúbulos estão conectados uns com os outros através de filamentos, bem como à parte interna da membrana plasmática e às cisternas periféricas do retículo endoplasmático, recebendo assim, a denominação de microtúbulos subpeliculares. Estas estruturas são resistentes às baixas temperaturas, bem como a inúmeras drogas empregadas usualmente na ruptura de microtúbulos, como colchicina, colcemida, taxol etc. (SOUZA, 2008).

3.2.1.2 Mitocôndria e Cinetoplasto

A mitocôndria possui um importante papel para o metabolismo celular, sendo considerada uma das mais importantes organelas das células eucarióticas. Os tripanossomatídeos, ao contrário das células de mamífero que possuem inúmeras mitocôndrias, apresentam apenas uma única mitocôndria ramificada, que se estende logo abaixo da camada de microtúbulos subpeliculares e percorre todo o corpo celular do parasito. A ultraestrutura mitocondrial pode variar de acordo com a espécie do parasito, mas geralmente possui uma matriz densa e finas cristas tubulares irregularmente distribuídas (SOUZA et al., 2009). Uma característica peculiar da mitocôndria destes protozoários da ordem kinetoplastida é que ela possui uma estrutura especializada com uma grande concentração de DNA mitocondrial (k-DNA), conhecida como cinetoplasto. O cinetoplasto foi o primeiro DNA extranuclear descrito, representa aproximadamente 30% do DNA total da célula e é constituído por uma rede gigante de milhares de moléculas de DNA circulares relaxadas e interconectadas, cuja morfologia irá variar de acordo com a forma evolutiva do parasito (DOCAMPO et al., 2014). Na maioria dos tripanossomatídeos, como as formas epimastigotas e amastigotas de *T. cruzi*, as diferentes espécies de *Leishmania* e em *T. brucei*,

o cinetoplasto apresenta uma estrutura em formato de bastão. Já as formas tripomastigotas de *T. cruzi* apresentam um cinetoplasto arredondado ou em formato de cesta (SOUZA et al., 2009). Dois tipos de moléculas de DNA estão presentes no cinetoplasto, os minicírculos e os maxicírculos. Os maxicírculos estão em menor número e são funcionalmente homólogos ao DNA mitocondrial de outros eucariotos, pois codificam RNAs ribossomais para algumas proteínas, a maioria envolvida na cadeia respiratória. Os milhares de minicírculos respondem por aproximadamente 90% do total da massa de DNA mitocondrial e sua principal função é codificar pequenos RNAs guias que, por sua vez, modificam os transcritos do maxicírculo por inserção/deleção de resíduos de uridina em um processo conhecido como edição de RNA, gerando RNAs mensageiros funcionais (LUKES et al., 2002).

3.2.1.3 Reservossomos

Reservossomos são grandes organelas encontradas na região posterior de formas epimastigotas de *T. cruzi*, consideradas como compartimentos relacionados aos lisossomos. Embora sua morfologia possa variar de acordo com as condições de crescimento e a cepa do parasito, os reservossomos são geralmente arredondados, envolvidos por uma unidade de membrana e constituídos por uma matriz elétron-densa com vesículas e inclusões lipídicas imersas (CUNHA-E-SILVA et al., 2006). Os reservossomos representam a última etapa da via endocítica do parasito, acumulando macromoléculas do meio extracelular ou vindas do sistema RE-Complexo de Golgi, como proteínas e enzimas relacionadas com a digestão de proteínas e o metabolismo lipídico (PEREIRA et al., 2011). Estudos demonstraram que o conteúdo armazenado nestas estruturas também é utilizado como fonte de energia para o processo de metaciclogênese, visto que durante a diferenciação das formas epimastigotas para tripomastigotas estas organelas desaparecem gradualmente (FIGUEIREDO et al., 2004).

3.2.1.4 Acidocalcissomos

Acidocalcissomos são estruturas com aparência vacuolar distribuída aleatoriamente dentro da célula, que podem ser vistas no microscópio eletrônico de transmissão contendo um depósito elétron-denso designado como grânulos de polifosfato ou volutina. Possuem morfologia esférica e também podem ser observados por microscopia óptica utilizando fluorocromos que são acumulados em compartimentos ácidos, como a laranja de acridina (DOCAMPO; MORENO, 2011). Nos tripanossomatídeos, os acidocalcissomos são

geralmente observados em contato próximo com outras organelas e estruturas intracelulares, tais como a mitocôndria, o núcleo, os microtúbulos subpeliculares e inclusões lipídicas. O contato com a mitocôndria pode estar relacionado com a função de regulação da bioenergética da célula, como ocorre entre o retículo endoplasmático e as mitocôndrias nas células de mamíferos (DOCAMPO, 2015). Os acidocalcissomos de *T. cruzi* são ricos em ortofosfato, pirofosfato inorgânico e polifosfatos complexados com cátions (sódio, potássio, magnésio, cálcio, zinco e ferro) e aminoácidos básicos. Além disso, também estão envolvidos na homeostase do pH e na osmorregulação em associação com o vacúolo contrátil (DOCAMPO et al., 2011).

3.2.1.5 Glicossomos

Os glicossomos, inicialmente descritos em *T. brucei*, são organelas similares aos peroxissomos dos eucariotos superiores cuja designação é decorrente de sua capacidade de conter a maior parte das enzimas envolvidas na via glicolítica. A compartimentalização da glicólise dentro de organelas é um evento único, visto que em outros organismos este processo metabólico é basicamente citosólico (MICHELS et al., 2006). Posteriormente, os glicossomos também foram encontrados em outros protozoários, todos pertencentes à ordem kinetoplastida, e caracterizados através da microscopia eletrônica como estruturas esféricas ou alongadas, envoltas por uma unidade de membrana e uma matriz homogênea (SOUZA, 2008). Ao contrário da mitocôndria, os glicossomos não apresentam material genético em seu interior, sendo todas as proteínas encontradas codificadas por genes nucleares, traduzidas em ribossomos livres e importadas para a organela. Todas as enzimas identificadas nesta organela até o momento estão envolvidas nos processos energéticos da célula e no metabolismo de carboidratos e lipídeos (RODRIGUES et al., 2014).

3.2.2 O Retículo Endoplasmático de Tripanossomatídeos

Como em outras células eucarióticas, o retículo endoplasmático (RE) de tripanossomatídeos é uma organela de fundamental importância para os processos que envolvem a síntese de proteínas e lipídeos, sendo rico em chaperonas e enzimas auxiliares. As estruturas tubulares do RE podem ser encontradas por todo o corpo da célula, em contato com organelas como o núcleo (em continuidade com a membrana nuclear), a mitocôndria e o complexo de Golgi (ENGSTLER et al., 2007). Muitas vezes há também uma maior

concentração de perfis de RE na região periférica da célula, próximo dos microtúbulos subpeliculares e da membrana plasmática (Figura 6) (SOUZA, 2008).

Figura 6 - Micrografia eletrônica de célula epimastigota de *T. cruzi*.

Fonte: Rocha et al. (2006).
Legenda: Célula epimastigota apresentando perfis de RE (cabeça de seta) próximos à membrana plasmática. A seta branca aponta para a área de adesão do flagelo ao corpo celular. f: flagelo, k: cinetoplasto. Barra = 1 μm.

Apesar do RE possuir estrutura e função semelhantes ao de outros eucariotos, os tripanossomatídeos apresentam várias características diferentes no que se refere ao controle de qualidade da síntese proteica. Por exemplo, na reação de formação de glicoproteínas, os oligossacarídeos adicionados às proteínas durante a N-glicosilação não possuem resíduos de glicose, e sua estrutura varia de acordo com a espécie (BANERJEE et al., 2007; CONTE et al., 2003). Esses parasitos também não possuem calnexina, que participaria do enovelamento das proteínas glicosiladas ou glicosidase I, que retiraria o primeiro resíduo externo de glicose. Também tem sido reportado que *T. brucei* não possui IRE1 ou ATF6 e uma proteína ortóloga a PERK está localizada na bolsa flagelar, sugerindo uma função divergente (FIELD et al., 2010). Esses achados sugerem que os tripanossomatídeos tenham uma maquinaria mais simples de controle de qualidade do RE do que outros eucariotos (MICHAELI, 2012).

Os oligossacarídeos monoglicosilados são formados pela UGGT em tripanossomatídeos exclusivamente durante a glicosilação de glicoproteínas mal enoveladas, assim como em outros eucariotos. A glicosidase II, responsável por retirar o resíduo externo de glicose, a BiP e a CRT, que auxiliam no enovelamento das proteínas, também tem sido descritas, apresentando as mesmas propriedades encontradas em outras espécies (Figura 7)

(CONTE et al., 2003). Em particular, a CRT de *T. cruzi* tem um papel importante na maturação da cruzipaína, uma protease lisossomal abundante considerada um fator de virulência desse parasito (LABRIOLA et al., 2010).

Figura 7 - Controle de qualidade da síntese proteica em tripanossomatídeos.

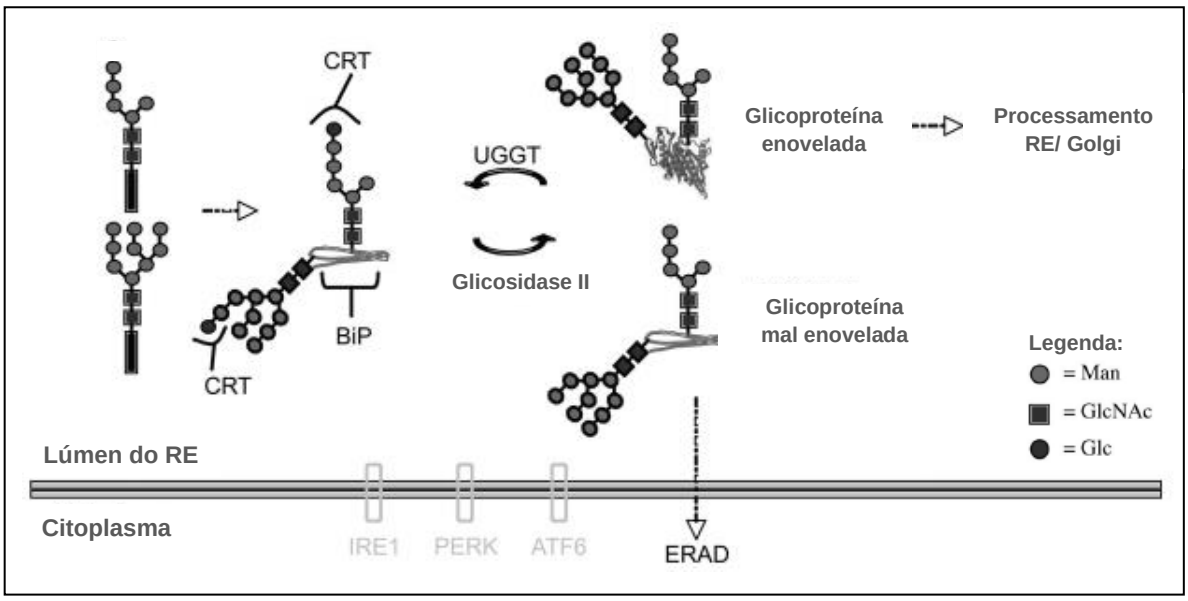

Fonte: Modificado de Izquierdo, et al. (2009).
Legenda: Fatores de controle de qualidade dependente de N-glicano na formação de dímeros de glicoproteína variante de superfície (VSG) de formas tripomastigotas de *T. brucei*. CRT, calreticulina; ERAD, degradação associada ao RE; Man, manose; GlcNac, N-acetilglicosamina; Glc, glicose.

3.2.3 Estresse de RE e Morte Celular em Tripanossomatídeos

Embora sejam altamente divergentes de mamíferos e fungos, as características gerais do sistema de endomembranas de tripanossomatídeos são bastante conservados (ENGSTLER et al., 2007; FIELD; CARRINGTON, 2004). No entanto, pouco se sabe sobre os mecanismos de resposta ao estresse de RE e o seu papel na morte celular do parasito. Alguns estudos utilizaram em tripanossomatídeos agentes farmacológicos que causam estresse de RE em eucariotos superiores, como a tunicamicina (TM), a tapsigargina (TG) e o ditiotreitol (DTT) (DUROSE et al., 2006).

A TM é um antibiótico natural originalmente isolado a partir de *Streptomyces lysosuperficus* e *S. chartreusis* (LI; YU, 2015), muito utilizado por inibir a glicosilação de proteínas em diferentes linhas celulares, incluindo tripanossomatídeos como *Leishmania major* (DOLAI et al., 2011), *L. donovani* (GOSLINE et al., 2011) e *T. brucei* (KOUMANDOU et al., 2008; TIENGWE et al., 2015). A maioria desses estudos não encontrou alteração na expressão de BiP, um dos marcos da UPR, com exceção da *L. major* que, durante o tratamento com a TM, parece aumentar a expressão de BiP e induzir morte celular por apoptose (DOLAI et al., 2011). Estudos anteriores também analisaram o efeito da TM sobre a interação entre *T. cruzi* e células de mamífero (PIRAS et al., 1982; ZINGALES et al., 1985; SOUTO-PADRÓN; de SOUZA, 1989), e demonstraram que o tratamento com a TM pode interferir na infecção da célula hospedeira. No entanto, o potencial da TM no estresse de RE do *T. cruzi* e os mecanismos de ação e os processos de morte celular programada (MCP) envolvidos ainda não foram explorados nesse parasito.

A TG inibe a ATPase dependente de Ca^{2+} do RE, causando a liberação de cálcio do RE para o citosol, comprometendo a sua capacidade de sintetizar proteínas corretamente (HARBUT et al., 2012). Alguns estudos analisaram o efeito da TG sobre a homeostase do cálcio em tripanossomatídeos (DOCAMPO et al., 1993, PÉREZ-GORDONES et al., 2015; VERCESI et al., 1993) porém, com exceção do trabalho de Tiengwe e colaboradores (2015), que demonstrou que a TG não induziu a expressão de nenhum indicador da UPR clássica em *T. brucei*, não foram encontrados estudos analisando o estresse de RE induzido pela TG em outros parasitos.

O DTT por sua vez, quebra ou previne a ligação de pontes dissulfeto, impedindo a conformação das estruturas terciárias e quaternárias das proteínas (BACK et al., 2005). O uso do DTT como estressor de RE tem sido reportado em *L. donovani* e *T. brucei* (GOLDSHMIDT et al., 2010; GOSLINE et al., 2011; KOUMANDOU, 2008), porém esses

estudos apresentam resultados divergentes quanto a regulação da expressão de BiP durante o estresse de RE. Em *T. brucei*, os autores acreditam que o parasito altere seu transcriptoma em resposta ao estresse do RE de maneira similar a fungos e metazoários. Estas alterações não seriam um produto de um programa de regulação transcricional como em outros eucariotos, mas através da estabilização de mRNA que é necessária para executar a resposta ao estresse do RE (GOLDSHMIDT et al., 2010). No entanto, um estudo mais recente em *T. brucei* apontou que o estresse oxidativo induzido pelo DTT é tão grande que pode levar à morte celular por outras vias que não envolvam a UPR clássica nem o aumento da expressão de chaperonas (TIENGWE et al., 2015). Assim, mais estudos ainda são necessários para validar a ação do DTT como estressor de RE, inclusive em outras espécies, como o *T. cruzi*.

Os tripanossomatídeos possuem um mecanismo de expressão de genes não convencional e, portanto, um alvo potencial para o desenvolvimento de novos agentes quimioterápicos. Este mecanismo inclui edição de RNA e o *trans-splicing*. O mecanismo de edição de RNA consiste na inserção ou deleção de resíduos de uridina para formação de uma fase aberta de leitura funcional (MOFFETT et al, 1997; OCHSENREITER et al., 2008). O *trans-splicing* é requerido para maturação de todos os mRNAs nestes parasitos e consiste na adição de uma sequência extremamente conservada, espécie-específica, de 39 nucleotídeos, denominada de sequência líder (SL; *spliced-leader*) ou mini-exon, à extremidade 5´ dos RNAs mensageiros nascentes (GOLDSHMIDT et al., 2010). Nesta reação, participam duas moléculas de RNA codificadas por genes situados em diferentes sítios do genoma, daí a denominação *trans-splicing*. A molécula doadora é um precursor do mini-exon e em *T. cruzi* possui cerca de 110 nucleotídeos (ZWIERZYNSKI; BUCK, 1991). A aceptora é um transcrito derivado da unidade policistrônica ao qual o mini-exon é transferido. Os genes para proteínas são arranjados em uma longa unidade policistrônica que é processada pós-transcricionalmente pela ação orquestrada do *trans-splicing* e da poliadenilação. O SL-RNA possui um promotor bem definido que se liga a fatores de transcrição específicos tais como t-SNAPs (SMIRLIS et al., 2010).

Para *T. brucei* parece existir um novo mecanismo regulatório induzido por estresse que controla o transcriptoma sob os mais variados estímulos. Este mecanismo é conhecido como silenciamento do SL-RNA (SLS) (LUSTIG et al., 2007). O SLS foi descoberto em células silenciadas para o receptor da partícula de reconhecimento de sinal (SRα), mas também foi descrito durante o tratamento com agentes farmacológicos, como o DTT (GOLDSHMIDT et al., 2010). Durante o estresse persistente de RE, o fator de transcrição tSNAP42 falha em ligar ao promotor do SL-RNA. O marco do SLS é, desta forma, o

desligamento da transcrição do RNA seguido por uma massiva acumulação de t-SNAP42 no núcleo, levando à morte das células por um processo semelhante a apoptose (Figura 8) (LUSTIG et al., 2007).

Figura 8 - Representação da via de SLS induzida por estresse de RE em *T. brucei.*

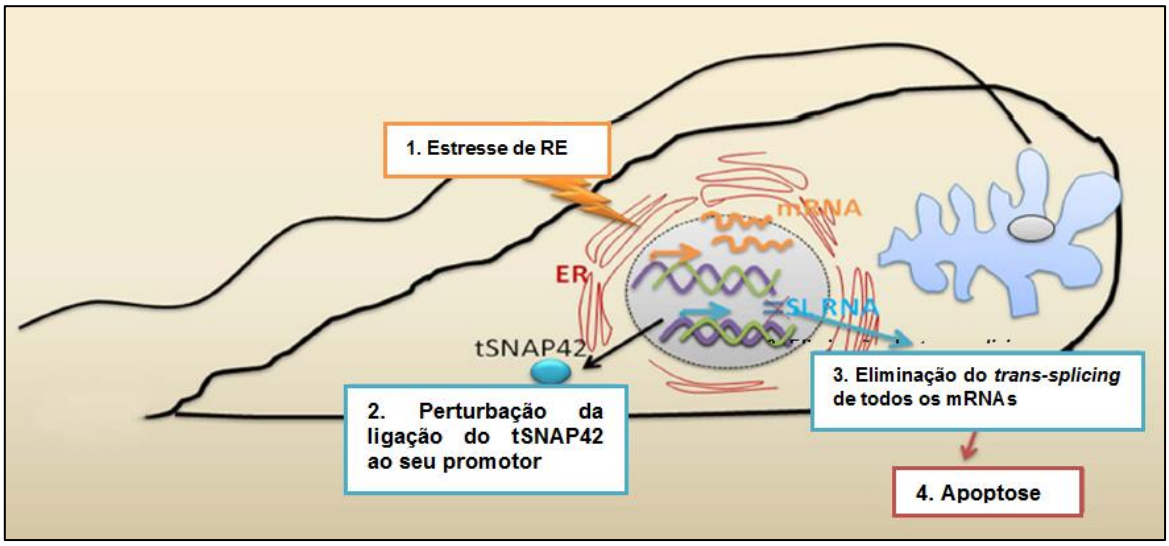

Fonte: Adaptado de Smirlis et al. (2010).
Legenda: O estresse persistente de RE (**1**) perturba a ligação de tSNAP42 ao promotor da sequência líder (SL-RNA) (**2**). Isto leva ao desligamento da transcrição do SL-RNA e à eliminação do *trans-splicing* de todos os mRNAs (**3**). A via de silenciamento do SL-RNA que, por sua vez, induz a morte celular por apoptose.

Muitas evidências têm demonstrado que os tripanossomatídeos podem apresentar características típicas de apoptose, embora não possuam algumas das moléculas chaves que contribuem para este processo em eucariotos superiores, como os genes das caspases, da família Bcl-2 e da família dos receptores relacionados com o fator de necrose tumoral (SMIRLIS et al., 2010). Uma justificativa para a ativação da morte celular é que esses parasitos possuem um complexo ciclo de vida envolvendo o hospedeiro vertebrado, nos quais passam por várias etapas de diferenciação e multiplicação e têm que lidar com ambientes muitas vezes hostis (MICHAELI, 2012). As alterações bioquímicas e morfológicas de apoptose observadas incluem a despolarização do potencial de membrana mitocondrial, liberação de citocromo c, ativação de proteases, formação de corpos apoptóticos, exposição de fosfatidilserina no folheto externo da membrana plasmática e condensação da cromatina (MENNA-BARRETO et al., 2009; ROY et al., 2008; MATTA et al., 2007).

Nos últimos anos, outras vias de morte celular independentes de caspases, como a autofagia, tem sido identificadas em tripanossomatídeos em resposta aos mais variados

estímulos, como estresse nutricional e o tratamento com drogas (ALVAREZ et al., 2007; MENNA-BARRETO et al., 2009; SANDES et al., 2014). Este tipo de MCP está envolvido na degradação de proteínas e na reciclagem de organelas durante estresse, como uma forma de garantir a sobrevivência das células (BRENNAND et al., 2011; RODRIGUES; SOUZA, 2008; UCHIYAMA et al., 2008).

Embora tanto o estresse do RE quanto o SLS pareçam ter um papel determinante na sobrevivência de *T. brucei*, seu papel na sobrevivência/morte celular dos demais tripanossomatídeos é pouco compreendido. Sabe-se, por exemplo, que a interação entre chaperonas como a BiP e a calreticulina é importante para maturação de glicoproteínas em *T. cruzi* (LABRIOLA et al., 2011). No entanto, não se sabe como estas proteínas respondem a condições de estresse do RE, já que nenhum estudo envolvendo o *T. cruzi* foi encontrado na literatura.

3.3 O *T. cruzi* e a doença de Chagas

Dentre os tripanossomatídeos, o *Trypanosoma cruzi*, usado como modelo de nosso estudo, é considerado um dos mais importantes protozoários patogênicos, sendo responsável pela doença de Chagas ou Tripanossomíase Americana. Esta patologia constitui um sério agravo para Saúde Pública com cerca de 6 a 7 milhões de pessoas infectadas, principalmente na América Latina, onde a doença de Chagas é endêmica, mas também foram reportados casos nos Estados Unidos da América, no Canadá, na Europa e em alguns países do Pacífico Ocidental, como Japão e Austrália (Figura 9) (PEREZ et al., 2015; ORGANIZAÇÃO MUNDIAL DA SAÚDE, 2015). A principal forma de transmissão da doença de Chagas aos seres humanos e para mais de 150 espécies de animais domésticos e selvagens é através de insetos pertencentes à família Reduviidae e subfamília Triatominae, popularmente conhecidos como “barbeiros”. No entanto, também existem outras vias de infecção que incluem transfusão sanguínea, transplante de órgãos e medula óssea, transmissão congênita, e via oral por alimentos contaminados com o *T. cruzi* (RASSI JR. et al., 2012).

Figura 9 - Distribuição global de casos da doença de Chagas, 2006 – 2010.

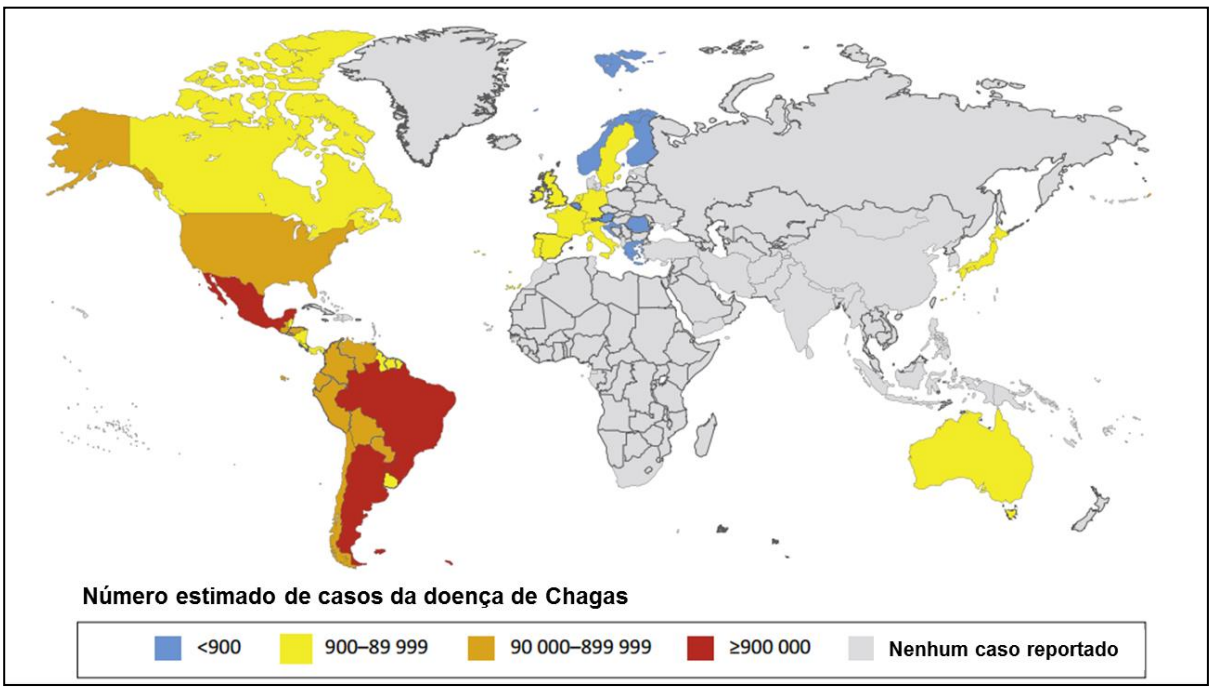

Fonte: Adaptado de Perez et al. (2015).

A progressão natural da doença de Chagas envolve uma fase aguda e uma fase crônica. Na fase aguda da doença, os sintomas são geralmente inespecíficos como febre, mal-estar e hepatoesplenomegalia. Em alguns casos, um nódulo cutâneo (chagoma) ou um edema palpebral (sinal de Romaña) pode indicar o local da inoculação. Por volta de 4 a 8 semanas a parasitemia e os sintomas desaparecem e a doença pode evoluir para a fase crônica indeterminada, que pode durar por toda a vida ou uma fase crônica determinada propriamente dita. Cerca de 20 a 30% das pessoas infectadas têm a progressão para a fase crônica determinada da doença, que é caracterizada por uma cardiomiopatia chagásica crônica e/ou pelo desenvolvimento de graves alterações gastrointestinais, como o megacólon e o megaesôfago (Figura 10) (BERN, 2015; PEREZ et al., 2015). Apesar da gravidade da doença, os medicamentos disponíveis ainda são os mesmos que foram utilizados cinco décadas atrás, Benzonidazol e Nifurtimox, que apresentam baixa eficácia na fase crônica da doença e provoca graves efeitos colaterais (BUSCHINI et al., 2009; GASPAR et al., 2015).

Figura 10 - As fases da doença de Chagas.

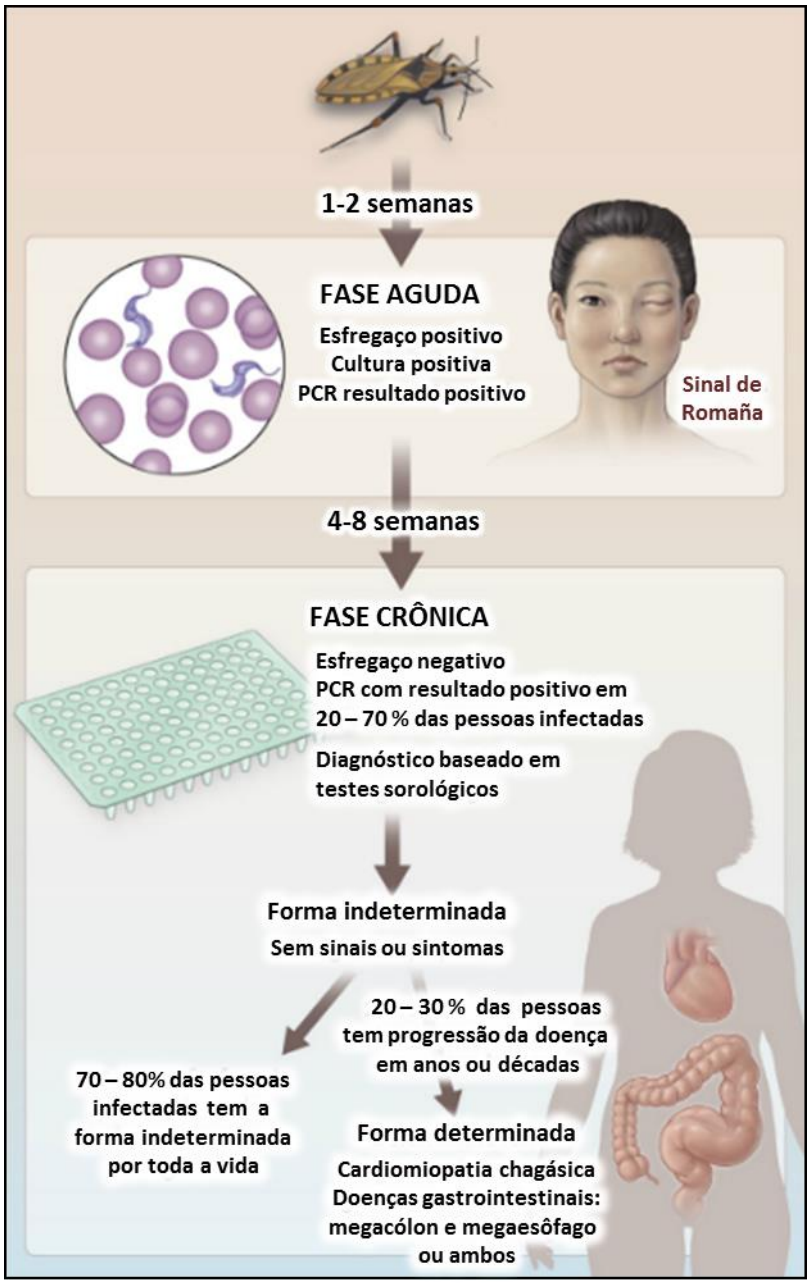

Fonte: Adaptado de Bern (2015).
Legenda: A fase aguda da doença de Chagas se inicia cerca de 1-2 semanas após a infecção pelo *T. cruzi* e é caracterizada pela detecção da parasitemia por até 4 a 8 semanas. Depois a parasitemia e os sintomas desaparecem e a doença evolui para a fase crônica indeterminada, que pode durar por toda a vida. Estima-se que 20 a 30% das pessoas podem progredir para a fase determinada da doença ao longo de anos ou décadas, tendo como principais complicações a cardiomiopatia chagásica e doenças gastrointestinais, como megacólon ou megaesôfago, ou ambos.

Tripanossomatídeos patogênicos possuem um complexo ciclo de vida que se alterna entre hospedeiros invertebrados e vertebrados. As diferentes formas evolutivas podem viver dentro das células hospedeiras, na corrente sanguínea ou no intestino de insetos. No caso do

T. cruzi, o ciclo de vida envolve a passagem por três formas evolutivas principais: tripomastigotas, amastigotas e epimastigotas, as quais diferem tanto morfologicamente quanto fisiologicamente (Figura 11). As formas epimastigotas são replicativas, não infectantes, encontradas no intestino do hospedeiro invertebrado e facilmente cultivadas em meios axênicos. Suas características morfológicas principais são o corpo celular alongado, o flagelo livre anteriormente e o cinetoplasto em forma de barra ou bastão anterior ao núcleo (Figura 11A). Os tripomastigotas não possuem capacidade de se multiplicar e são as formas infectivas tanto para os hospedeiros vertebrados (tripomastigotas sanguíneas) como para os invertebrados (tripomastigotas metacíclicas na porção final do intestino). Possuem um cinetoplasto arredondado localizado na região posterior ao núcleo e um flagelo que emerge lateralmente aderido ao longo do corpo do parasito até tornar-se livre na região anterior (Figura 11B). As formas amastigotas são encontradas exclusivamente no interior de células de mamíferos, onde se multiplicam. Apresenta morfologia arredondada, cinetoplasto em forma de bastão na região anterior ao núcleo e um flagelo curto restrito ao interior da bolsa flagelar (Figura 11C) (SOUZA, 2008).

Figura 11 - Formas evolutivas do *Trypanosoma cruzi*.

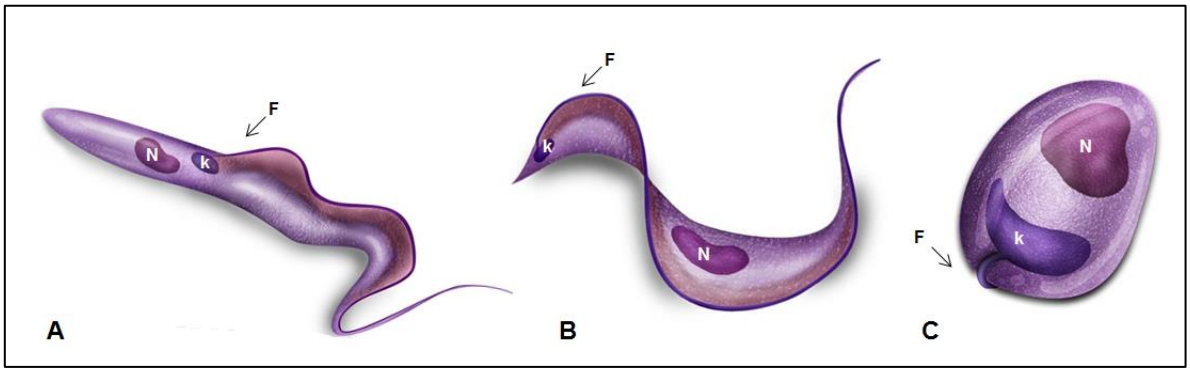

Fonte: Modificado de Eschenazi (2009).
Legenda: (A) Epimastigota, **(B)** Tripomastigota, **(C)** Amastigota. N= núcleo, k= cinetoplasto, F= flagelo.

Os hospedeiros invertebrados se tornam infectados através da ingestão de formas tripomastigotas circulantes no sangue de mamíferos infectados. No trato digestivo dos triatomíneos, as formas tripomastigotas se diferenciam em epimastigotas (forma multiplicativa) e, em seguida, em tripomastigotas metacíclicas na porção final do intestino (Figura 12) (ESCH; PETERSEN, 2013; RODRIGUES et al., 2014). Durante um novo repasto sanguíneo, formas tripomastigotas metacíclicas infectivas, eliminadas junto com as fezes dos

triatomíneos, podem eventualmente infectar um hospedeiro vertebrado através das mucosas ou pela ferida causada pelo ato de coçar. Os tripomastigotas invadem as células perto do local da infecção e se diferenciam em amastigotas intracelulares, que se replicam por fissão binária. No citoplasma das células, as formas amastigotas se diferenciam em tripomastigotas, os quais podem romper as células e cair na corrente sanguínea invadindo tecidos adjacentes e se espalhando pelos vasos linfáticos e pela corrente sanguínea para locais distantes, principalmente células musculares (cardíacas, lisas e esqueléticas), onde se submetem a novos ciclos de multiplicação intracelular. O ciclo de transmissão se reinicia quando formas tripomastigotas circulantes são ingeridas durante o repasto sanguíneo do vetor (RASSI JR. et al., 2012).

Figura 12 - Ciclo de vida do *Trypanosoma cruzi*.

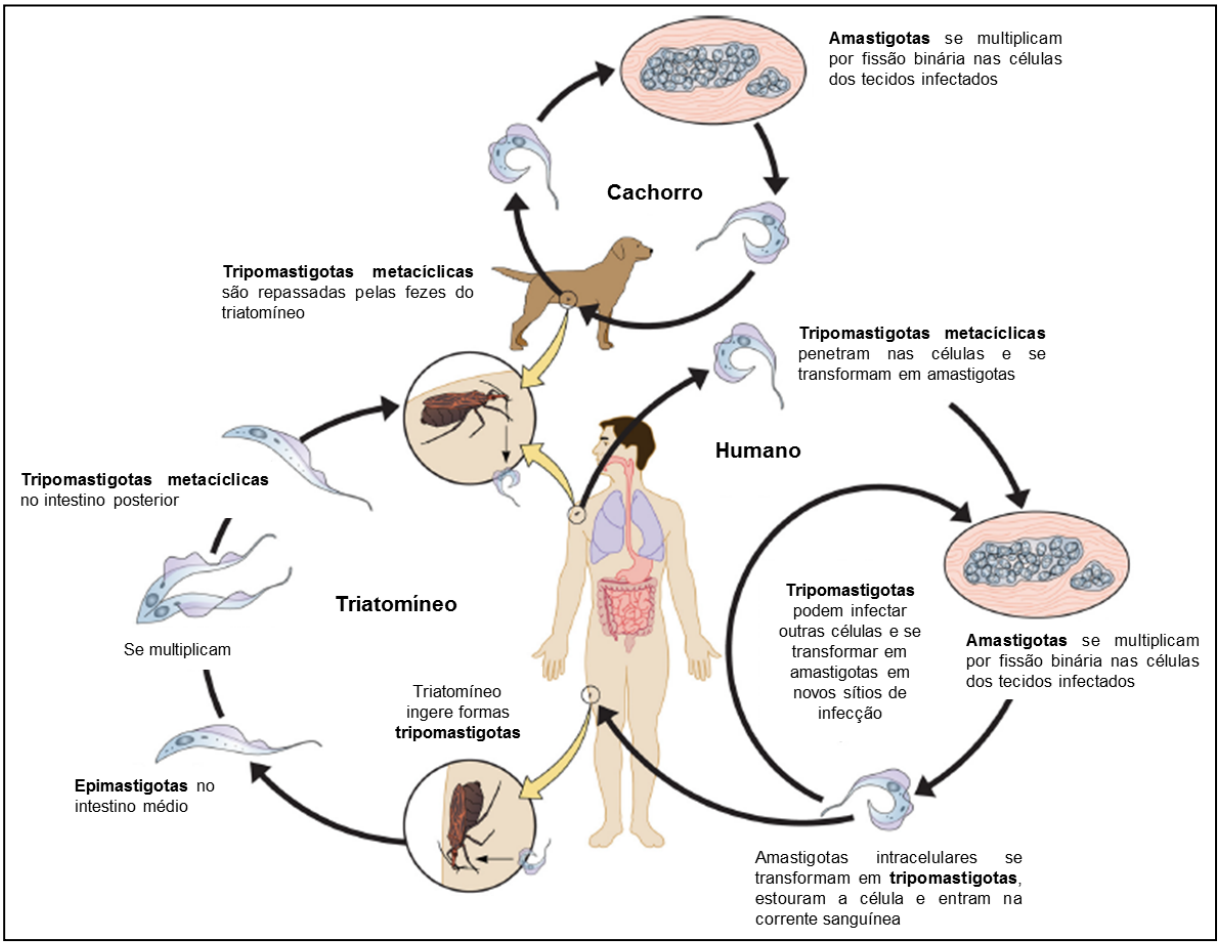

Fonte: Adaptado de Esch; Petersen (2013).
Legenda: Um vetor triatomíneo ou "barbeiro" infectado durante seu repasto sanguíneo no hospedeiro mamífero, como o ser humano ou o cachorro, libera tripomastigotas infectivas nas fezes perto do local da picada ou de mucosas. Tripomastigotas infectivas entram no hospedeiro pela ferida causada pelo ato de coçar, mas também pode penetrar em mucosas intactas, como a conjuntiva, ou oralmente após exposição de origem alimentar. As tripomastigotas invadem as células perto do local da infecção e se diferenciam em amastigotas intracelulares. As amastigotas se replicam por fissão binária dentro dos

vacúolos parasitóforos e depois escapam para o citoplasma, onde se diferenciam em tripomastigotas. As tripomastigotas são liberadas da célula, muitas vezes rompendo-a, e atingem a corrente sanguínea. Insetos triatomíneos se tornam infectados através da ingestão de tripomastigotas circulantes no sangue de mamíferos infectados, que irão se transformar em epimastigotas dentro do intestino médio do triatomíneo, e se diferenciar em tripomastigotas infectivas dentro do intestino posterior do inseto.

3.4 O *T. cruzi* como Modelo de Estudo do Estresse de RE

Apesar da importância como patógeno do *T. cruzi*, agente etiológico da doença de Chagas, nenhuma estratégia de intervenção e controle ao parasita é considerada eficaz, fazendo com que esta doença seja considerada um sério problema de saúde pública, uma vez que as drogas utilizadas no tratamento desta patologia possuem sérios efeitos colaterais devido à falta de especificidade em relação às células do hospedeiro (GASPAR et al., 2015). Dessa forma, pesquisas para identificação de genes, proteínas e vias metabólicas essenciais para a sobrevivência do parasito e que não sejam encontrados no hospedeiro vertebrado surgem como uma estratégia valiosa para o desenvolvimento racional de drogas.

Tem sido demonstrado que os tripanossomatídeos de maneira geral respondem ao estresse do RE de modo diferente das células eucarióticas de mamíferos (MICHAELI, 2012). Vários estudos têm avaliado o estresse do RE e seu potencial como indutor de uma resposta do tipo da UPR e/ou de eventos de MCP em *T. brucei* e *Leishmania* sp. (DOLAI et al., 2011; GOLDSHMIDT et al., 2010; GOSLINE et al., 2011; KOUMANDOU et al, 2008; TIENGWE et al., 2015). No entanto, aspectos da biologia celular relacionados ao papel do RE na morte celular em *T. cruzi* são totalmente desconhecidos, o que despertou o interesse do nosso grupo de pesquisa e cujos resultados serão apresentados em formato de artigo nos itens a seguir. Esperamos com a realização do presente estudo não só contribuir para o entendimento dos processos que medeiam os eventos de morte celular induzidos por estresse de RE, como fornecer subsídio para o desenvolvimento de drogas mais eficientes contra a doença de Chagas.

REFERÊNCIAS

ALVAREZ, V. E. et al. Autophagy is involved in nutritional stress response and differentiation in *Trypanosoma cruzi*. **J. Biol. Chem**. v. 283, p. 3454-3464, 2007.

APPENZELLER-HERZOG, C; HAURI, H. P. The ER-Golgi intermediate compartment (ERGIC): in search of its identity and function. **J Cell Sci.** v. 119, p. 2173-2183, 2006.

BACK, S. H. et al. ER stress signaling by regulated splicing: IRE1/HAC1/XBP1. **Methods.** v. 35, p. 395-416, 2005.

BANERJEE, S. et al. The evolution of N-glycan-dependent endoplasmic reticulum quality control factors for glycoprotein folding and degradation. **Proc. Natl. Acad. Sci.** v. 104, p. 11676-11681, 2007.

BERN, C. Chagas' Disease. **N. Engl. J. Med.** v. 373, p. 456-466, 2015.

BRAVO, R. et al. Endoplasmic reticulum and the unfolded protein response: dynamics and metabolic integration. **Int. Rev. Cell. Mol. Biol.** v. 301, p. 215-290, 2013.

BRENNAND, A., et al. Autophagy in parasitic protists: unique features and drug targets. **Mol. Biochem. Parasitol**. v. 177, p. 83-99, 2011.

BRODSKY, J. L.; SKACH, W. R. Protein folding and quality control in the endoplasmic reticulum: Recent lessons from yeast and mammalian cell systems. **Curr. Opin. Cell. Biol.** v. 23, p. 464-475, 2011.

BUSCHINI, A. et al. Genotoxicity revaluation of three commercial nitroheterocyclic drugs: nifurtimox, benznidazole, and metronidazole. **J. Parasitol. Res.** v. 2009, p. 463-575, 2009.

CHEN, X. et al. Molecular characterization of the endoplasmic reticulum: insights from proteomic studies. **Proteomics**. v. 10, p. 4040-4052, 2010.

CONTE, I. et al. The interplay between folding-facilitating mechanisms in *Trypanosoma cruzi* endoplasmic reticulum. **Mol. Biol. Cell.** v. 14, p. 3529-3540, 2003.

CUNHA-E-SILVA, N. et al. Reservosomes: multipurpose organelles? **Parasitol. Res.** v. 99, p. 325-327, 2006.

DIEHL, J. A.; FUCHS, S. Y.; KOUMENIS, C. The cell biology of the unfolded protein response. **Gastroenterology**. v. 141, p. 38-41, 2011.

DOCAMPO, R. The origin and evolution of the acidocalcisome and its interactions with other organelles. **Mol. Biochem. Parasitol.** 2015. No prelo.

DOCAMPO, R.; MORENO, S. N. Acidocalcisomes. **Cell Calcium.** v. 50, p. 113- 119, 2011.

DOCAMPO, R. et al. Acidocalcisomes: conserved from bacteria to man. **Nat. Ver. Microbiol.** v. 3, p. 251-261, 2005.

DOCAMPO, R. et al. The role of acidocalcisomes in the stress response of *Trypanosoma cruzi*. **Adv. Parasitol.** v. 75, p. 307-324, 2011.

DOCAMPO, R.; MORENO, S. N.; VERCESI, A. E. Effect of thapsigargin on calcium homeostasis in *Trypanosoma cruzi* trypomastigotes and epimastigotes. **Mol. Biochem. Parasitol.** v. 59, p. 305-313, 1993.

DOCAMPO, R.; VERCESI, A. E.; HUANG, G. Mitochondrial calcium transport in trypanosomes. **Mol. Biochem. Parasitol.** v. 196, p. 108-116, 2014.

DOLAI, S. et al. Endoplasmic reticulum stress-induced apoptosis in *Leishmania* through Ca2+-dependent and caspase-independent mechanism. **J. Biol. Chem.** v. 286, p. 13638-13646, 2011.

DUDEK, J.; BENEDIX, J.; JALAL, C. The Role of BiP and Its Co‐ Chaperones. In: Protein Transport into the Endoplasmic Reticulum, ed. Richard Zimmermann. **Landes Bioscience.** Cap. 6, p. 65-76, 2009.

DUJARDIN, J. C. et al. Research priorities for neglected infectious diseases in Latin America and the Caribbean region. **PLoS. Negl. Trop. Dis.** v. 26, p. e780. 2010.

DUROSE, J. B.; TAM, A. B.; NIWA, M. Intrinsic capacities of molecular sensors of the unfolded protein response to sense alternate forms of endoplasmic reticulum stress. **Mol. Biol. Cell.** v. 17, p. 3095-3107, 2006.

ELLGAARD, L.; FRICKEL, E. M. Calnexin, calreticulin, and ERp57: teammates in glycoprotein folding. **Cell. Biochem. Biophys.** v. 39, p. 223-247, 2003.

ENGSTLER, M.; BANGS, J. D.; FIELD, M. C. Intracellular transport systems in trypanosomes: function, evolution and virulence. In: Trypanosomes – After the Genome, J. D. Barry et al. (ed.). **Horizon Press**. p. 281-317, 2007.

ESCH, K. J.; PETERSEN, C. A. Transmission and epidemiology of zoonotic protozoal diseases of companion animals. **Clin. Microbiol. Rev.** v. 26, p. 58-85, 2013.

ESCHENAZI, B. *Trypanosoma cruzi* forms - Job for association Medecins Sans Frontieres. Rio de Janeiro, 2009. Disponível em: <http://www.coroflot.com/eschenazi/scientific-and-medical>. Acesso em: 12 fev. 2016.

FIELD, M. C.; CARRINGTON, M. Intracellular membrane transport systems in *Trypanosoma brucei*. **Traffic**. v. 5, p. 905-913, 2004.

FIELD, M. C. et al. Chaperone requirements for biosynthesis of the trypanosome variant surface glycoprotein. **PLoS One**. v. 5, p. e8468, 2010.

FIGUEIREDO, R. C. et al. Reservosome: an endocytic compartment in epimastigote forms of the protozoan *Trypanosoma cruzi* (Kinetoplastida: Trypanosomatidae). Correlation between endocytosis of nutrients and cell differentiation. **Parasitology.** v.129, p.431-438, 2004.

GARDNER, B. M.; WALTER, P. Unfolded proteins are ire1-activating ligands that directly induce the unfolded protein response. **Science.** v. 333, p. 1891-1894, 2011.

GASPAR, L. et al. Current and Future Chemotherapy for Chagas Disease. **Curr. Med. Chem.** v. 22, p. 4293-4312.

GOLDSHMIDT, H. et al. Persistent ER stress induces the spliced leader RNA silencing pathway (SLS), leading to programmed cell death in *Trypanosoma brucei*. **Plos Pathog**. v. 6, p. e1000731, 2010.

GOSLINE, S. J. Intracellular eukaryotic parasites have a distinct unfolded protein response. **PLoS One.** v. 6, p. e19118, 2011.

HARBUT, M. B. et al. Targeting the ERAD pathway via inhibition of signal peptide peptidase for antiparasitic therapeutic design. **Proc. Natl. Acad. Sci.** v. 109, p. 21486-21491, 2012.

HEGDE, R. S.; PLOEGH, H. L. Quality and quantity control at the endoplasmic reticulum. **Curr. Opin. Cell. Biol.** v. 22, p. 437-446, 2010.

HEUSER, J. E. A critical comparison between the two current methods of viewing frozen, live cells in the electron microscope: cryoelectron microscopic tomography versus "deep-etch" electron microscopy. **Biomed. Rev.** v. 12, p. 11-29, 2001.

HOTAMISLIGIL, G. S. Endoplasmic reticulum stress and the inflammatory basis of metabolic disease. **Cell.** v. 140, p. 900-917, 2010.

IURLARO, R.; MUÑOZ-PINEDO, C. Cell death induced by endoplasmic reticulum stress. **FEBS J.** 2015. No prelo.

IZQUIERDO L. et al. Distinct donor and acceptor specificities of *Trypanosoma brucei* oligosaccharyl-trasferases. **EMBO Journal.** v. 28, p. 2650-2661, 2009.

KABACHINSKI, G.; SCHWARTZ, T. U. The nuclear pore complex – structure and function at a glance. **J Cell Sci** v.128, p. 423–429, 2015.

KIEL, J. A. Autophagy in unicellular eukaryotes. **Philos. Trans. R. Soc. Lond. B. Biol. Sci.** v. 365, p. 819-830, 2010.

KIM, R. et al. Role of the unfolded protein response in cell death. **Apoptosis** v. 11, p. 5-13, 2006.

KOUMANDOU, V. L. et al. The trypanosome transcriptome is remodeled during differentiation but displays limited responsiveness within life stages. **BMC Genomics.** v. 9, p. 298-326, 2008.

LABRIOLA, C. A. et al. Endoplasmic reticulum calcium regulates the retrotranslocation of *Trypanosoma cruzi* calreticulin to the cytosol. **PLoS One.** v. 5, p. e13141, 2010.

LABRIOLA, C. A. et al. Functional cooperation between BiP and calreticulin in the folding maturation of a glycoprotein in *Trypanosoma cruzi*. **Mol. Biochem. Parasitol.** v. 175, p. 112-117, 2011.

LAI, E.; TEODORO, T.; VOLCHUK, A. Endoplasmic reticulum stress: signaling the unfolded protein response. **Physiology (Bethesda).** v. 22, p. 193-201, 2007.

LAVOIE, C.; PAIEMENT, J. Topology of molecular machines of the endoplasmic reticulum: a compilation of proteomics and cytological data. **Histochem. Cell. Biol.** v. 129, p. 117-128, 2008.

LAVOIE, C. et al. Taking organelles apart, putting them back together and creating new ones: lessons from the endoplasmic reticulum. **Prog. Histochem. Cytochem.** v. 46, p. 1-48, 2011.

LUKES, J. et al. Kinetoplast DNA network: evolution of an improbable structure. **Eukaryot Cell.** v. 1, p. 495-502, 2002.

LI, J.; YU, B. A modular approach to the total synthesis of tunicamycins. **Angew. Chem. Int. Ed. Engl.** v. 54, p. 6618-6621, 2015.

LUSTIG, Y. et al. Spliced-leader RNA silencing: a novel stress-induced mechanism in *Trypanosoma brucei*. **EMBO reports.** v. 8, p. 408-413, 2007.

MATTA, R. A. da et al. *Trypansoma cruzi* exposes phosphatidylserine as an evasion mechanism. **FEMS Microbiol. Lett.** v. 266, p. 29-33, 2007.

MENNA-BARRETO, R. F. et al. Different cell death pathways induced by drugs in *Trypanosoma cruzi*: an ultrastructural study. **Micron.** v. 40, p. 157-168, 2009.

MICHAELI, S. Spliced leader RNA silencing (SLS): a programmed cell death pathway in *Trypanosoma brucei* that is induced upon ER stress. **Parasit. Vectors**. v. 5, p. 107, 2012.

MICHELS, P. A. et al. Metabolic functions of glycosomes in trypanosomatids. **Biochim. Biophys. Acta.** v. 1763, p. 1463-1477, 2006.

MOFFETT, L. K.; STEFAN, H.; KENNETH, D. S. RNA editing: getting U into RNA. **Trends Biochem. Sci** v. 22, p. 162-166, 1997.

OCHSENREITER, T.; CIPRIANO, M.; HAJDUK, S. L. Alternative mRNA editing in trypanosomes is extensive and may contribute to mitochondrial protein diversity. **PLoS One**. v. 3, p. e1566, 2008.

ORGANIZAÇÃO MUNDIAL DA SAÚDE. Chagas disease (American trypanosomiasis). **Fact sheet N°340**. 2015. Disponível em: <http://www.who.int/mediacentre/factsheets/fs340/en/>. Acesso em: 30 dez. 2015.

PAGLIASSOTTI, M. J. Endoplasmic reticulum stress in nonalcoholic fatty liver disease. **Annu. Rev. Nutr.** v. 32, p. 17-33, 2012.

PALIWAL, S. K.; VERMA, A. N.; PALIWAL, S. Neglected disease – African Sleeping Sickness: Recent Synthetic and Modeling Advances. **Sci. Pharm**. v. 79, p. 389-428, 2011.

PEREIRA, M. G. et al. *Trypanosoma cruzi* epimastigotes are able to store and mobilize high amounts of cholesterol in reservosome lipid inclusions. **PLoS One**. v. 6, p. e22359, 2011.

PEREZ, C. J.; LYMBERY, A. J.; THOMPSON, R. C. Reactivation of Chagas Disease: Implications for Global Health. **Trends Parasitol.** v. 31, p.595-603, 2015.

PÉREZ-GORDONES, M. C. et al. Presence of a thapsigargin-sensitive calcium pump in *Trypanosoma evansi*: Immunological, physiological, molecular and structural evidences. **Exp. Parasitol.** v. 159, p. 107-117, 2015.

PIRAS, R.; PIRAS, M. M, Henriquez D. The effect of inhibitors of macromolecular biosynthesis on the in vitro infectivity and morphology of *Trypanosoma cruzi* trypomastigotes. **Mol. Biochem. Parasitol.** v. 6, p. 83-92, 1982.

RASHID, H. O. et al. ER stress: Autophagy induction, inhibition and selection. **Autophagy**. v. 2, p. 1956-1977, 2015.

RASSI JR., A.; RASSI, A.; MARCONDES de REZENDE, J. American trypanosomiasis (Chagas disease). **Infect. Dis. Clin. North Am.** v. 26, p. 275-291, 2012.

ROCHA, G. M. et al. The flagellar attachment zone of *Trypanosoma cruzi* epimastigote forms. **J. Struct. Biol.** v. 154, p. 89-99, 2006.

RODRIGUES, J. C.; SOUZA, W. de. Ultrastructural alterations in organelles of parasitic protozoa induced by different classes of metabolic inhibitors. **Curr. Pharm. Des.** v. 14, p. 925-938, 2008.

RODRIGUES, J. C.; GODINHO, J. L.; de SOUZA, W. Biology of human pathogenic trypanosomatids: epidemiology, lifecycle and ultrastructure. **Subcell. Biochem**. v. 74, p. 1-42, 2014.

RON, D.; WALTER, P. Signal integration in the endoplasmic reticulum unfolded protein response. **Nat. Rev. Mol. Biol.** v. 8, p. 519-29, 2007.

ROY, A. et al. Mitochondria-dependent reactive oxygen species-mediated programmed cell death induced by 3,3'-diindolylmethane through inhibition of F0F1-ATP synthase in unicellular protozoan parasite *Leishmania donovani*. **Mol. Pharmacol**. v. 74, p. 1292-1307, 2008.

SANDES, J. M. et al. *Trypanosoma cruzi* cell death induced by the Morita-Baylis-Hillman adduct 3-Hydroxy-2-methylene-3-(4-nitrophenylpropanenitrile). **PLoS One.** v. 9, p. e93936, 2014.

SANO, R.; REED, J. C. ER stress-induced cell death mechanisms. **Biochimica et Biophysica Acta**. v. 1833, p. 3460–3470, 2013.

SENFT, D.; RONAI, Z. A. UPR, autophagy, and mitochondria crosstalk underlies the ER stress response. **Trends Biochem. Sci.** v. 40, p. 141-148, 2015.

SHIELS, H.A.; GALLI, G. L. The sarcoplasmic reticulum and the evolution of the vertebrate heart. **Physiol.** v. 29, p. 456-69, 2014.

SMIRLIS, D. et al. Targeting essential pathways in trypanosomatids gives insights into protozoan mechanisms of cell death. **Parasit. Vectors**. v. 17, p. 107, 2010.

SOUTO-PADRÓN, T.; de SOUZA, W. The effect of tunicamycin and monensin on the association of *Trypanosoma cruzi* with resident macrophages. **Parasitol. Res.** v. 76, p. 98-106, 1989.

SOUZA, W. de. Electron microscopy of trypanosomes: A historical view. **Mem. Inst. Oswaldo Cruz**. v. 103, p. 313-325, 2008.

SOUZA, W. de; SANT'ANNA, C.; CUNHA-E-SILVA, N. L. Electron microscopy and cytochemistry analysis of the endocytic pathway of pathogenic protozoa. **Prog. Histochem. Cytochem.** v. 44, p. 67-124, 2009.

SOVOLYOVA, N. et al. Stressed to death: mechanisms of ER stress-induced cell death. **Biol. Chem.** v. 395, p. 1-13, 2014.

SZEGEZDI, E. et al. Mediators of endoplasmic reticulum stress-induced apoptosis. **EMBO Rep.** v. 7, p. 880-885, 2006.

TIENGWE, C.; BROWN, A. E.; BANGS, J. D. Unfolded Protein Response Pathways in Bloodstream-Form *Trypanosoma brucei*? **Eukaryot Cell.** v. 14, p. 1094-1101, 2015.

UCHIYAMA, Y. et al. Autophagy–physiology and pathophysiology. **Histochem. Cell. Biol.** v. 129, p.407–420, 2008.

VERCESI, A. E. et al. Thapsigargin causes Ca2+ release and collapse of the membrane potential of *Trypanosoma brucei* mitochondria in situ and of isolated rat liver mitochondria. **J. Biol. Chem**. v. 268, p. 8564-8568, 1993.

WALTER, P.; RON, D. The unfolded protein response: from stress pathway to homeostatic regulation. **Science**. v. 334, p. 1081-1086, 2011.

WATANABE, M. M.; LAURINDO, F. R.; FERNANDES, D. C. Methods of measuring protein disulfide isomerase activity: a critical overview. **Front. Chem.** v. 2, p. e00073, 2014.

ZINGALES, B. et al. Correlation of tunicamycin-sensitive surface glycoproteins from *Trypanosoma cruzi* with parasite interiorization into mammalian cells. **Mol. Biochem. Parasitol**. v. 16, p. 21-34, 1985.

ZWIERZYNSKI, T. A.; BUCK, G. A. RNA-protein complexes mediate in vitro capping of the spliced-leader primary transcript and U-RNAs in *Trypanosoma cruzi*. **Proc. Natl. Acad. Sci.** v. 88, p. 5626-5630, 1991.

4 ARTIGOS

4.1 Artigo 1 - The effects of the endoplasmic reticulum stressor agent dithiothreitol (DTT) on *Trypanosoma cruzi*.

Manuscrito a ser submetido na revista indexada *Scientific Reports*, Qualis Capes A1 (Ciências Biológicas I), JCR 5,578, formatado segundo suas regras. Neste artigo avaliamos o efeito do ditiotreitol, um composto comumente utilizado como estressor do retículo endoplasmático em células eucarióticas, sobre a viabilidade de formas epimastigotas de *T. cruzi*, a expressão de proteínas envolvidas na resposta ao estresse do RE, bem como o perfil de morte celular programada induzido.

The effects of the endoplasmic reticulum stressor agent dithiothreitol (DTT) on *Trypanosoma cruzi*.

[1,2,*]Jana Messias Sandes, [3]Danielle Maria Nascimento Moura, [2]Moana Divina da Silva Santiago, [2]Gustavo Barbosa de Lima, [1]Paulo Euzébio Cabral Filho, [2]Suênia da Cunha Gonçalves de Albuquerque, [2]Milena de Paiva Cavalcanti, [2,+]Regina Célia Bressan Queiroz Figueiredo and [1,+]Adriana Fontes.

[1] Universidade Federal de Pernambuco, Departamento de Biofísica e Radiobiologia, Recife 50670-901, Pernambuco, Brazil.
[2] Centro de Pesquisas Aggeu Magalhães/FIOCRUZ-PE, Departamento de Microbiologia, Recife. 50670-420, Pernambuco, Brazil.
[3] Centro de Pesquisas Aggeu Magalhães, Departamento de Imunologia, Recife, 50670-420, Brazil.

[*] Corresponding author
janasandes@gmail.com
[+] These authors contribute equally to this work

ABSTRACT

The endoplasmic reticulum (ER) is a vital organelle for all eukaryotic cells, being responsible for lipid and protein synthesis, folding and secretion. Imbalance in the inner environment of ER can lead to an ER stress condition, which can trigger the Unfolded Protein Response (UPR). Although ER stress has a decisive role in mammalian cells survival, studies concerning this organelle in *Trypanosoma cruzi*, the etiological agent of Chagas' disease, are still inexistent. This work aimed to determine the effects of dithiothreitol (DTT), a well-known ER stressor, in *T. cruzi* epimastigote forms. The parasites were treated with different concentrations of DTT (2 – 16 mM) from 24 to 96 h. DTT treatment inhibited the growth of *T. cruzi* in a dose dependent manner. Recovery experiments demonstrated that cells treated with 16 mM DTT for 60 - 240 min. are able to restore the culture growth when the drug was removed. Western blotting analysis showed that DTT treatment did not alter the expression of of the chaperone BiP (binding protein). Moreover, in general RT-qPCR showed a reduction of BiP and CRT mRNA levels. The persistent ER stress caused drastic morphological and physiological changes compatible with cell death by late apoptosis/necrosis.

INTRODUCTION

The endoplasmic reticulum (ER) is a multifunctional organelle involved in many physiological processes, such as the lipid and protein synthesis, folding and secretion of proteins, drug metabolism, vesicle trafficking, and calcium homeostasis[1,2]. In order to perform the correct folding, assembling and glycosylation of proteins the inner environment of ER must be precisely controlled. A number of chaperones, such as BiP (binding protein), calnexin, calreticulin and a family of protein disulfide isomerases plays an essential role in quality control by assisting polypeptide folding, translocation and assembly of newly made proteins[3]. Polypeptides that fail to acquire proper conformation or incorporate into functional complexes are retained and addressed for degradation by a process termed ER-associated degradation (ERAD)[1,4]. It is well known that perturbations on protein folding homeostasis in the ER cause accumulation of misfolded or unfolded polypeptides, which triggers the Unfolded Protein Response (UPR). The UPR is well characterized in yeast and higher eukaryotic cells and represents a reaction to a physiological or pathological imbalance in the ER[5-7]. Three ER-resident transmembrane proteins, inositol-requiring enzyme (IRE1), PKR-like ER kinase (PERK) and the activating transcription factor 6 (ATF6) have been identified as sensors of stress in ER of mammalian cells[2]. The activation of UPR leads, as an immediate reaction, to the inhibition of general translation and the upregulation of ER molecular chaperones, as BiP. Macroautophagy (ER-phagy) is also activated to eliminate damaged ER and abnormal protein aggregates throughout the lysosomal pathway[8]. Overall, these mechanisms reduce the influx of proteins into the ER to allow adaptive and repair mechanisms. However, the persistent stress of ER can lead to prolonged UPR response, which ultimately activates the programmed cell death (PCD)[9].

Trypanosomatids such as *Trypanosoma brucei*, *Leishmania* and *Trypanosoma cruzi* are unicellular protozoans of medical and economical relevance because they are the etiologic agents of severe infectious diseases in humans as well as livestock[10]. As in other eukaryotic cells, the ER has fundamental importance for survival of these parasites. Studies using ER stressors as tunicamycin (TM), thapsigargin (TG) and dithiothreitol (DTT) have demonstrated that the ER stress response in these parasites differs from those found in mammalian cells and yeast[11-13]. In trypanosomatids, for instance, the ER stress sensors IRE1 and ATF6 are lacking. Furthermore, at least for *T. brucei*, is hypothesized that a post-transcriptional program, the spliced leader silencing (SLS) is elicited in response to ER stress, which shuts off the *trans*-splicing and consequently the production of all mRNAs [14]. These singular features of ER

stress response in trypanosomatids make them an interesting model from a cell biology point of view[15,16.]

Trypanosoma cruzi is a trypanosomatid protozoan that causes Chagas' disease in Latin America, a poverty-related neglected illness, responsible for high rates of mortality and morbidity[17]. In this parasite both rough and smooth ER profiles are observed[18]. However, aspects of protein processing and the physiology of ER in *T. cruzi* are poorly understood. In this study we aimed to investigate the effects of DTT, a compound commonly used as stressor of ER in mammalian cells, on the viability, morphology and chaperones expression in epimastigote forms of *T. cruzi*. We expected to improve not only the knowledge on cell biology of the parasite concerning the role of ER, but also lead to further identification of useful specific targets on this organelle that can be able to activate a persistent ER stress, leading to parasite death.

RESULTS

The effects of DTT on growth and viability of *T. cruzi*.

To analyse the effects of ER stressor on the viability of *T. cruzi* epimastigotes, the parasites were treated with 2 - 16 mM DTT for up to 96 h. The DTT treatment inhibited the growth of parasites in a dose-dependent manner, as compared with non-treated cells (Fig. 1A). After 96 h of incubation with 16 mM DTT, the cell growth was almost completely inhibited. In order to verify whether the growth inhibition induced by DTT could be reverted, epimastigotes were firstly exposed to 16 mM DTT for different times of incubation (60 - 240 min). Then, the drug was washed out and the cell growth monitored for up to 96 h. Our results showed an inversed correlation between the time of exposure to DTT and the ability of parasites to resume cell growth. However, in all conditions evaluated, the growth of treated cells was always lower than control (Fig. 1B).

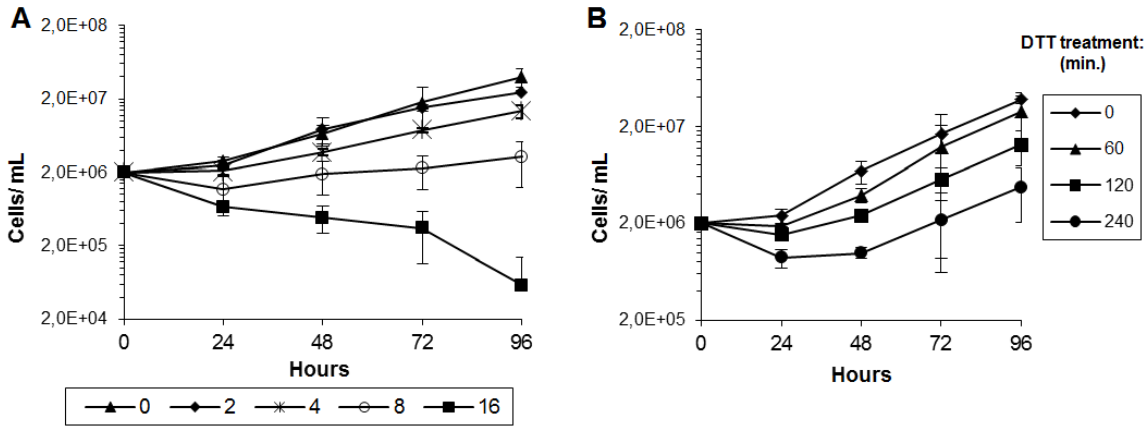

Figure 1. Effect of DTT on the growth of *T. cruzi*.
(A) Growth curve in the presence or absence of DTT (2 – 16 mM). **(B)** Growth recovery curve after exposure to 16 mM DTT. Each point corresponds to the mean ± standard deviation of at least two independent experiments in triplicate in (A) or duplicate (B).

The effects of DTT treatment on BiP and CRT expression

To determine whether DTT can induce an UPR-like response in *T. cruzi*, the epimastigote forms were submitted to DTT treatment for 24 h at 4 or 8 mM, and analysed for BiP expression, an ER resident chaperone that is usually upregulated under ER stress during the UPR. The Western blotting analysis (Fig. 2A and 2B) showed no major differences in BiP expression neither in cells treated with 4 mM or 8 mM of DTT when compared with non-

treated cells, with exception of a slight increase in BiP expression only at the point of 24 h, in both conditions.

We also investigated the expression of BiP and calreticulin (CRT) chaperones at mRNA level by quantitative real-time RT-PCR analysis (RT-qPCR) (Fig. 2C and 2D). The RT-qPCR analysis showed no significant change in the expression of the CRT mRNA in cells treated with 4 mM DTT for 2 h. For other incubation times and concentrations tested there was a significant reduction in the expression of both chaperones in dose and time dependent manner. The treatment with 8 mM DTT for 4 h resulted in a 3.3-fold decrease in the BiP mRNA level relative to the control (non-treated). At this experimental condition, the decrease of the level of CRT expression was comparatively higher to those found for BiP (5.27-fold). These results suggested that DTT treatment did not induce a classical UPR response at short-term treatment (2 – 24 h) in epimastigotes of *T. cruzi*.

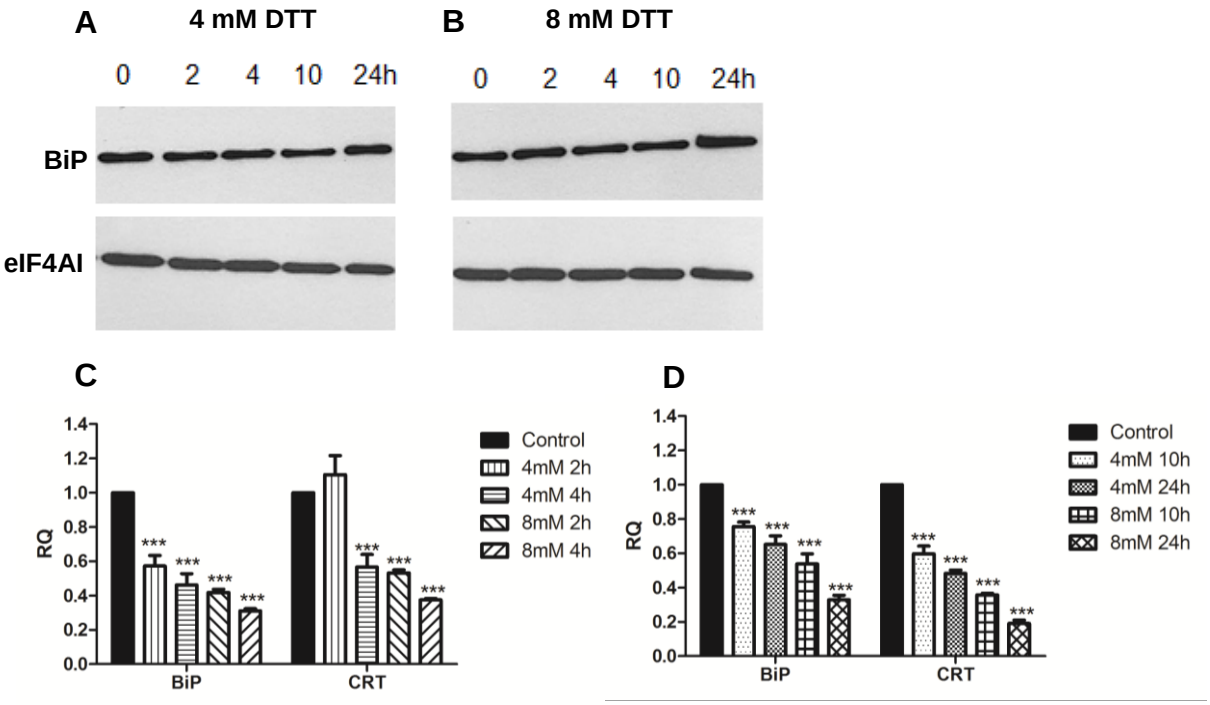

Figure 2. Western blotting and RT-qPCR analysis of chaperone expression.
(A-B) Western blotting analysis of BiP expression during the treatment with 4 mM DTT **(A)** or 8 mM DTT **(B)** on *T. cruzi* epimastigote forms from 0 to 24 h. EIF4AI, a protein that is expressed constitutively, was used as loading control. **(C - D)** RT-qPCR analysis of epimastigotes treated with 4 and 8 mM DTT for 2 – 4 h **(C)**, or 10 – 24 h **(D)**. The BiP and CRT signals were normalized by 18S rRNA levels and expressed as a ratio to the control treatment values. RQ: Relative quantification.
*** p< 0.0001 compared to control.

The effects of DTT on *T. cruzi* ultrastructure

Because the treatment with DTT did not induce upregulation of chaperones expression levels, but led to significant inhibition on cell growth and decrease of mRNA for CRT and BiP, we further investigated the effects of long-term treatment with DTT on the ultrastructure of *T. cruzi* epimastigote forms. The parasites were exposed to different concentrations of DTT for 72 hours and processed as routine for scanning (SEM) and transmission (TEM) electron microscopy. SEM analysis showed that untreated epimastigote forms displayed typical elongated morphology; an anterior flagellum and an intact smooth plasma membrane (Fig. 3A and 3B). This profile changed considerably in cells treated with DTT (Fig. 3C – H). Although the severity of cell morphology alterations was dependent on the concentration of DTT used, the most prominent effects of this compound were the shrinkage and rounding of parasite cell body and shortening of parasite flagellum. As a consequence of whole-cell shrinkage, the plasma membrane assumed a corrugated aspect. At 16 mM DTT, only few partially elongated parasites could be observed (Fig. 3G and 3H).

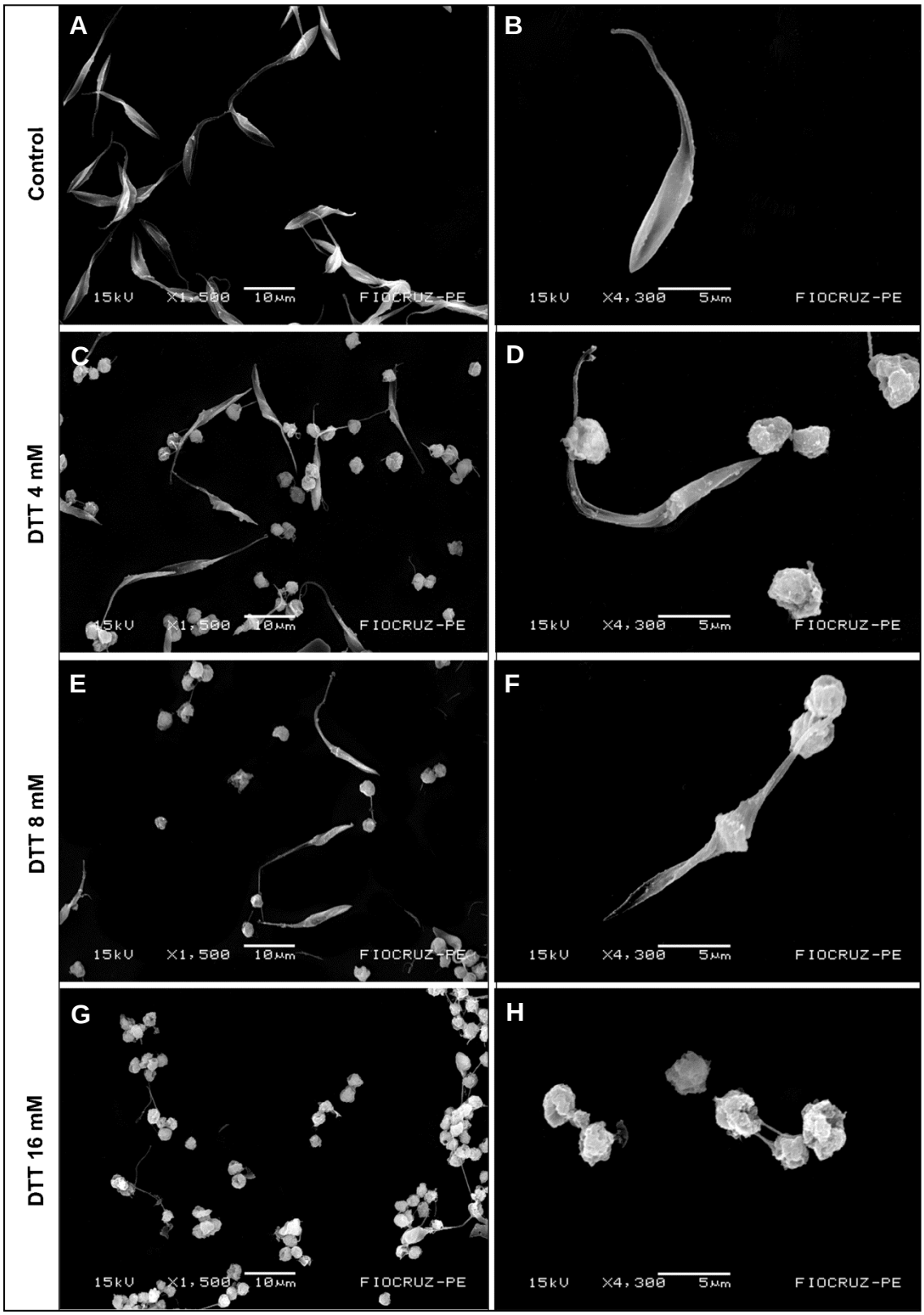

Figure 3. SEM of control and DTT treated cells.
(**A-B**) Control *T. cruzi* epimastigotes exhibiting elongated cell body, anterior flagellum and plasma membrane with no apparent damage. (**C-H**) DTT-treated cells (4 – 16 mM) exhibiting a dose-dependent alteration on cell morphology, with rounding of the cell body, and decrease in cell volume and in the flagellum length.

The ultrastructural analysis by TEM showed control epimastigote forms presenting typical morphology(Fig. 4A and 4B). The centrally located nucleus showed a well-preserved heterochromatin with evident nucleolus. A single mitochondrion just underneath the plasma membrane could be seen running along the cell body of parasite. Endoplasmic reticulum profiles could be observed throughout the cytoplasm. Few ultrastructural alterations could be detected in parasites treated with 4 mM of DTT (Fig. 4C and 4D). An increased number of vesicles and tubular processes could be observed in both sides of Golgi complex (Fig. 4C). In some cells this organelle was partially disorganized. Regardless the concentration of DTT tested the mitochondrion was the most affected organelle in treated parasites. A drastic swelling and disorganization of this structure can be observed even at low concentrations of DTT. An unusual organization of mitochondrial cristae, which assume a lamellar appearance, was often observed in parasites treated with 16 mM of DTT (Fig. 4G). These results suggested that the mitochondrion is a major target of DTT action. In addition to above mentioned changes, cells treated with 8 mM DTT presented an unexpected increase of lipid droplets in the cytoplasm (Fig. 4E) and membrane-derived vesicles resembling exosomes budding from plasma membrane (Fig. 4F). At the highest concentration analysed (16 mM) the cells were drastically affected with loss of cytoplasmic content and the presence of several ER profiles involving portions of cytoplasm and partially degraded organelles (Fig. 4H), which is indicative of autophagy.

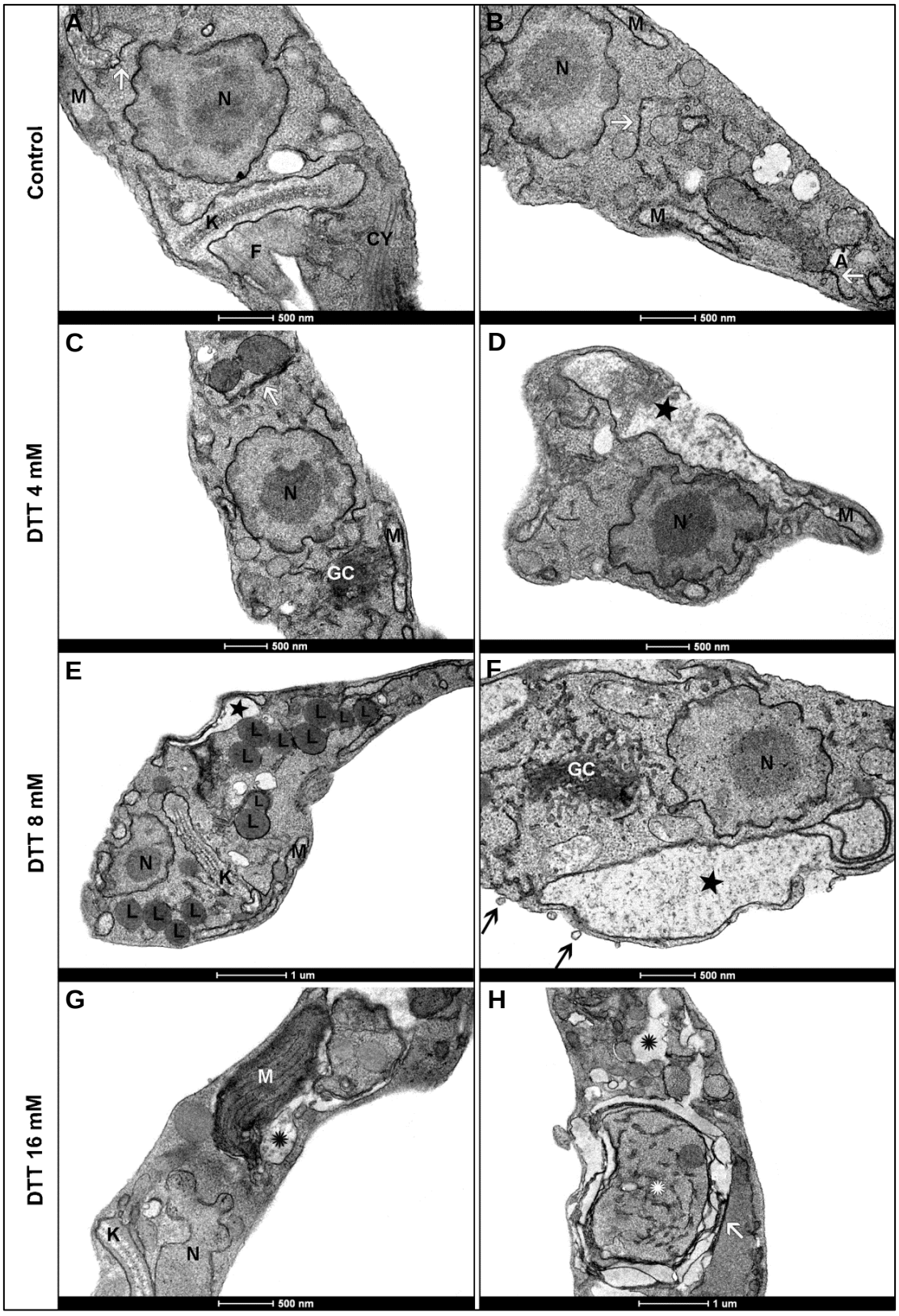

Figure 4. DTT effect on the ultrastructure of *T. cruzi*.
(**A-B**)Control cells (no treatment) showing organelles with characteristic morphology. (**C-H**) Treated cells (4 - 16 mM) for 72 h showing several ultrastructural alterations such as dismantled Golgi complex (GC) (**C**), mitochondrion swelling and eventual disruption of the plasma membrane (black star) (**D-F**). Increased lipid droplets (L) in the cytoplasm (**E**) and the presence of small vesicles

budding from plasma membrane (black arrow) (**F**) were usually found in the cytoplasm of treated cells, mainly at high concentrations of DTT. Electron lucent spaces (**G-H**) and the appearance of ER profiles enclosing bulk of cytoplasm and partially degraded organelles (**H**) were also found (white asterisk). ER (white arrow), nucleus (N), mitochondrion (M), kinetoplast (K), acidocalcisome (A) and cytostome (CY).

Cell death induced by DTT

To assess whether DTT treatment triggers programed cell death in the parasites we used the fluorescent probes Annexin V/Alexa 488 (AV), which binds to externalized phosphatidylserine during early apoptosis and propidium iodide (PI), which binds to nucleic acid in cells where the membrane permeability was lost, a late apoptosis/ necrosis phenotype[19]. Flow cytometry demonstrated that more than 90% of the control cells (Fig. 5A) and 80% of the cells treated with 2 mM of DTT (Fig. 5B) for 72 h were negative for both probes (AV^-/ PI^-). However the treatment with DTT at 4 to 16 mM (Fig. 5C and 5D) resulted in increased cell death, as demonstrated by the appearance of AV^+/PI^+ (late apoptosis) and AV^-/PI^+ (necrotic cells) phenotypes. At 16 mM, 92.1% of total cell population were double labeled with annexin V and PI (Fig. 5E). The confocal microscopy analysis corroborated the data obtained by flow cytometry (Fig. 6).

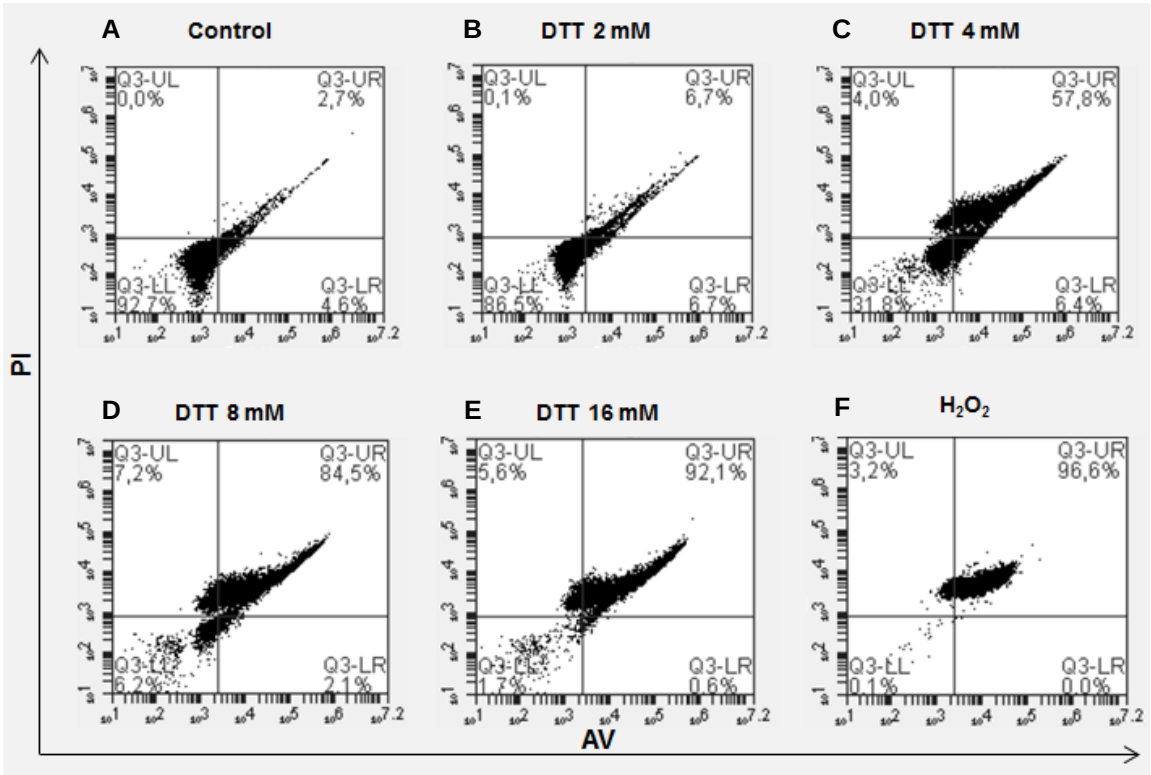

Figure 5. Annexin V(AV)/ propidium iodide (PI) labeling analysis by flow cytometry.
Labeling analysis of AV/ PI on *T. cruzi* control cells (no treatment) (**A**) or treated with DTT 2 – 16 mM (**B-E**) for 72 h. The upper left (UL) quadrant represents stained cells only with PI and the lower right (LR) quadrant the cells marked only with AV. The upper right (UR) and lower left (LL) quadrants represent, respectively, the double positive and the double negative cells for both markers. The dot plots are representative of duplicate experiments with 20,000 events per sample.

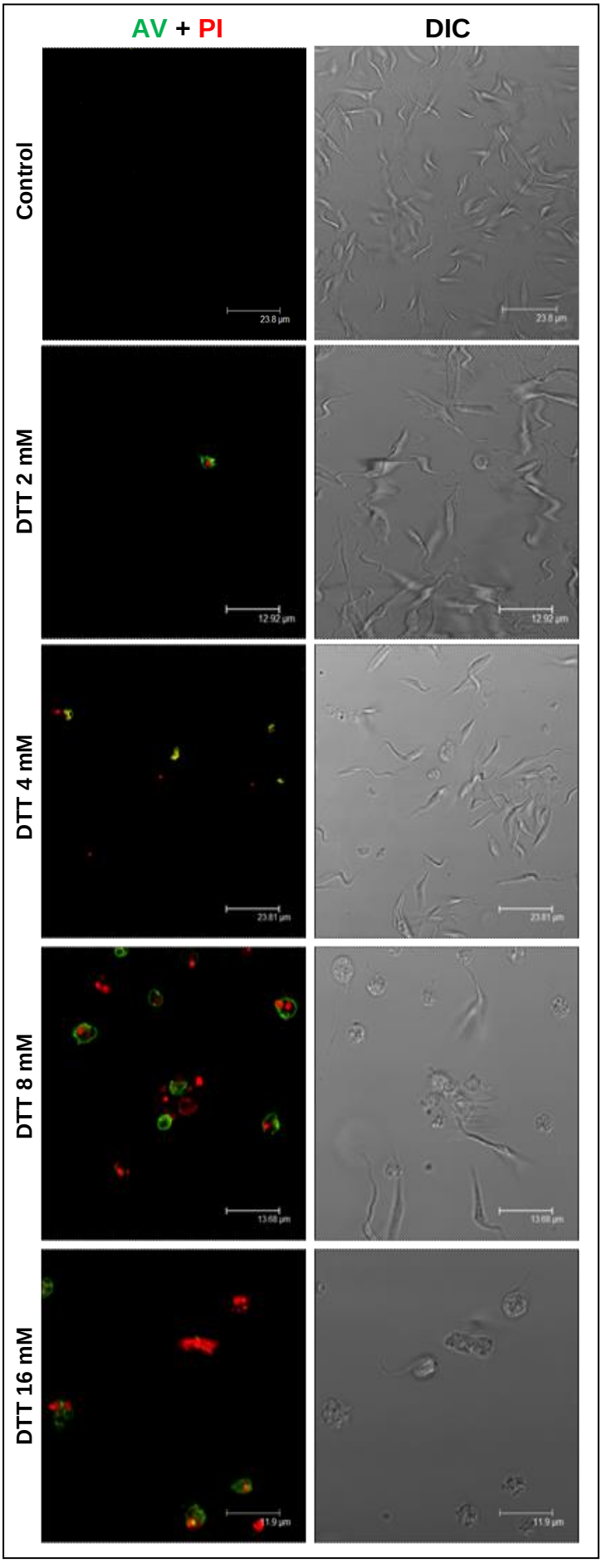
AV + PI
DIC
Control
DTT 2 mM
DTT 4 mM
DTT 8 mM
DTT 16 mM

Figure 6. Annexin V/ propidium iodide labeling analysis by confocal microscopy.
Analysis by confocal laser scanning microscopy of AV (green)/ PI (red) labeling of *T. cruzi* epimastigote cells control or treated with 2 -16 mM in the incubation period of 72 h. The phenotypes suggesting late apoptosis (AV^+/ PI^+) and/or necrosis (AV^- / PI^+) were frequently observed in the cells treated with 8 and 16 mM, confirming the data obtained by flow cytometry. Morphological changes such as rounded cell body were also observed by differential interference contrast (DIC, right column) from the above-mentioned concentrations.

Because DTT treatment induced alterations on the mitochondrion morphology, we investigated whether the DTT-induced cell death is related to changes in the mitochondrial membrane potential ($\triangle\psi m$). For this, epimastigotes were labeled with rhodamine 123 (Rho 123), a cationic fluorochrome that is attracted by the potential of mitochondrial membrane of metabolically active cells[20]. As expected, the mitochondrion of control cells emitted intense bright green fluorescence (Fig. 7). However, in treated cells there was a gradual decrease in fluorescence intensity with little or no labeling observed in cells treated with 8 or 16 mM of DTT.

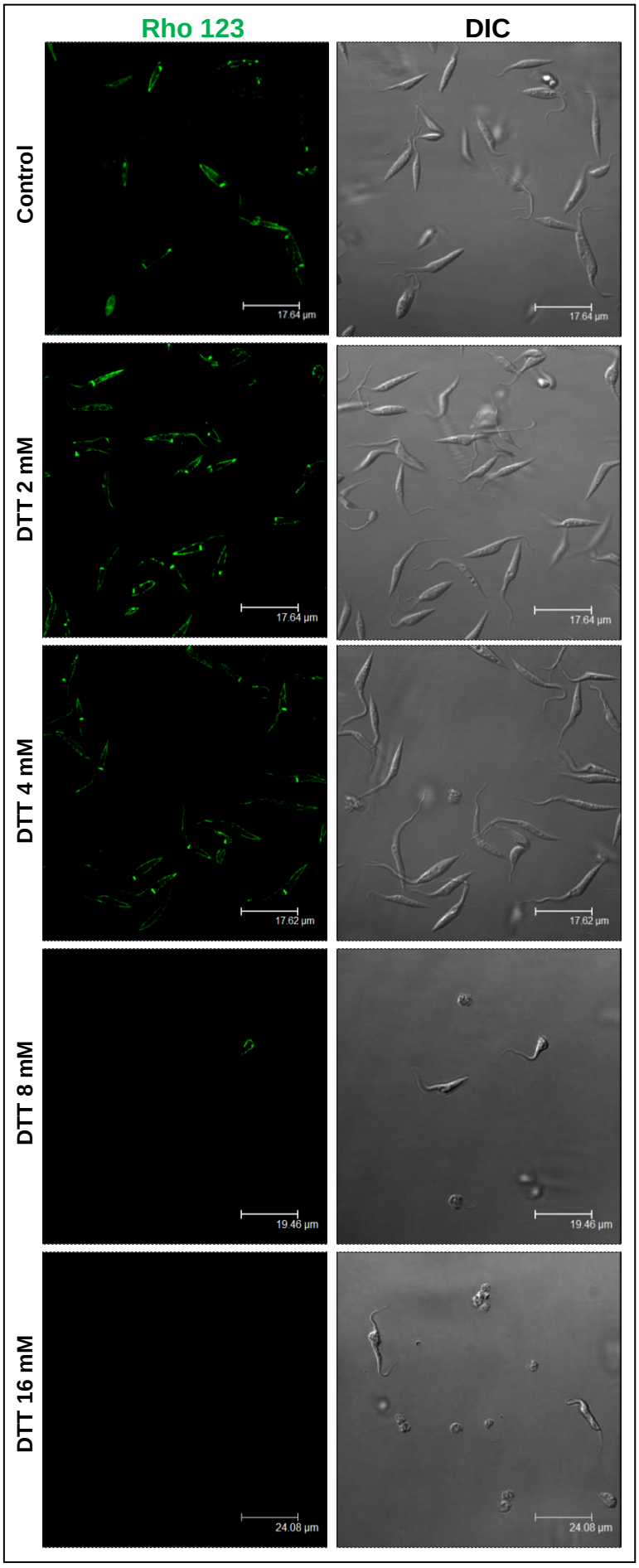
Rho 123
DIC
Control
DTT 2 mM
DTT 4 mM
DTT 8 mM
DTT 16 mM
17.64 µm
17.64 µm
17.64 µm
17.64 µm
17.62 µm
17.62 µm
19.46 µm
19.46 µm
24.08 µm
24.08 µm

Figure 7. Rhodamine 123 staining analysis by confocal microscopy.
Epimastigotes forms of *T. cruzi* treated or not with 2 - 16 mM DTT for 72 h. It is possible to notice the gradual decrease in the fluorescence intensity of the treated cells, with almost no stained cells in cultures treated with 8 and 16 mM. DIC, differential interference contrast.

The flow cytometry data were consistent with those obtained by confocal microscopy, showing a gradual depolarization of the mitochondrial membrane as indicated by a dose-dependent reducing values of the index of variation (IV) after the following DTT treatments: 2 mM (IV= -0.10), 4 mM (IV= -0.40), 8 mM (IV= -0.62) and 16 mM (IV= -0.65). These results showed that DTT induced physiological changes on the parasite mitochondrion that may activate intrinsic pathways of cell death.

We also examined whether the changes in mitochondrial membrane potential was due to an increased production of superoxide radicals by mitochondria by labeling treated and control with MitoSOX™, a specific permeable fluorochrome used to detect reactive oxygen species (ROS) in this organelle[21]. Flow cytometric data showed that treatment with DTT gradually increases ROS production by the parasite mitochondrion (Fig. 8B-E), in a dose dependent manner when compared to control cells, which presents only a basal production of mitochondrial superoxide (2.2%) (Fig. 8A). Parasite cultures treated with 9% hydrogen peroxide, used as positive control, showed about 98% of cell population positive for MitoSOX (Fig. 8F).

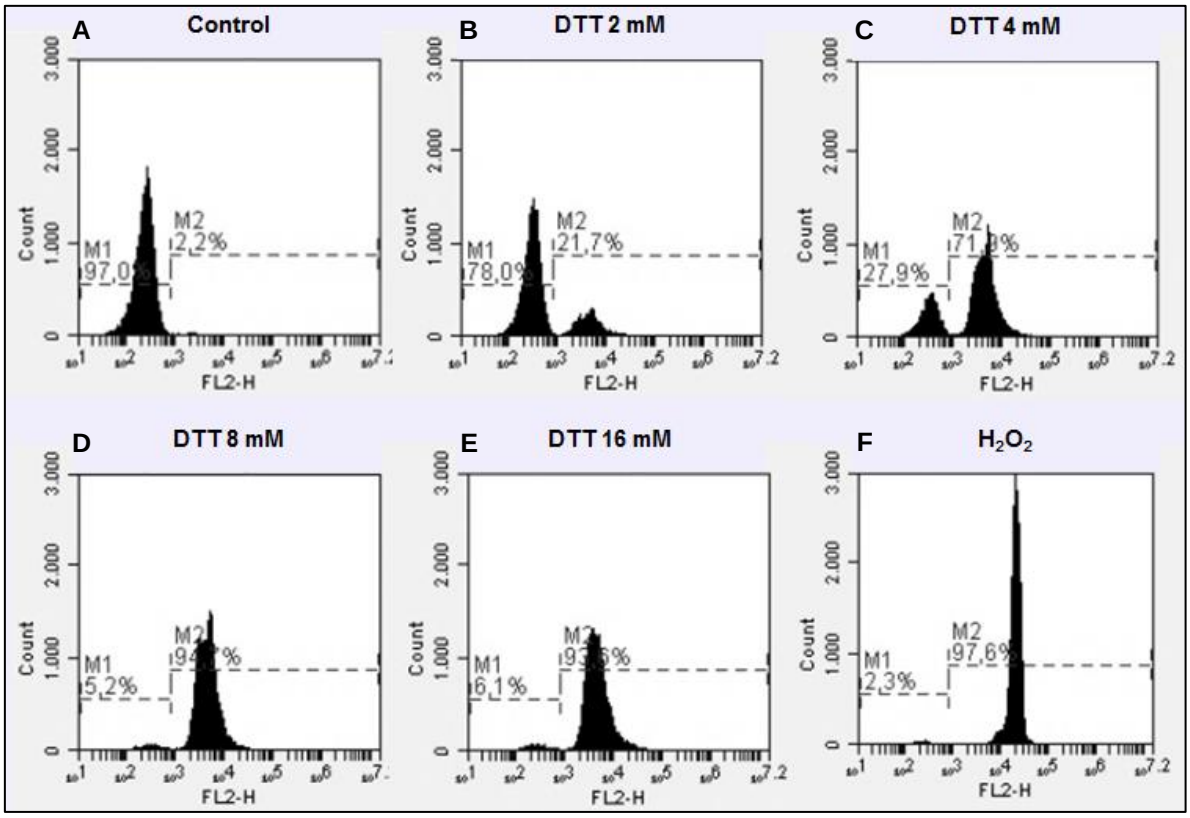

Figure 8. MitoSOX labeling analysis by flow cytometry.
Control (**A**) and treated (**B-E**) *T. cruzi* epimastigotes (2 – 16 mM DTT) at 72 h. Hydrogen peroxide (H_2O_2) 9% (**F**) was used as the positive control. The region delimited by the M1 marker corresponds to the percentage of negative cells for MitoSOX while the M2 region correspond to the percentage of positive labeled cells. The analysis was done with 20,000 events per sample. FL2-H = MitoSOX fluorescence intensity.

DISCUSSION

The unfolded protein response (UPR) is a process by which eukaryotic cell cope with the stress of unfolded secretory proteins in the endoplasmic reticulum[22.] DTT is a well-known ER stressor agent that inhibits the formation of protein disulfide bonds preventing the protein to reach its correct tertiary and quaternary structure[23,24]. The ability of DTT to activate the ER stress pathway has been examined in higher eukaryotes, fungus and more recently in trypanosomatid species as *Leishmania* and *T. brucei*[11-13,22]. This study investigated for the first time the effects of DTT on *Trypanosoma cruzi*, the etiological agent of Chagas' disease, in attempt to improve the knowledge about the physiology of endoplasmic reticulum in this parasite.

Our results showed that DTT inhibited the growth of epimastigote forms of *T. cruzi* in a dose dependent manner. However, *T. cruzi* showed to be more resistant to DTT-induced stress than other trypanosomatids. In *T. brucei* bloodstream forms (BSF), DTT treatment at concentrations that invoke UPR in other eukaryotic cells (1 – 10 mM) led to rapid cell death in less than 24 h, even at the lowest concentration (1 mM)[11]. Tiwngwe *et al* [22] using the same evolutive forms of *T. brucei*, argued that 1 mM DTT was enough to induce 100 % of cell death after 4 h of incubation. On the other hand, Gosline and co-works[13] demonstrated that *Leishmania donovani* promastigotes are not able to grow at 4 mM of DTT. In contrast, in our work, the growth of *T. cruzi* was severely affected only during incubation with DTT at 8mM or higher, leading to cell death at 16 mM after 96 h. Furthermore, *T. cruzi* were also able to recover growth after short-term exposition to DTT at 16 mM, whereas *T. brucei*, fail to retrieve the cell growth after 120 min of exposure at 4mM DTT[12]. The existing difference in the susceptibility of different species of trypanosomatids to DTT may be partially due to the difficulty in establish the correct concentration and time of incubation able to elicit the endoplasmic reticulum stress without triggering programed cell death.

BiP is one of the major chaperones of the ER participating in many functions such as importation of proteins to the ER, folding of newly synthesized proteins, conduction of misfolded proteins for degradation, UPR regulation and Ca^{2+} homeostasis[25]. This protein is highly conserved between the species of *T. cruzi* and *T. brucei* and studies with mammals and plants cells showed that BiP is regulated positively by transcription during the UPR response[26]. In our work, however, we failed to demonstrate a significant change in the expression of this protein in *T. cruzi* treated with DTT. Previous work by Gosline *et al* [13]did not observe any change on BiP expression in *L. donovani* promastigotes treated with 1 mM DTT for 8 h either. Koumandou *et al*[11] and Tiengwe *et al*[22] also failed to demonstrate any

alteration in BiP expression in bloodstream forms of *T. brucei* treated with 1 mM or 0.5 mM DTT for up 4 h, respectively. Conversely, studies made by Goldshmidt *et al*[12] working on procyclic forms of *T. brucei* showed that DTT treatment at the same concentration utilized in our study (4 mM) for 2 or 4 h resulted in increased levels of BiP expression (protein levels).

Calreticulin (CRT), as well as BiP, is an abundant ER resident protein and plays a central role on the glycoprotein folding quality control system, being also one of the main ER calcium buffers[27]. Both chaperones act together in *T. cruzi* for proper folding of glycosylated proteins in the ER[28]. Our RT-qPCR analysis showed a dose dependent decrease in the mRNA of both chaperones in cells submitted to DTT treatment, contradicting the steady levels of BiP observed by Western blotting. Many reports showed that the steady state of mRNA and protein levels in *T. cruzi*, as in others trypanosomatids, are not coordinately regulated[22]. The polycistronic nature of kinetoplastid transcription means that the amount of mRNA is almost always determined post-transcriptionally by the rate of mRNA degradation and the expression of protein by the rates of translation initiation, elongation, and protein turnover[29]. Therefore, it seems to us that, despite the lower availability of BiP and CRT mRNAs, DTT-treated cells are able to maintain the steady state of chaperones, probably by enhancing the translation process of these proteins, to circumvent the stress induced by DTT treatment.

As previously mentioned, the response to DTT treatment in *T. brucei* procyclics was once the only experimental link between an UPR-like response and the SLS pathway in trypanosomes, having as characteristics the increase in BiP levels and reduction of SL transcripts[12]. However more recent data has challenged these findings as being part of a general response since no major changes in BiP expression or other chaperones have been detected during DTT treatment in bloodstream forms[11,22] or other species of trypanosomatids[13]. In our work, we did not attempt to measure SL transcripts (or tSNAP42 upregulation), and so the existence of a similar SLS response in *T. cruzi* has yet to be investigated.

Although DTT treatment did not elicit an UPR-like response in *T. cruzi* epimastigote forms, this compound induced a strong inhibition on cell growth. This fact prompts us to investigate the changes in morphology and physiology of the parasites during persistent ER stress induced by DTT treatment. Our results showed that DTT altered drastically the ultrastructure of *T. cruzi*. The parasite mitochondrion seems to be the major target of DTT action. The morphological changes observed in this organelle are followed by a decrease in the mitochondrial membrane potential and increased production of mitochondrial superoxide. The mitochondria have fundamental importance for cell survival being directly related to the

activation of cell death signalling cascades in response to cell detrimental stimulus[30]. Several studies have demonstrated the close spatial and physiological association between the mitochondria and ER. In this regard, an imbalance in the ER could have a severe impact on the mitochondria physiology, allowing pro survival adaptations or initiation of programmed cell death depending on the duration and/or intensity of ER stress[31].

Similarly, it is reasonable to think that any disturbance in the mitochondria can also elicit an ER stress response in attempt to re-establish cellular homeostasis. Another common morphological feature of DTT treated cells was the appearance of lipid droplets (LD) dispersed in the cytoplasm. Accumulation of LD in presence of ER stress has been reported in other eukaryotic cells such as fungi[32], plants[33] and animals[34]. Kim *et al* [33] demonstrated that the treatment of algae *Chlamydomonas reinhardtii* and *Chlorella vulgaris* with Brefeldin A (BFA), a chemical inducer of ER stress, lead to rapid accumulation of neutral lipid droplets in the algae cytoplasm. These authors suggested that LD formation might be a resistance mechanism against BFA toxicity. On the other hand, the LD could protect exposed hydrophobic residues of unfolded proteins upon ER stress from aggregation in the cytoplasm, which can be extremely toxic to cells[33].

Our TEM analysis also showed that the treatment of cell with DTT induced morphological changes with features of non-selective autophagy. ER membrane profiles encircling bulks of cytoplasm containing organelles were seen mainly at high concentrations of the drug. Autophagy is a highly dynamic multi-step process by which cells engulf organelles and/or cytoplasm to be degraded into double membrane structures called autophagosomes[35]. In trypanosomatids, autophagy plays an important role in parasite differentiation and development in the host. Furthermore, several compounds have proven to cause ultrastructural changes in these parasites compatible with autophagy[36]. In this regard, the presence of autophagic compartments in cells treated with DTT can serve as a survival mechanism to circumvent the deleterious effects of DTT. However, as the stressor stimulus persists the treated parasites can evolve to the programed cell death by apoptosis or necrosis. Consistently our results showed an increase rate of cell double labeled with Annexin V/PI, an indicative of late apoptosis or necrosis, what was previously reported in *T. cruzi* epimastigotes[37].

In conclusion, our results showed that DTT is not able to induce classical UPR response in epimastigote forms of *T. cruzi* at any time and concentration tested as observed by the analysis of BiP and CRT chaperones expression. However, this parasite is able to efficiently mount a defence response to DTT injury, by triggering autophagic process and

increasing the LD in the cytoplasm. Nonetheless, when the mechanisms of cell defence are not enough robust to face the oxidative stress imposed by DTT treatment; the energetic homeostasis of this mitochondrion is ruptured leading to parasite death by late apoptosis or necrosis.

METHODS

Parasites - All experiments were carried out using *T. cruzi* epimastigote forms (Dm28c) from axenic cultures, maintained in liver infusion tryptose (LIT) medium pH 7,4 supplemented with 10% Fetal Bovine Serum (FBS) at 28 °C and harvested during the exponential phase of growth.

Drugs - Dithiothreitol (DTT) (Sigma-Aldrich, St Louis, USA), was dissolved in ultrapure water at a concentration of 1 M and then immediately diluted in LIT medium for experiments (2 – 16 mM).

Viability Assay - Epimastigotes in the log phase of growth ($2x10^6$ parasites/mL) were incubated at 28 °C in LIT medium supplemented with 10% FBS in the absence or presence of different concentrations of DTT for up to 96 h. The inhibitory effect on cell growth was then estimated by daily cell counting using a Neubauer chamber. For recovery experiments, parasites were exposed to 16 mM DTT by different time periods (60 - 240 min.). After incubation, the drug was washed out, and daily cell countings were performed as described above.

Western blotting analysis - Whole cell extracts were resolved by SDS-PAGE 15%, transferred to PVDF membranes (Millipore) and probed with *T. brucei* anti-BiP (diluted 1:40,000), kindly provided by Prof. James Bangs (University of Wisconsin- Madison, Madison, USA), or anti-eIF4AI (diluted 1:5,000), kindly provided by Dr. Osvaldo de Melo-Neto (Aggeu Magalhães Research Center, Recife, Brazil) as loading control. The bound antibodies were detected with goat anti-rabbit IgG coupled to horseradish peroxidase (Jackson Immunoresearch), and were visualized by chemioluminescence.

Quantitative real-time RT-PCR - Multiple alignments of BiP and calreticulin sequences of *Trypanosoma cruzi* available in GenBank were analyzed using Mega 6.06.[38]. Primers were

then designed with the PRIMER BLAST software (http://www.ncbi.nlm.nih.gov/tools/primer-blast), using the criteria described elsewhere[39], based on the following sequences: L23420.1 (TcBiP), and XM_799098.1 (TcCRT). The specific primers sequences selected were (5' to 3'): TcBIP-F (AAGCAGTCGAAGAAGGGGTG) and TcBIP-R (GAAAAGGCAACCAGAGCAGC); TcCRT-F (GCTCGAAGAAGACTGGAGCC) and TcCRT-R (GGATCATTGCGGGTTCGTTG). Amplification efficiency was determined from the slope of the calibration curve for each primer using 1:10 serial dilution of genomic *T. cruzi* DNA (1 ng/µL – 1 fg/µL). Total RNA was extracted from treated and control epimastigote forms (c. a. 1×10^8 cells) using the RNeasy Mini kit (Qiagen, Hilden, Germany), according to the manufacturer's instructions, with an additional DNase (Invitrogen, Carlsbad, CA, USA) digestion step. RNA was converted to cDNA with reverse transcriptase and random primers of TaqMan Reverse Transcription Reagents (Invitrogen), in a final volume of 40 µL. Quantitative real-time RT-PCR was performed using Power SYBR Green PCR Master Mix (Applied Biosystems, Foster City, USA) with reaction mixture containing c. a. 100 ng of template cDNA and 3 µM of primers in 25 µL of final volume. Amplifications were carried out in triplicate, in two independent experiments and *T. cruzi* 18S rRNA (Tc18S-F: TTACGTCCCTGCCATTTGTA and Tc18S-R: TTCGGTCAAGTGAAGCACTC)[40] was used as reference gene for relative quantification by $2^{-\Delta\Delta CT}$ method. All reactions were performed on an ABI 7500 Real-time PCR system (Applied Biosystems) with default run method. All calculations and normalizations were done using 7500 system v2.0.5 and data were analysed with two-way ANOVA and Bonferroni post-test performed with Prism software, version 5 (GraphPad Software, Inc., San Diego, CA).

Ultrastructural analysis by electronic microscopy – For Transmission electron microscopy (TEM), control and treated epimastigote forms were fixed for 2 h at 4 °C in a solution containing 2.5% glutaraldehyde and 4% paraformaldehyde in 0.1 M phosphate buffer, pH 7.2. After washing in the same buffer, the cells were post-fixed for 1 h with 1% osmium tetroxide/ 0.8% potassium ferricyanide/ 5 mM $CaCl_2$ in 0.1 M cacodylate buffer at pH 7.2. The parasites were then dehydrated in graded acetone series and embedded in Epon-812 (Sigma-Aldrich, St Louis, USA). Ultrathin sections were stained with 5% uranyl acetate and 2% lead citrate and observed in a FEI Tecnai^{TM} Spirit G^2 BioTWIN. For Scanning Electron Microscopy (SEM), the cells were fixed as described above for TEM and were subsequently adhered to cover slips containing poly-L-lysine for 20 min. The samples were then post-fixed in OsO_4 solution,

dehydrated in increasing ethanol concentration, dried by the critical point method, metallized with gold (20 nm) and observed in the Jeol 510.

Annexin V and Propidium Iodide labeling - Untreated (control) or DTT treated cells (2 – 16 mM) for 24 - 72 h, were incubated with the Cell Apoptosis Kit with Annexin V Alexa Fluor™ 488 & Propidium Iodide (Molecular Probes, Eugene, Oregon, USA), following the manufacturer's instructions. Parasites were incubated with 5 µL Alexa Fluor® 488 annexin V (AV) and 1 µL 100 µg/mL propidium iodide (PI) in 1x annexin-binding buffer at 28 °C. After 15 min of loading, cells were immediately analysed on a flow cytometer or a confocal laser scanning microscope (CLSM). Flow cytometric analysis were performed on a BD Accuri C6 flow cytometer (Becton-Dickinson, San Jose, CA, USA) and the data were expressed as the percentage of cells in each population phenotype: unstained, stained only with PI (FL2-H), stained only with AV (FL1-H) or stained with both markers, accordingly to the total number of cells analyzed (20,000 events). Parasites were also observed by confocal microscopy using a 488 nm diode laser and the fluorescence emission was recorded at 510 nm (for AV) and 560 nm (for PI). The samples were observed under a Leica SPII/AOBS (Mannheim, Germany) scanning confocal microscope.

Rhodamine 123 (Rho 123) - Treated and non-treated parasites were washed and suspended in 0.5 mL PBS with 10 µg/mL Rho 123 (Sigma-Aldrich, St Louis, USA) for 15 min. After loading time, the parasites were immediately washed in PBS and analysed by flow cytometry. A total of 20,000 events were acquired and changes in the fluorescence intensities of Rho 123 (FL1-H) were quantified by the index of variation (IV) that was obtained by the equation (TM − CM)/CM, where TM and CM are the mean of fluorescence for treated and control parasites, respectively. Rho 123-labeled parasites were also observed at CLSM using 488 nm laser.

Mitochondrial superoxide production - Treated and control parasites were washed and incubated in 0.5 mL PBS with 5 µM MitoSOX^{TM} Red mitochondrial superoxide indicator (Molecular Probes) for 10 min., protected from light. After loading time, the cells were washed with PBS and analysed by flow cytometry.

ACKNOWLEDGMENTS

We are thankful to Mrs. Cassia Docena and Mrs. Viviane Carvalho for their technical assistance and the Program for Technical Development of Health Inputs (PDTIS)/FIOCRUZ for the use of its facilities. This work was supported by CPqAM/FIOCRUZ and FACEPE.

AUTHOR CONTRIBUTIONS STATEMENT

J.M.S, D.M.N.M., M.P.C., R.C.B.Q.F. and A.F. wrote the main manuscript text; J.M.S, D.M.N.M., M.D.S.S., G.B.L., P.E.C.F. and S.C.G.A. performed the experiments. All authors reviewed the manuscript

REFERENCES

1. Chen, X., Karnovsky, A., Sans, M.D., Andrews, P.C. & Williams, J.A. Molecular characterization of the endoplasmic reticulum: insights from proteomic studies. *Proteomics*. **10**, 4040-4052 (2010).
2. Dolai, S., Swati, P., Yadav, R. K. & Adak, S. Endoplasmic reticulum stress-induced apoptosis in Leishmania through Ca^{2+}-dependent and caspase independent mechanism. *J. Biol. Chem*. **286**, 13638-13646 (2011).
3. Díaz-Villanueva, J.F., Díaz-Molina, R. & García-González, V. Protein Folding and Mechanisms of Proteostasis. *Int. J. Mol. Sci*. **16**, 17193-17230. (2015).
4. Zhang, T., Ye, Y. The final moments of misfolded proteins en route to the proteasome. *DNA Cell Biol*. **33**, 477-483 (2014).
5. Mori, K. Signalling pathways in the unfolded protein response: development from yeast to mammals. *J. Biochem*. **146**,743-750 (2009).
6. Kohno, K. Stress-sensing mechanisms in the unfolded protein response: similarities and differences between yeast and mammals. *J. Biochem*. **147**, 27-33 (2010).
7. Zeng, L. *et al*. Small heat shock proteins and the endoplasmic reticulum: potential attractive therapeutic targets? *Curr. Mol. Med*. **15,** 38-46 (2015).
8. Ron, D. & Walter, P. Signal integration in the endoplasmic reticulum unfolded protein response. *Nat. Rev. Mol. Cell Biol*. **8**, 519-529 (2007).
9. Hetz, C. The unfolded protein response: controlling cell fate decisions under ER stress and beyond. *Nat. Rev. Mol. Cell Biol* **13**, 89-102 (2012).
10. Bartholomeu, D. C. *et al.* Unveiling the intracellular survival Gene kit of trypanosomatid parasites. *PLoS Pathog*. **10**, e1004399 doi:10.1371/journal.ppat.1004399 (2014).
11. Koumandou, V. L., Natesan, S. K., Sergeenko, T. & Field, M. C. The trypanosome transcriptome is remodelled during differentiation but displays limited responsiveness within life stages. *BMC Genomics* **9**, 298-326, (2008).
12. Goldshmidt, H. *et al*. Persistent ER stress induces the spliced leader RNA silencing pathway (SLS), leading to programmed cell death in *Trypanosoma brucei*. *Plos Pathog.* 6, e1000731 doi: 10.1371/journal.ppat.1000731 (2010).
13. Gosline, S. J. *et al.* Intracellular eukaryotic parasites have a distinct unfolded protein response. *PLoS One***.** 6,e19118 doi: 2011. 10.1371/journal.pone.0019118 (2011).
14. Dolai, S. & Adak, S. Endoplasmic reticulum stress response in *Leishmania*. *Mol. Biochem. Parasitol.* **197**, 1-8 (2014).

15. Banerjee, S. *et al.* The evolution of N-glycan-dependent endoplasmic reticulum quality control factors for glycoprotein folding and degradation. *Proc. Natl. Acad. Sci*. **104**, 11676-11681 (2007).
16. Durose, J. B., Tam, A. B., Niwa, M. Intrinsic capacities of molecular sensors of the unfolded protein response to sense alternate forms of endoplasmic reticulum stress. *Mol. Biol. Cell.* **17**, 3095-3107 (2006).
17. World Health Organization. Chagas disease (American trypanosomiasis). *Fact sheet N°340.* (2015). Available at: <http://www.who.int/mediacentre/factsheets/fs340/en/> (Accessed 30/12/15).
18. De Souza, W. Structural organization of *Trypanosoma cruzi*. *Mem. Inst. Oswaldo Cruz*. **104**, 89-100 (2009).
19. Kroemer *et al.* Classification of cell death: recommendations of the Nomenclature Committee on Cell Death. *Cell Death Differ*. **16**, 3-11 (2009).
20. Huang *et al*. Mitochondrial inner membrane electrophysiology assessed by Rhodamine-123 transport and fluorescence. *Annals of Biomed. Eng.* **35**, 1276-1285 (2007).
21. Kuznetsov *et al*. Mitochondrial ROS production under cellular stress: comparison of different detection methods. *Anal. Bioanal. Chem*. **400**, 2383-2390 (2011).
22. Tiengwe, C., Brown, A. E. & Bangs, J. D. Unfolded protein response pathways in bloodstream-form *Trypanosoma brucei*? *Eukaryot. Cell*. **14**, 1094-1101 (2015).
23. Back, S. H., Schröder, M., Lee, K., Zhang, K. & Kaufman, R. J. ER stress signaling by regulated splicing: IRE1/HAC1/XBP1. *Methods.* **35**, 395-416 (2005).
24. Witte, I & Horke, S. Assessment of endoplasmic reticulum stress and the unfolded protein response in endothelial cells in unfolded protein response and cellular stress. *Methods Enzymol.* **489**, 127-146 (2011).
25. Otero, J. H., Lizák, B. & Hendershot, L. M. Life and death of a BiP substrate. *Semin. Cell. Dev. Biol.* **21**, 472-478 (2010).
26. Martinez, I. M. & Chrispeels, M. J. Genomic analysis of the unfolded protein response in *Arabidopsis* shows its connection to important cellular processes. *Plant Cell* **15**, 561–576 (2003).
27. Labriola, C.A., Conte, I. L., López, M. M., Parodi, A. J. & Caramelo, J. J. Endoplasmic reticulum calcium regulates the retrotranslocation of *Trypanosoma cruzi* calreticulin to the cytosol. *PLoS One***. 5**, e13141 doi:10.1371/journal.pone.0013141 (2010).

28. Labriola, C. A., Giraldo, A. M. V., Parodi, A. J. & Caramelo, J. J. Functional cooperation between BiP and calreticulin in the folding maturation of a glycoprotein in *Trypanosoma cruzi*. *Mol. Biochem. Parasitol.* **175**, 112-117 (2011).
29. Clayton, C. mRNA turnover in Trypanosomes in *Nucleic acids and molecular biology* (Ed. Albrecht, B.) 28 (Springer-Verlag Berlin Heidelberg, 2012).
30. Shang, X. J. *et al*. Procyanidin induces apoptosis and necrosis of prostate cancer cell line PC-3 in a mitochondrion-dependent manner. *J. Androl.* **30**, 122–126 (2009).
31. Vannuvel, K., *et al*. Effects of a sublethal and transient stress of the endoplasmic reticulum on the mitochondrial population. *J. Cell. Physiol*. doi: 10.1002/jcp.25292 *ahead to print* (2016).
32. Fei, W., Wang, H., Fu, X., Bielby, C. & Yang H. Conditions of endoplasmic reticulum stress stimulate lipid droplet formation in *Saccharomyces cerevisiae*. *Biochem. J.* **424**, 61–67 (2009).
33. Kim *et al*. Rapid Induction of Lipid Droplets in *Chlamydomonas reinhardtii* and Chlorella vulgaris by Brefeldin A. *PLoS One* **8**, e81978. doi:10.1371/journal.pone.0081978 (2013).
34. Yamamoto *et al*. Induction of liver steatosis and lipid droplet formation in ATF6 alpha-knockout mice burdened with pharmacological endoplasmic reticulum stress. *Mol. Biol. Cell.* **21**, 2975–2986 (2010).
35. Klionsky *et al*. Guidelines for the use and interpretation of assays for monitoring autophagy (3rd edition). *Autophagy.* **12**, 1-222 (2016).
36. Duszenko *et al.* Autophagy in protists *Autophagy.* 7, 127-158 (2011).
37. Sandes *et al*. *Trypanosoma cruzi* cell death induced by the Morita-Baylis-Hillman adduct 3-Hydroxy-2-methylene-3-(4-nitrophenylpropanenitrile). *PLoS One* **9**, e93936. doi: 10.1371/journal.pone.0093936. (2014).
38. Tamura, K., Dudley, J., Nei, M. & Kumar, S. MEGA4: molecular evolutionary genetics analysis (MEGA) software version 4.0. *Mol. Biol. Evol.* **24,** 1596e9 (2007).
39. Sharrocks, A. D. The design of primers for PCR in *PCR technology, current innovations* (eds Griffin, H.G. & Griffin, A.M.) p. 5e11 (CRC Press, 1994).
40. Franzén *et al*. Comparative genomic analysis of human infective *Trypanosoma cruzi* lineages with the bat-restricted subspecies *T. cruzi marinkellei*. *BMC Genomics* **5,** 531 doi: 10.1186/1471-2164-13-531 (2012).

4.2 Artigo 2 - Endoplasmic Reticulum Stress Induced by Tunicamycin on *Trypanosoma cruzi*

Manuscrito a ser submetido na revista indexada *Cell Death & Disease*, Qualis Capes A1 (Ciências Biológicas I – III), JCR 5,014, formatado conforme suas regras, exceto as figuras e tabelas que foram inseridas no texto para facilitar a compreensão dos leitores. Neste artigo, avaliamos o efeito da tunicamicina (TM) sobre a viabilidade do *T. cruzi*, a expressão de proteínas envolvidas na resposta ao estresse do RE, bem como o perfil de morte celular programada induzido por esta droga.

Endoplasmic Reticulum Stress Induced by Tunicamycin on *Trypanosoma cruzi*

[1,2,+]Jana Messias Sandes, [3]Danielle Maria Nascimento Moura, [2]Moana Divina da Silva Santiago, [2]Gustavo Barbosa de Lima, [1]Paulo Euzébio Cabral Filho, [2]Suênia da Cunha Gonçalves de Albuquerque, [2]Milena de Paiva Cavalcanti, [1,*]Adriana Fontes and [2,*]Regina Célia Bressan Queiroz Figueiredo.

[1] Universidade Federal de Pernambuco, Departamento de Biofísica e Radiobiologia, Recife 50670-901, Pernambuco, Brazil.

[2] Centro de Pesquisas Aggeu Magalhães/FIOCRUZ-PE, Departamento de Microbiologia, Recife. 50670-420, Pernambuco, Brazil.

[3] Centro de Pesquisas Aggeu Magalhães, Departamento de Imunologia, Recife, 50670-420, Brazil.

[+] Corresponding author

janasandes@gmail.com

[*] These authors contribute equally to this work

Running title: ER stress induced by tunicamycin on *T. cruzi*.

ABSTRACT

The endoplasmic reticulum (ER) is responsible for protein synthesis, folding and modification. Adverse conditions to ER homeostasis, including nutrient deprivation, loss of calcium homeostasis and inhibition of glycosylation may lead to ER stress and induction of the unfolded protein response (UPR). In higher eukaryotes, UPR increases chaperone expression, reduces protein synthesis and promotes degradation of unfolded proteins and, if all these strategies fail, UPR lead to cell death usually by apoptosis. Trypanosomatids lack classical UPR machinery and some studies presented controversial results about how they respond to ER stress or whether they possess an UPR-like response. Thus, the aim of this work was to evaluate the effect of ER stress induced by tunicamycin (TM), which inhibits N-glycosylation, on *Trypanosoma cruzi*. Our results showed that TM had a trypanostatic effect in all concentrations tested, without growth recovery after withdrawal of the drug. At 2.5 µg/mL TM we did not observe increase of BiP protein levels, but the mRNA levels of both BiP and CRT increased significantly between 4 and 10 h. By flow cytometry we observed that only ≈ 10% of the cells treated with 2.5 – 20 µg/mL of TM presented apoptotic phenotype, and rhodamine 123 and MitoSOX labeling indicated depolarization of mitochondrial membrane without pronounced ROS production. SEM and TEM analysis showed rounding of cell body, reduction of flagellum length, presence of lipid inclusions and ER profiles surrounding cytoplasmic structures in degradation process. Altogether, these results indicate that TM treatment induced ER-stress response as observed by increase of ER chaperones mRNA levels, increase of ER profiles and autophagic activity. However, the steady levels of BiP protein suggest that *T. cruzi* may have a different UPR response than higher eukaryotes.

INTRODUCTION

The endoplasmic reticulum (ER) is considered one of the major vital organelles of eukaryotic cells, being responsible for protein synthesis, posttranslational modification, peptide chain folding, regulation of glucose concentration, calcium homeostasis and lipid metabolism[1]. The ER provides an oxidative compartment, which facilitates disulfide bond formation, and is loaded with molecular chaperones such as: Hsp40 (J-proteins), Hsp70 (Grp78/BiP) and Hsp90 (Grp94); the lectin-based chaperones calnexin (CNX) and calreticulin (CRT); and protein disulfide isomerases (PDIs) that augment folding and prevent the formation of protein aggregates[2]. Correctly folded proteins are transported to the Golgi apparatus for further maturation and distribution to their destinations[3].

Cellular perturbations including nutrient deprivation, alterations in the oxidative-reduction balance, loss of calcium homeostasis and failure to glycosylate proteins may lead to accumulation of misfolded or unfolded proteins in ER lumen[4]. This unfolded protein accumulation, in turn, triggers an ER stress response knowing as the unfolded protein response (UPR) that activates intracellular signal transduction pathways in attempt to maintain cell homeostasis[5]. The major ER stress sensors involved in UPR induction are IRE1 (Inositol-requiring enzyme 1), PERK (PKR-like ER kinase) and ATF6 (activating transcription factor 6). At basal state, these proteins are inactivated by association with the chaperone BiP (binding protein), but during ER stress BiP disassociates from its ligands to assist in protein folding, allowing the activation of IRE1, PERK, and ATF6 (ref. 6). The UPR increases chaperones expression to prevent protein aggregation and facilitates the correct protein folding. In a similar way, UPR also reduces the ER load via inhibiting translation and increasing the degradation of the unfolded proteins via ER-associated degradation (ERAD). If these steps fail to overcome the ER stress, the UPR then induces cell death usually by apoptosis[2].

Trypanosoma cruzi, a protozoan parasite of the trypanosomatidae family, is the causative agent of Chagas disease, which affects about 6 – 7 millions of people worldwide, mostly in Latin America where it is endemic[7]. Although trypanosomes are highly divergent from yeast and mammals, the ER is also an important organelle for their survival, playing basically the same function found in superior eukaryotic organisms. However, little is known concerning protein folding factors in these parasites once trypanosomes lacks some UPR proteins as IRE1, ATF6, calnexin and glucosidade I, suggesting that they may have a simpler machinery for ER-quality control than other eukaryotes[8]. In fact, for *T. brucei* the initial ER stress seems to induce changing of mRNAs stability and, under severe ER stress, the silencing

of the spliced leader RNA (SL), a specie specific mini-exon donated to all pre-mRNA by trans-splicing and whose silencing leads to programmed cell death (PCD) by apoptosis[9].

In attempt to better understand the physiological mechanisms by which *T. cruzi* responses to ER stress, we have previously showed that the treatment with an traditional ER stressor dithiothreitol (DTT), that disrupts the formation of protein disulfide bonds, did not elicit a classical UPR-like response under short-term ER stress but lead to cell death, by mechanisms suggestive of late apoptosis/necrosis dependent on mitochondrion, during persistent ER stress[10]. However, it was not clear if the DTT affected specifically the ER once it also induces a strong oxidative stress. The purpose of the present study is therefore to investigate if the effect of tunicamycin (TM), another well-known ER stressor that inhibits N-glycosylation, would be more specific to ER and also evaluate the *T. cruzi* viability, protein expression and PCD induction under initial and persistent ER stress induced by TM.

RESULTS

ER stress affects cell viability

The treatment with TM (2.5 - 20 µg/mL) for up to 96 h had a strong trypanostatic effect on *T. cruzi* epimastigotes with cessation of cellular growth independently of the dose, as compared with control cells (no treatment) (Fig. 1A). To determine whether *T. cruzi* can recover growth after removal of TM, parasites were exposed to TM 20 µg/mL for 60 - 240 min., washed and growth was monitored by direct counting in a Neubauer chamber for up to 72 h (Fig. 1B). Our results demonstrated that TM-treated cells were not able to recover growth to the initial cell concentration (≅ 2×10^6 cells/mL) independently of time exposition, which indicates that TM acts irreversibly in the conditions evaluated.

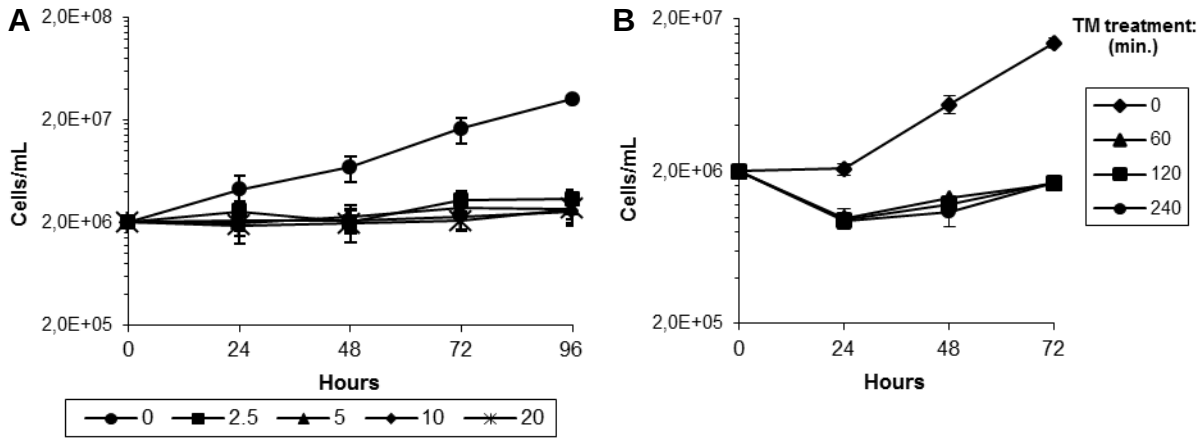

Figure 1. Effect of TM on the growth of *T. cruzi*.
(A) Growth curve of *T. cruzi* epimastigotes control and treated with different concentrations of TM (2.5 – 20 µg/mL), for 96 h. **(B)** Growth recovery of *T. cruzi* exposed to 20 µg/mL TM for up to 240 min. Each point represents the mean ± standard deviation of at least two independent experiments performed in triplicate (A) or duplicate (B).

ER stress and chaperone expression

To evaluate whether TM treatment would be able to upregulate the expression of the ER chaperone BiP, one of the hallmarks of the mammalian UPR[11], *T. cruzi* epimastigotes were submitted to short-term (2 – 4 h) or long-term (10 - 24 h) treatment with 2.5 µg/mL TM and the whole cell extracts were analyzed by Western blotting. Our results showed that, despite the inhibitory effect on the parasite growth, TM-treated cells were not able to alter the steady-state levels of BiP in any time of incubation evaluated, when compared to non-treated cells (0 h) (Fig. 2A).

Because BiP and calreticulin (CRT) chaperones cooperate with each other to assist the protein quality control within the ER[12], we further investigated whether TM treatment would be able to induce some alteration in the mRNA levels of both chaperones. The RT-qPCR analysis showed that BiP expression increased significantly in cells treated for 4 h (1.42-fold) and 10 h (1.72-fold), when compared to control (non-treated) cells (Fig. 2B). A significant increase in the CRT mRNA levels could be observed earlier after 2 h of TM treatment (1.46-fold). After 4 and 10 hours of treatment the level of CRT mRNA increase 1.79 and 1.53-fold comparing to the control cells. However an abrupt decrease in this level could be observed at 24 h (-2.45-fold).

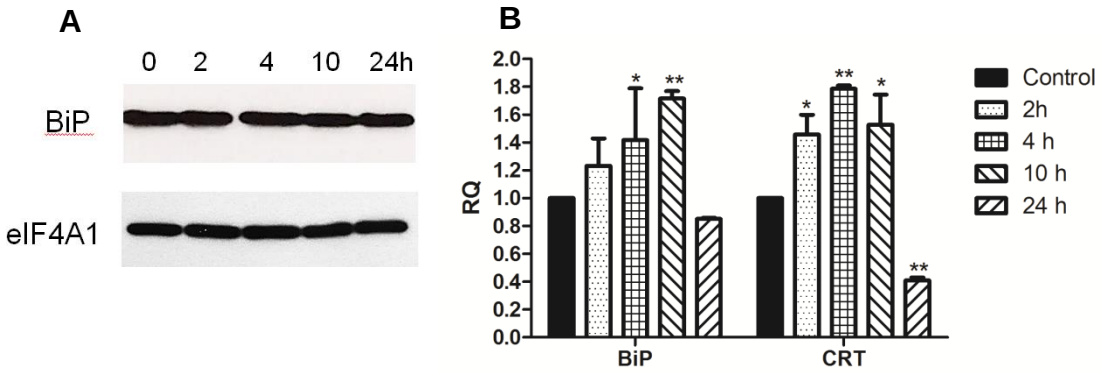

Figure 2. Western blotting and RT-qPCR analysis of BiP and/or CRT.
(A) Western Blotting assay of epimastigote submitted to TM treatment (2.5 µg/mL). EIF4A1, a protein that is expressed constitutively[42], was used as loading control. **(B)** Analysis of Bip and CRT mRNA expression by RT-qPCR. *p< 0.05; ** p< 0.01 compared to control.

ER stress and PCD

Our cytometric assay demonstrated that more than 90% of the control cells (no treatment) and 80% of the treated cells did not show any labeling for both probes (AV^-/IP^-) at 24 h, indicating that necrosis or apoptosis processes are not occurring in most cells analyzed (Table 1). However, after 72 h we observed in TM-treated cells a small increase (≈ 10 %) in the percentage of cells stained only with AV (AV^+/IP^-), suggesting that even on persistent ER stress only a small portion of the cells is undergoing PCD by apoptosis, in a dose-independent manner. The treatment of the cells with 9 % hydrogen peroxide (H_20_2) used as positive control of the experiment, cause intense necrosis in epimastigote forms of *T. cruzi*, with about 97.6% presenting AV^+/PI^+ phenotype.

Table 1. Flow cytometry analysis of AV/PI labeling of *T. cruzi* treated or not with TM

	24h				72h			
Sample	**AV^-/PI^+**	**AV^+/PI^+**	**AV^-/PI^-**	**AV^+/PI^-**	**AV^-/PI^+**	**AV^+/PI^+**	**AV^-/PI^-**	**AV^+/PI^-**
Control	0.06	3.16	93.50	3.29	0.03%	2.87	92.36	4.75
TM 2.5 µg/mL	0.07	7.76	86.56	5.62	0.09%	3.87	85.28	10.77
TM 5 µg/mL	0.11	5.90	90.18	3.81	0.10%	6.64	81.29	11.97
TM 10 µg/mL	0.06	4.17	92.70	3.07	0.10%	5.31	81.44	13.16
TM 20 µg/mL	0.09	5.53	89.51	4.87	0.14%	4.32	83.09	12.46
H_2O_2	0.06	97.60	2.20	0.14	3.22%	96.63	0.14	0.02

*The values represent the mean of two independent experiments with 20,000 events each and are expressed as % of cells in each phenotype.

Mitochondrial alterations on persistent ER stress

Comparing to control cells our flow cytometry analysis showed a decrease in the Rhodamine 123 (Rho 123) mean fluorescence intensity in cells treated with TM, with negative IV of -0.44 at 20 µg/mL. The analysis of MitoSOX ™ labeling, however demonstrated that TM treatment did not influence the production of mitochondrial reactive species, with the percentage of labeled cells ranging from 10 - 15% in treated cells. Cells treated with 9% hydrogen peroxide (H_2O_2) showed that more than 97 % of the cells were labeled for MitoSOX.

Table 2. Rho 123 and MitoSOX labeling analysis of *T. cruzi* treated with TM for 72 h.

	Rho 123		MitoSOX™
Sample	Fluorescence intensity (FI)	Index of variation (IV)	Positive cells (%)
Control	405,655.40	0.00	5.95
TM 2.5 µg/mL	264,669.12	-0.35	11.00
TM 5 µg/mL	269,478.50	-0.34	10.55
TM 10 µg/mL	261,379.07	-0.36	10.25
TM 20 µg/mL	225,513.86	-0.44	14.45
H_2O_2	-	-	97.85

* The values represent the mean of two independent experiments with 20,000 events each.

An increased production of ATP, probably due to cell proliferation, could be observed during the cultivation of control cells. However, the levels of ATP in treated cells were maintained unaltered in all concentrations or times of cultivation tested (Fig. 3)

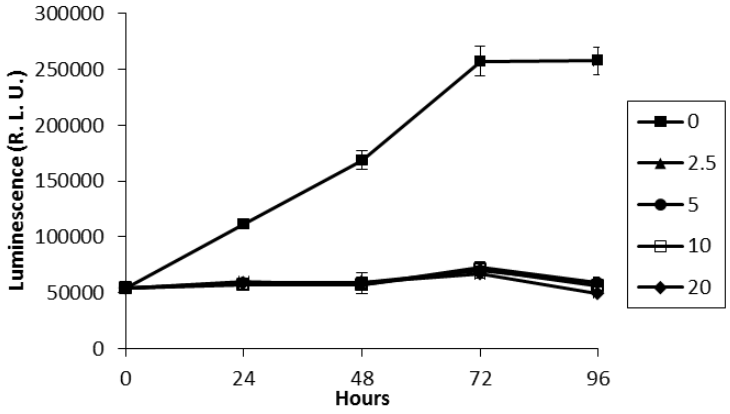

Figure 3. *T. cruzi* intracellular ATP relative levels by Luminescence analysis.
T. cruzi cells were treated or not with TM (2.5, 5, 10 or 20 µg/mL) and the levels of ATP were assessed using the bioluminescent assay CellTiter-Glo® 2.0. RLU: relative light units.

Ultrastructural changes on persistent ER stress

As shown by SEM in Fig. 4A, control epimastigote forms of *T. cruzi* exhibited typical elongated morphology, twisted cell body and smooth membrane. The treatment with TM at 2.5 µg/mL (Fig. 4B-D) led to a drastic cell rounding and shortening of the flagellum (arrow). At 10 - 20 µg/mL of TM (Fig. 4C-D) it was possible to observe cells with increased cell body twisting and shortening of cell body (thick arrow), and flagellum length. TM treatment also induced abnormal division process (asterisk) and flagellum detachment of the cell body (arrowhead). No ruptured cells or cell debris were observed.

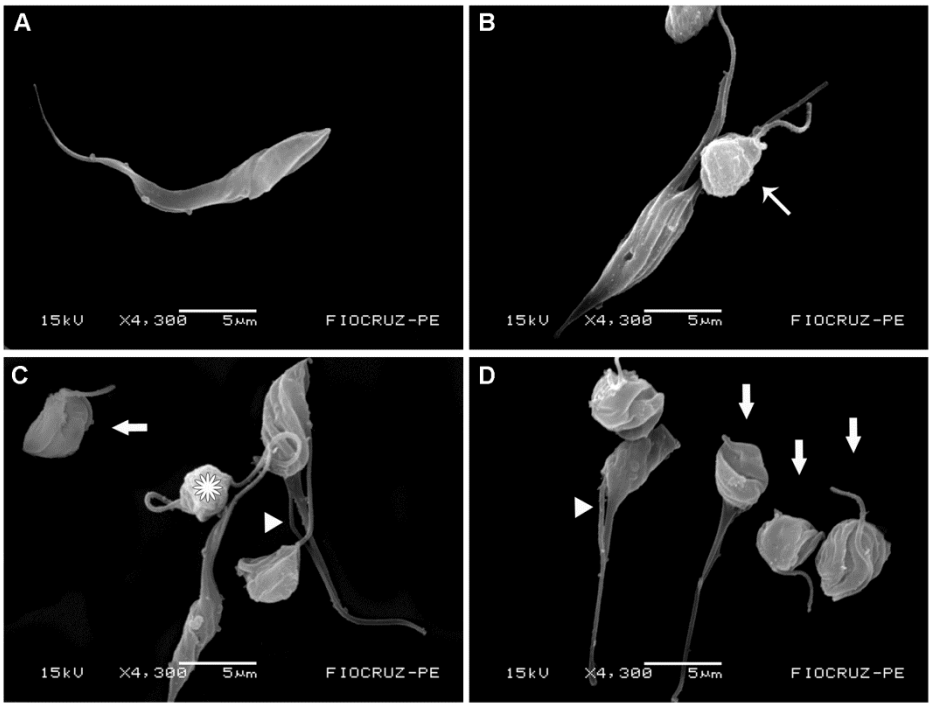

Figure 4. Scanning electron microscopy of *T. cruzi* treated with TM.

(A) Controls of *T. cruzi* epimastigote forms exhibiting typical morphology. **(B - D)** Cells treated with 2.5 µg/mL **(B)**, 10 µg/mL **(C)** or 20 µg/mL of TM showing round shape and shortening of the flagellum (arrow), increasing of body twisting and reduction of cell body (thick arrow), flagellum detaching of the cell body (arrowhead) and incomplete division process (asterisk).

The TEM analysis also showed that the control epimastigote cells presented characteristic morphology, as an elongated shape and a centrally located nucleus. A single mitochondrion, containing a specialized structure named kinetoplast where the mitochondrial DNA is concentrated, could be observed along the cell body. Reservosomes, a characteristic pre-lysosomal compartment of epimastigotes, and scarce ER profiles scattering along the cytoplasm or in association with plasma membrane were also observed (Fig. 5A and B). Treatment of parasites with TM induced an increase in ER profiles surrounding portions of cytoplasm and partially degraded organelles (Fig. 5B-H), suggesting that autophagy process is taking a place. Furthermore we also observed an increase in the number and electrondensity of cytoplasmic lipid inclusions closer to the ER and the mitochondrion (Fig. 5D). At 10 µg/mL of TM (Fig. 5E and F) we also found a great number of ER profiles around partially degraded organelles, including the reservosomes (Fig. 5F). Besides the above-mentioned changes, at higher concentrations of TM an increased in number of vesicles and tubular process budding from morphologically altered Golgi complex could be observed (Fig. 5G). Loss of cellular organization, condensation of nuclear chromatin, reservosomes with altered shape and a large number of membrane-bound electron-lucent vesicles (Fig. 5H) were also found in these cells.

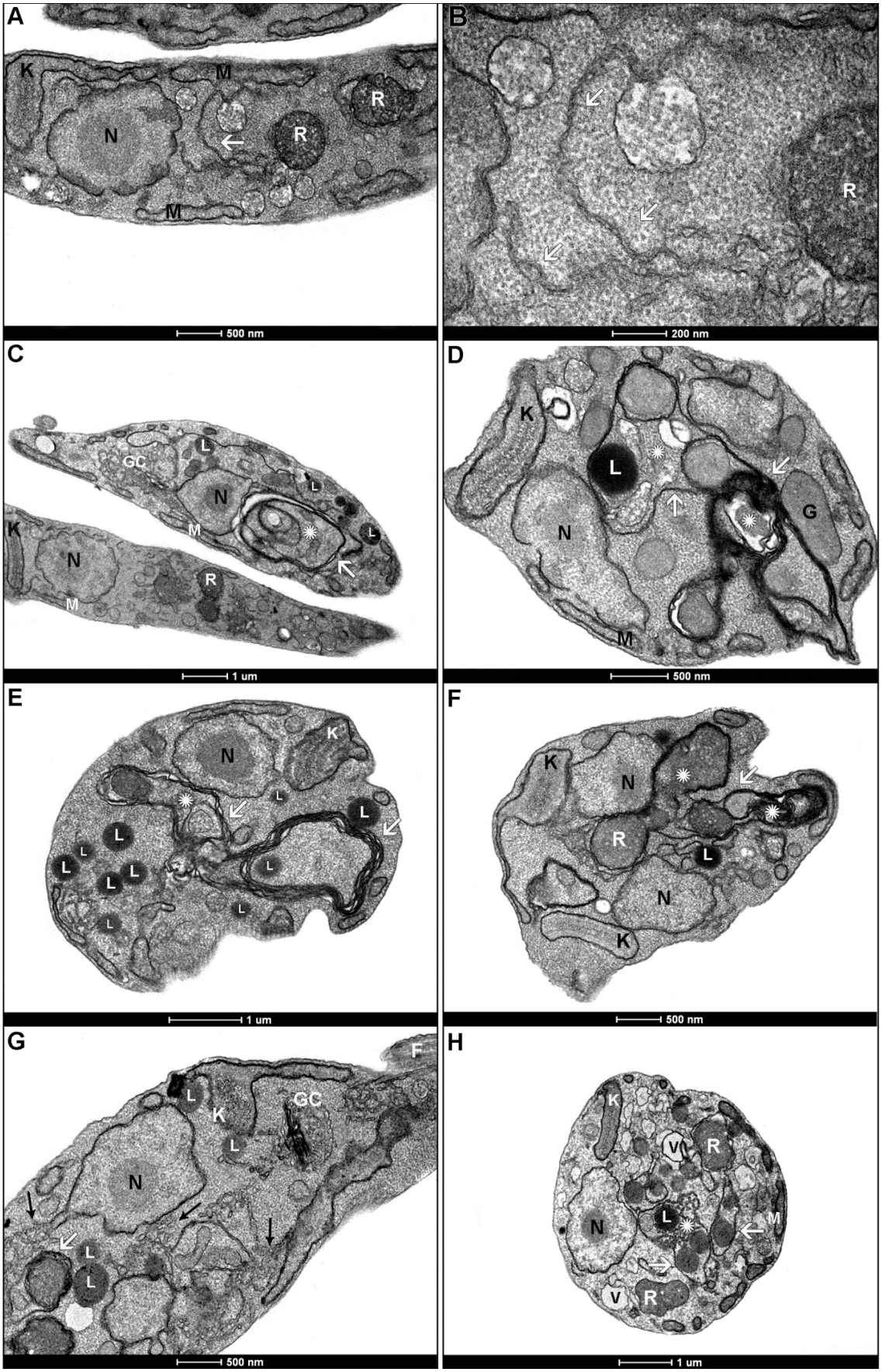

Figure 5. Transmission electron microscopy of *T. cruzi* treated with TM.

(A-B) *T. cruzi* epimastigotes control cells (no treatment) showing preserved organelles as ER (white arrow), nucleus (N), mitochondrion (M), kinetoplast (K), acidocalcisome (A) and reservosomes (R). **(C-F)** Cells treated with 2.5 µg/mL **(C-D)** or 10 µg/mL **(E-F)** of TM presenting several ER profiles (white arrow) surrounding cytoplasmic structures (white asterisk) and numerous lipid inclusions (L). **(G-H)** Cells treated with 20 µg/mL showing vesicles and tubular processes budding from Golgi complex (GC) **(G)**, loss of cellular organization, condensation of nuclear chromatin and electron-lucent vesicles (V) **(H).** G: glicosome.

DISCUSSION

The endoplasmic reticulum (ER) is an organelle found in eukaryotes responsible for synthesis, folding and structural maturation of proteins that are translated by ER membrane associated ribosomes whereas they are carried into the ER lumen for posterior transport to other organelles and plasma membrane[4]. Pharmacological agents as dithiothreitol (DTT), thapsigargin (TG), or tunicamycin (TM) have been used to induce ER stress and UPR response in a number of cell types[13]. Despite being one of the most used in the study of ER stress, the validity of the DTT as stressor agent has been questioned in several studies. Tiengwe et al.[14] showed that besides its toxicity the DTT in *T. brucei* failed to upregulate BiP, a hallmark of UPR response. These authors argued that due to its strong oxidative effect, DTT compromised the whole cell function rather than acts as a specific inductor of ER stress. Similar results were obtained by our previous work using DTT to study the ER in *T. cruzi*[10].

The tunicamycin (TM), originally isolated from *Streptomyces lysosuperficus* and *S. chartreusis*, consists of five structural units: uracil, ribose, galactosamine (GalN), N-acetylglucosamine (GlcNAc), and a fatty acid (LY; YU 2015). This antibiotic inhibits the first step in the biosynthesis of N-linked oligosaccharides inducing ER stress in different cell lines, including trypanosomatids as *Leishmania major*[15], *L. donovani*[16] and *Trypanosoma brucei*[17,14]. Previous studies analyzed the effect of TM on the interaction of *T. cruzi* with mammalian cells[18-20], showing that TM treatment interfered in the host cell infection. However, the potential roles of TM in *T. cruzi* ER stress response are still unknown. The viability analysis of TM-treated cells showed that this drug has a strong trypanostatic effect on *T. cruzi*, since no cell growth was observed independently of the dose or time of incubation. Furthermore, the cells were not able to resume the cell growth after removal of TM.

The UPR in higher eukaryotes initially leads to the suppression of protein synthesis and upregulation of ER chaperones such as calreticulin (CRT) and BiP in attempt to prevent protein aggregation and increase the protein folding[21]. Indeed, *L. major* treated with TM revealed a 4-fold increase in BiP protein expression when treated with 20 µg/mL of TM[15]. In our study we failed to demonstrate alterations in the profile of BiP expression in *T. cruzi* treated with 2.5 µg/mL of TM at any time of cultivation tested. Unchanged BiP expression was also found in *L. donovani*[16] and in *T. brucei*[17] in response of TM. These results suggest that a canonical UPR response with increase of BiP expression could not be found in these parasites in response to TM.

Previous study with *T. cruzi* epimastigotes treated with 2 µg/mL of TM for 10 h showed that, although the BiP protein levels were not altered, the levels of BiP mRNA had an increase of 5.4-fold compared with non-treated cells[14]. Thus, we investigated whether the mRNA levels of BiP and CRT would be upregulated on TM treatment. We observed that the increase of CRT mRNA preceded those found for BiP. In eukaryotic cells the chaperone selection in ER depends on two factors: The structural features of the folding intermediates that favors their interaction with particular set of chaperones, and the competitive effect between the chaperones. Many proteins entering the ER interact first with BiP whereas others associate first with CRT instead of BiP, a process triggered by the presence of N-glycans near the N-terminus of the translocating polypeptide[12]. It is reasonable to assume that the early increase of CRT mRNA compared to BiP may be due to the differential function and specificity exerted by these proteins during TM-induced stress.

The possible reasons for the transcriptional alterations did not interfere to the protein levels of BiP may be due to a translational attenuation pathway, which in mammals can be activated in UPR by PERK and eIF2a phosphorylation[22]. However, in trypanosomatids, that lacks the classic UPR machinery[8], the mechanism behind translational attenuation still need to be elucidated. Another possibility is that the Western Blotting technique is not sensible enough to detect minor variations in a small population of nascent BiP induced by TM[23]. Moreover, in a previous study carried out by our group we have demonstrated that DTT treatment also failed to alter BiP protein levels even when this protein mRNA was down regulated[10].

When the ER stress becomes more severe or persistent the UPR-induced mechanisms in higher eukaryote cells may fail to alleviate the unfolded protein accumulation, and can activate apoptosis by both the intrinsic and extrinsic pathways[24]. In *T. brucei,* the severe ER stress induced by drugs elicits the spliced leader silencing (SLS) pathway, which blocks the trans-splicing to all nascent mRNAs and leads to cell death[8]. In order to investigate if TM treatment could induce PCD pathways in *T. cruzi* we submitted the treated parasites to AV/PI labeling. Our results demonstrated that TM-treatment did not induced important parasite death neither after 24 h (initial ER stress) nor 72 h of treatment (persistent ER stress), since most of epimastigote cells were negative for both markers. Approximately 10% of the cells were stained only with AV (AV^+/PI^-), suggesting that even on persistent ER stress just a small portion of the cells may be undergoing PCD by apoptosis.

The ER stress can directly affect the mitochondrial functions and depending on the extent of cellular stress can result in pro-survival or pro-apoptotic pathways[25]. In *T. cruzi* cells

we observed that TM treatment induced depolarization of the mitochondrial membrane, but without inducing significant oxidative stress or interfering with ATP production in most cells. One possible explanation is that the ER stress can be transmitted to mitochondria by alterations in the transfer of metabolites such as Ca^{2+}(ref. 25), which lead to alterations in mitochondrial membrane potential, but is not sufficiently strong to provoke a pronounced increase in ROS production or attenuation of ATP production.

To better evaluate the effect of TM in *T. cruzi* persistent ER stress we analyzed the cells by SEM and TEM and investigated the possible target organelles and mechanisms of action. We observed by SEM that TM treatment induced rounding of the cell body, reduction of flagellum length, and in some cells flagellum detachment of the cell body, which may indicate destabilization of cytoskeleton components or microtubule-associated proteins[26]. Such alterations were found inclusive in cells during an incomplete division process, which suggests that TM-treated cells were not be able to divide and would explain the trypanostatic action of TM.

The most prominent effect induced by TM in treated cell was the increase of ER profiles surrounding bulk cytoplasm and organelles, suggestive of autophagy process. Autophagy is a highly conserved degradation pathway that is responsible for elimination of damaged cellular components. This process is implicated in several physiological and pathological processes leading to cell survival or cell death. It has been demonstrated that the presence of autophagy protects cells from apoptosis induced by ER stress[27]. The protective role of autophagy could explain the low level of cell undergoing apoptosis as demonstrated in our AV/PI assays. Several studies have highlighting the direct relationship between the ER stress and the autophagy as an alternative route of protein degradation[28,29]. A second function of autophagy could be the degradation of own damaged ER, the ER-phagy, in attempt to promote their replacement and homeostasis[30-32].

We also observed numerous vesicles and tubular process in the vicinity of Golgi complex in a TM-treated cell. Thus, it is possible that the Golgi complex would be helping to alleviate the ER overload, once it is known that in mammalian cells the misfolded substrates can be transported to the Golgi and then sorted for lysosomal degradation, or modified by Golgi mannosidase II and targeted for degradation by ERAD[2]. In *T. cruzi*, the Golgi vesicles would be translocating the misfolded proteins to reservosomes, which has an important function in digestive, autophagic and recycling processes in epimastigote forms of *T. cruzi*[33].

Accumulation of lipid inclusions in response to ER stress was also found in our previous study using DTT and by other authors in fungus, plants and mammalian cells

submitted to ER-stress[10,34-36]. These authors suggested that lipid inclusion formation might be a resistance mechanism against ER stressors. On the other hand that the LD could protect exposed hydrophobic residues of unfolded proteins upon ER stress from aggregation in the cytoplasm, which can be extremely toxic to cells[10,35]. It has been demonstrated that the increase in number and volume of ER profiles is a common feature during the UPR[29]. Likewise, the appearance of lipid inclusions closer to the ER and the mitochondrion in TM treated cells could be also supporting the ER expansion[37].

Taken together, our results suggest that TM treatment induces a specific response to ER stress in *T. cruzi* that increases the ER-chaperones mRNAs levels, alters the number of ER profiles and possibly the transport of cargo to Golgi complex. As a consequence, the cell elicits autophagy/ER-phagy process, coping with ER stress without causing substantial injury to cell or cell death by apoptosis, as observed in our study. However, the steady levels of BiP protein suggests that the *T. cruzi*, as others trypanosomatids, has a different UPR response that diverge from other eukaryotic cells.

MATERIALS AND METHODS

Parasites. *T. cruzi* epimastigote forms (Dm28c) were maintained in liver infusion tryptose (LIT) medium supplemented with Fetal Bovine Serum 10% at 28 °C and harvested during the exponential phase of growth for experiments.

Drugs. Tunicamycin (TM) (Sigma-Aldrich) was initially dissolved in dimethyl sulfoxide (DMSO) at 5 mg/mL, aliquoted and stored at -20ºC. For experiments, the aliquots were diluted in LIT medium (2.5 – 20 µg/mL). DMSO final concentration never exceeds 0.4%, a non-toxic concentration to the parasite.

Viability Assay. Epimastigotes in the log phase of growth ($2x10^6$ parasites/mL) were incubated at 28 °C in LIT medium supplemented with 10% FBS in the absence or presence of different concentrations of TM for 24 to 96 h. The inhibitory effect of TM on cell growth was then estimated by daily cell counting using a Neubauer chamber. To examine if *T. cruzi* can recover following removal of TM treatment, parasites were exposed to TM 20 µg/mL by different time periods (60 - 240 min.). After incubation, the drug was washed out, and growth was monitored by daily cell counting as mentioned above.

Western blotting analysis. Whole cell extracts were resolved by SDS-PAGE 15%, transferred to PVDF membranes (Millipore) and probed with *T. brucei* anti-BiP (diluted 1:40,000), kindly provided by Prof. James Bangs (University of Wisconsin- Madison, Madison, USA), or anti-EIF4AI (diluted 1:5,000), kindly provided by Dr. Osvaldo de Melo-Neto (Aggeu Magalhães Research Center, Recife, Brazil) as loading control. The bound antibodies were detected with goat anti-rabbit IgG coupled to horseradish peroxidase (Jackson Immunoresearch), and were visualized by chemioluminescence.

Quantitative real-time RT-PCR. Multiple alignments of BiP and calreticulin sequences of *Trypanosoma cruzi* available in GenBank were analyzed using Mega 6.06. (ref. 38). Primers were then designed with the PRIMER BLAST software (http://www.ncbi.nlm.nih.gov/tools/primer-blast), using the criteria described elsewhere[39], based on the following sequences: L23420.1 (TcBiP) and XM_799098.1 (TcCRT). The specific primers sequences selected were (5’ to 3’): TcBIP-F (AAGCAGTCGAAGAAGGGGTG) and TcBIP-R (GAAAAGGCAACCAGAGCAGC);

TcCRT-F (GCTCGAAGAAGACTGGAGCC) and TcCRT-R (GGATCATTGCGGGTTCGTTG). Amplification efficiency was determined from the slope of the standard curve for each primer using 1:10 serial dilution of genomic *T. cruzi* DNA (1 ng/µL – 1 fg/µL). Total RNA was extracted from treated and control epimastigote forms (c. a. 1×10^8 cells) using the RNeasy Mini kit (Qiagen, Hilden, Germany), according to the manufacturer's instructions, with an additional DNase (Invitrogen, Carlsbad, CA, USA) digestion step. RNA was converted to cDNA with reverse transcriptase and random primers of TaqMan Reverse Transcription Reagents (Invitrogen), in a final volume of 40 µL. Quantitative real-time RT-PCR was performed using Power SYBR Green PCR Master Mix (Applied Biosystems, Foster City, USA) with reaction mixture containing c. a. 100 ng of template cDNA and 3 µM primers in 25 µL of final volume. Amplifications were carried out in triplicate, in two independent experiments. *T. cruzi* 18S rRNA (Tc18S-F: TTACGTCCCTGCCATTTGTA and Tc18S-R: TTCGGTCAAGTGAAGCACTC)[40] was used as reference gene for relative quantification by $2^{-\Delta\Delta CT}$ method. All reactions were performed on an ABI 7500 Real-time PCR system (Applied Biosystems) with default run method. All calculations and normalizations were done using 7500 system v2.0.5 and data were analyzed using two-way ANOVA and Bonferroni post-test performed with Prism software, version 5 (GraphPad Software, Inc., San Diego, CA).

Annexin V and Propidium Iodide labeling. To assess whether PCD processes by apoptosis or necrosis could be trigger by ER stress response we use annexin V-Alexa 488 (AV), in order to detect external exposure of phosphatidylserine (feature of early apoptosis); and propidium iodide (PI), which detects the rupture of the plasma membrane (feature of necrosis)[41]. Parasites treated with 2,5 – 20 µg/mL TM, for 24 or 72 h, as well as, control untreated parasites were incubated with the Dead Cell Apoptosis Kit with Annexin V Alexa Fluor™ 488 & Propidium Iodide (Molecular Probes, Eugene, Oregon, USA), following the manufacturer's instructions. Briefly, the parasites were incubated with 5 µL Alexa Fluor® 488 annexin V (AV) and 1 µL 100 µg/mL propidium iodide (PI) in 1x annexin-binding buffer at 28 °C. After 15 min of loading, cells were immediately analyzed on a BD Accuri C6 flow cytometer (Becton-Dickinson, San Jose, CA, USA) and the data were expressed as the percentage of cells in each population phenotype: unstained, stained only with PI (FL2-H), stained only with AV (FL1-H) or stained with both markers, accordingly to the total number of cells analyzed (20,000 events).

Rhodamine 123 (Rho 123) assay. Treated and non-treated parasites were washed and suspended in 0.5 mL PBS with 10 µg/mL Rho 123 (Sigma-Aldrich, St Louis, USA) for 15 min. After loading time, the parasites were immediately washed in PBS and analysed by flow cytometry. A total of 20,000 events were acquired and changes in the fluorescence intensities of Rho 123 (FL1-H) were quantified by the index of variation (IV) that was obtained by the equation (TM − CM)/CM, where TM and CM are the mean of fluorescence for treated and control parasites, respectively.

Mitochondrial superoxide production. Treated and control parasites were washed and incubated in 0.5 mL PBS with 5 µM MitoSOX^{TM} Red mitochondrial superoxide indicator (Molecular Probes) for 10 min., protected from light. After loading time, the cells were washed with PBS and analyzed by flow cytometry.

ATP production. To assess the effect of TM on the levels of intracellular ATP, the kit CellTiter-Glo® 2.0 Assay (Promega, Fitchburg, WI) was used according to the manufacturer's instructions. Briefly, treated and control parasites (2×10^6 cells/ml) were exposed to different concentrations of TM for 24, 48, 72 and 96 h. After that, 100 µL of each sample plus the same volume of the CellTiter-Glo® 2.0 reagent was added in a white 96-well plate and incubated for 10 min. at room temperature (22–25°C). Luminescence was obtained by the reaction between luciferase and the ATP that was released after cell lysis. Light emission levels were measured on a GloMax®-Multi Detection System (Promega) at 570 nm. Two independent experiments were performed in triplicate.

Ultrastructural analysis by electronic microscopy. Epimastigote forms incubated or not with different concentrations of TM for 72 h, were processed for Transmission Electron Microscopy (TEM). The parasites were fixed for 2h at 4°C in a solution containing 2.5% glutaraldehyde and 4% paraformaldehyde in 0.1 M phosphate buffer, pH 7.2. After washing in the same buffer, the cells were post-fixed for 1 h with 1% osmium tetroxide/ 0.8% potassium ferricyanide/ 5 mM $CaCl_2$ in 0.1 M cacodylate buffer at pH 7.2. They were then dehydrated in graded acetone series and embedded for 72 h at 60°C in Epon-812 (Sigma-Aldrich, St Louis, USA). Ultrathin sections were stained with 5% uranyl acetate and 2% lead citrate and observed in a FEI Tecnai^{TM} Spirit G^2 BioTWIN. For Scanning Electron Microscopy (SEM), the cells at the same conditions were fixed as described for TEM and were subsequently adhered to cover slips containing poly-L-lysine for 20 min.. The samples

were post-fixed as described previously, dehydrated in increasing ethanol concentration, dried by the critical point method, metallized with gold (20 nn) and observerd in the Jeol 510.

ACKNOWLEDGMENTS

We are thankful to Mrs. Cassia Docena and Mrs. Viviane Carvalho for their technical assistance and the Program for Technical Development of Health Inputs (PDTIS)/FIOCRUZ for the use of its facilities. This work was supported by CPqAM/FIOCRUZ and FACEPE.

CONFLICT OF INTEREST

The authors declare no conflict of interest.

REFERENCES

1. Liu Z, Lv Y, Zhao N, Guan G, Wang J. Protein kinase R-like ER kinase and its role in endoplasmic reticulum stress-decided cell fate. *Cell Death Dis* 2015; **6**: e1822.
2. Brodsky JL, Skach WR. Protein folding and quality control in the endoplasmic reticulum: Recent lessons from yeast and mammalian cell systems. *Curr Opin Cell Biol* 2011; **23**: 464-475.
3. Dolai S, Adak S. Endoplasmic reticulum stress responses in *Leishmania*. *Mol Biochem Parasitol* 2014; **197**: 1-8.
4. Hetz C, Chevet E, Oakes SA. Proteostasis control by the unfolded protein response. *Nat Cell Biol* 2015; **17**: 829-838.
5. Walter P, Ron D. The unfolded protein response: from stress pathway to homeostatic regulation. *Science* 2011; **334**: 1081-1086.
6. Pagliassotti MJ. Endoplasmic reticulum stress in nonalcoholic fatty liver disease. *Annu Rev Nutr* 2012; **32**: 17-33.
7. World Health Organization. Chagas disease (American trypanosomiasis). *Fact sheet N°340.* 2015. Available at: <http://www.who.int/mediacentre/factsheets/fs340/en/> (Accessed 30/12/15).
8. Michaeli S. Spliced leader RNA silencing (SLS) - a programmed cell death pathway in *Trypanosoma brucei* that is induced upon ER stress. *Parasit Vectors* 2012; **5**: 107.
9. Goldshmidt H, Matas D, Kabi A, Carmi S, Hope R, Michaeli S. Persistent ER stress induces the spliced leader RNA silencing pathway (SLS), leading to programmed cell death in *Trypanosoma brucei*. *Plos Pathog* 2010; **6**: e1000731.
10. Sandes JM, Moura DMN, Santiago MDS, de Lima GB, Cabral Filho PE, Albuquerque SCG *et al.* The effects of the endoplasmic reticulum stressor agent dithiothreitol (DTT) on *Trypanosoma cruzi*. 2016. Unpublished data.
11. Mori K. Signalling pathways in the unfolded protein response: development from yeast to mammals. *J Biochem* 2009; **146**: 743-750.
12. Labriola CA, Giraldo AM, Parodi AJ, Caramelo JJ. Functional cooperation between BiP and calreticulin in the folding maturation of a glycoprotein in *Trypanosoma cruzi*. *Mol Biochem Parasitol* 2011; **175**: 112-117.
13. Durose JB, Tam AB, Niwa M. Intrinsic capacities of molecular sensors of the unfolded protein response to sense alternate forms of endoplasmic reticulum stress. *Mol Biol Cell* 2006; **17**: 3095-3107.

14. Tiengwe C, Brown AE, Bangs JD. Unfolded Protein Response Pathways in Bloodstream-Form *Trypanosoma brucei*? *Eukaryot Cell* 2015; **14**: 1094-1101.
15. Dolai S, Pal S, Yadav RK, Adak S. Endoplasmic reticulum stress-induced apoptosis in *Leishmania* through Ca2+-dependent and caspase-independent mechanism. *J Biol Chem* 2011; **286**: 13638-13646.
16. Gosline SJ, Nascimento M, Mccall LI, Zilberstein D, Thomas DY, Matlashewski G *et al.* Intracellular eukaryotic parasites have a distinct unfolded protein response. *PLoS One* 2011; **6**: e19118.
17. Koumandou VL, Natesan SK, Sergeenko T, Field MC. The trypanosome transcriptome is remodelled during differentiation but displays limited responsiveness within life stages. *BMC Genomics* 2008; **9**: 298-326.
18. Piras R, Piras MM, Henriquez D. The effect of inhibitors of macromolecular biosynthesis on the in vitro infectivity and morphology of *Trypanosoma cruzi* trypomastigotes. *Mol Biochem Parasitol* 1982; **6**: 83-92.
19. Zingales B, Katzin AM, Arruda MV, Colli W. Correlation of tunicamycin-sensitive surface glycoproteins from *Trypanosoma cruzi* with parasite interiorization into mammalian cells. *Mol Biochem Parasitol* 1985; **16**: 21-34.
20. Souto-Padrón T, de Souza W. The effect of tunicamycin and monensin on the association of *Trypanosoma cruzi* with resident macrophages. *Parasitol Res* 1989; **76**: 98-106.
21. Wang Q, Groenendyk J, Michalak M. Glycoprotein Quality Control and Endoplasmic Reticulum Stress. *Molecules* 2015; **20**: 13689-13704.
22. Iurlaro R, Muñoz-Pinedo C. Cell death induced by endoplasmic reticulum stress. *FEBS J* 2015; e-pub ahead of print 20 November 2015; doi: 10.1111/febs.13598.
23. Tibbetts RS, Kim IY, Olson CL, Barthel LM, Sullivan MA, Winquist AG *et al.* Molecular cloning and characterization of the 78-kilodalton glucose-regulated protein of *Trypanosoma cruzi*. *Infect Immun* 1994; **62**: 2499-2507.
24. Sano R, Reed JC. ER stress-induced cell death mechanisms. *Biochimica et Biophysica Acta* 2013; **1833**: 3460–3470.
25. Rainbolt TK, Saunders JM, Wiseman RL. Stress-responsive regulation of mitochondria through the ER unfolded protein response. *Trends Endocrinol Metab* 2014; **25:** 528-537.
26. Salomão K, de Souza EM, Carvalho SA, da Silva EF, Fraga CA, Barbosa HS *et al.* In vitro and in vivo activities of 1,3,4-thiadiazole-2-arylhydrazone derivatives of megazol against *Trypanosoma cruzi*. *Antimicrob Agents Chemother* 2010; **54**: 2023-2031.

27. Hassan M, Selimovic D, Hannig M, Haikel Y, Brodell RT, Megahed M. Endoplasmic reticulum stress-mediated pathways to both apoptosis and autophagy: Significance for melanoma treatment. *World J Exp Med* 2015; **5**: 206-217.
28. Hotamisligil GS. Endoplasmic reticulum stress and the inflammatory basis of metabolic disease. *Cell* 2010; **140**: 900-917.
29. Kiel JA. Autophagy in unicellular eukaryotes. *Philos Trans R Soc Lond B Biol Sci* 2010; **365**: 819-830.
30. Bernales S, Mcdonald KL, Walter P. Autophagy counterbalances endoplasmic reticulum expansion during the unfolded protein response. *PLoS Biol* 2006; **4**: e423.
31. Bravo R, Parra V, Gatica D, Rodriguez AE, Torrealba N, Paredes F *et al.* Endoplasmic reticulum and the unfolded protein response: dynamics and metabolic integration. *Int Rev Cell Mol Biol* 2013;**301**: 215-290.
32. Schuck S, Gallagher CM, Walter P. ER-phagy mediates selective degradation of endoplasmic reticulum independently of the core autophagy machinery. *J Cell Sci* 2014;**127**: 4078-4088.
33. De Souza W, Sant'anna C, Cunha-e-Silva NL. Electron microscopy and cytochemistry analysis of the endocytic pathway of pathogenic protozoa. *Prog Histochem Cytochem* 2009; **44**: 67-124.
34. Fei W, Wang H, Fu X, Bielby C, Yang H. Conditions of endoplasmic reticulum stress stimulate lipid droplet formation in *Saccharomyces cerevisiae*. *Biochem J* 2009;**424**: 61–67.
35. Kim S, Kim H, Ko D, Yamaoka Y, Otsuru M, Kawai-Yamada M *et al*. Rapid Induction of Lipid Droplets in *Chlamydomonas reinhardtii* and *Chlorella vulgaris* by Brefeldin A. *PLoS One* 2013; **8**, e81978.
36. Yamamoto K1, Takahara K, Oyadomari S, Okada T, Sato T, Harada A, *et al*. Induction of liver steatosis and lipid droplet formation in ATF6 alpha-knockout mice burdened with pharmacological endoplasmic reticulum stress. *Mol Biol Cell* 2010; **21**, 2975–2986.
37. Green DR, Galluzzi L, Kroemer G. Cell biology. Metabolic control of cell death. *Science* 2014; **345**: 1250256.
38. Tamura K, Dudley J, Nei M, Kumar S. MEGA4: molecular evolutionary genetics analysis (MEGA) software version 4.0. *Mol Biol Evol* 2007; **24**: 1596e9.
39. Sharrocks AD. The design of primers for PCR. In: Griffin HG, Griffin AM, (eds.) *PCR technology, current innovations*. London: CRC Press; 1994. p. 5e11.

40. Franzén O, Talavera-López C, Ochaya S, Butler CE, Messenger LA, Lewis MD et al. Comparative genomic analysis of human infective *Trypanosoma cruzi* lineages with the bat-restricted subspecies *T. cruzi marinkellei*. *BMC Genomics* 2012; **13**: 531.
41. Atale N, Gupta S, Yadav UC, Rani V. Cell-death assessment by fluorescent and nonfluorescent cytosolic and nuclear staining techniques. *J Microsc* 2014; **255**: 7-19.
42. Dhalia R1, Marinsek N, Reis CR, Katz R, Muniz JR, Standart N et al. The two eIF4A helicases in *Trypanosoma brucei* are functionally distinct. *Nucleic Acids Res* 2006; **34**: 2495-2507.

4.3 Artigo 3 - The Endoplasmic Reticulum Stress in Trypanosomatids

Artigo de opinião a ser submetido na revista indexada *Frontiers in Microbiology*, Qualis Capes A2 (Ciências Biológicas I), JCR 4,0. Neste manuscrito, discutimos sobre os recentes trabalhos envolvendo o estresse de retículo endoplasmático em diferentes espécies da família Trypanosomatidae.

The endoplasmic reticulum stress in trypanosomatids

[1,2,*]Jana Messias Sandes, [3]Danielle Maria Nascimento Moura, [1,+]Adriana Fontes and [2,+]Regina Célia Bressan Queiroz Figueiredo

[1] Departamento de Biofísica e Radiobiologia, Universidade Federal de Pernambuco, Recife, Pernambuco, Brazil.
[2] Departamento de Microbiologia, Centro de Pesquisas Aggeu Magalhães/FIOCRUZ-PE, Recife, Pernambuco, Brazil.
[3] Departamento de Imunologia, Centro de Pesquisas Aggeu Magalhães, Recife, Pernambuco, Brazil.

[*] Corresponding author
janasandes@gmail.com

[+] These authors contribute equally to this work

Running Title: ER stress in trypanosomatids

Key words: ER stress, unfolded protein response, *Trypanosoma cruzi*, *Leishmania*, *Trypanosoma brucei*, dithiothreitol, tunicamycin, thapsigargin.

Introduction

The endoplasmic reticulum (ER) is a vital organelle, being responsible for the folding and assembly of nascent polypeptides in the secretory pathway (Zhang and Ye, 2014). Cellular perturbations interfere with its folding capacity and induce ER stress (Iurlaro and Muñoz-Pinedo, 2015). The accumulation of newly synthesized unfolded proteins activates the unfolded protein response (UPR), which can contribute to reestablish the cell homeostasis or, under prolonged ER stress, trigger cell death mainly by apoptosis (Diehl et al., 2011). The UPR pathway is well characterized in higher eukaryotes but little is known about ER stress in protozoan parasites, such as the trypanosomatids. Some of them are responsible for several infectious diseases including leishmaniasis, caused by different species of *Leishmania*, Chagas' disease, caused by *Trypanosoma cruzi* and sleeping sickness, caused by *Trypanosoma brucei* (Bartholomeu et al., 2014). Recent studies applied pharmacological agents including dithiothreitol (DTT), which disrupts the protein disulfide bonds; tunicamycin (TM), which inhibits N-glycosylation; or thapsigargin (TG), which disrupts Ca^{2+} homeostasis, to study ER stress in these parasites (Dolai et al., 2011; Goldshmidt et al., 2010; Gosline et al., 2011; Koumandou et al, 2008; Sandes et al., 2016a and b; Tiengwe et al., 2015). However, their results were very discrepant among the different species and it is still unclear whether they have or not an UPR-like response. Thus, in this opinion article we attempted to compare all the works about ER stress in trypanosomatids in order to better understand the mechanisms involved in this process and also to provide information that may stimulate research interest in this area.

A brief review on ER stress in higher eukaryotes

The ER is a highly dynamic organelle involved in protein synthesis, folding and translocation, lipids synthesis, metabolism of carbohydrates and calcium homeostasis (Liu et al., 2015). To perform such functions the ER environment is precisely controlled by an oxidative compartment, with the presence of ER-resident chaperone proteins, such as BiP (binding protein), protein disulfide isomerase (PDI), calnexin (CNX) and calreticulin (CRT), as well as glycosylating enzymes (Brodsky and Skach, 2011). Perturbations in this environment induced by starvation, hypoxia, acidosis, glycosylation inhibition, and calcium or redox imbalances can lead to an ER stress condition, characterized by increased levels of unfolded/misfolded proteins in the ER lumen (Schönthal, 2012). This accumulation of unfolded proteins induces

the BiP dissociation of three ER transmembrane proteins to help in protein folding. These transmembrane proteins, PERK (PKR-like ER kinase), ATF6 (activating transcription factor 6) and IRE1 (Inositol-requiring enzyme 1), in turn, become activated and trigger the UPR, whose intracellular signal transduction pathways lead to global changes in gene expression in order to restore the cell homeostasis (Sovolyova et a., 2014).

PERK activation leads to eIF2α (α-subunit of the translation initiation factor eIF2) phosphorylation, which consequently promotes the attenuation of protein translation and induces the transcription of specific genes, as ATF4 (activating transcription factor-4) (Pagliassotti, 2012). ATF4 is responsible for inducing the expression of the pro-apoptotic transcription factor CHOP (C/EBP-homologous protein), and GADD34 (growth arrest and DNA damage–inducible 34), which dephosphorylates eIF2α to reestablish protein translation (Walter and Ron, 2011). The ATF6 pathway activation involves its translocation from the ER to the Golgi complex for proteolytic processing and then to the nucleus to activate the transcription of chaperones, such as BiP, which will assist in the folding of the misfolded proteins. ATF6 also induces the transcription of CHOP and XBP-1 (X-box protein), which will be subsequently processed by IRE1 (Szegezdi et al., 2006). IRE1 is a bifunctional protein that acts as a kinase and an endonuclease. When activated, IRE1 regulates the transcription of some ER-targeted mRNA, such as XBP-1 transcription factor, which is processed by splicing in the cytoplasm and then is translocated to the nucleus, where becomes competent to bind to the promoter of UPR target genes (Lai et al., 2007).

Taken together, the three UPR branches are responsible for: increasing chaperone expression, which prevents protein aggregation and facilitates correct protein folding; reducing the ER load, via translation inhibition induced by eIF2α phosphorylation; and for increasing the unfolded proteins degradation, via ER-associated degradation (ERAD) or autophagy (Rashid et al., 2015). If these steps fail to overcome the ER stress, the UPR then induces cell death usually by apoptosis (Iurlaro and Muñoz-Pinedo, 2015).

ER stress in trypanosomatids

Trypanosomes gene regulation is primarily posttranscriptional and, as they lack classical UPR machinery such as IRE1 and ATF6, the major response to ER stress in these cells is by mRNA stabilization of essential genes in order to reestablish cell homeostasis (Hope et al., 2014). These singularities make them an interesting subject of investigation, however only

few studies were found concerning this issue. In the following sections we will discuss the recent discoveries in this area and the major findings are summarized in Table 1.

ER stress in *Leishmania*

In *Leishmania major* the ER stress response seems to be related to UPR as Dolai et al. (2011) showed that the TM treatment (20 µg/mL) induced an increase in BiP expression and programmed cell death (PCD) phenotypes characteristic of apoptosis. TM-induced apoptosis included PS exposure, DNA fragmentation, intracellular release of Ca^{2+}, reactive oxygen species (ROS) production, mitochondrial membrane potential ($\Delta\Psi m$) depolarization and decline in ATP production. Some of these effects were abolished by the pretreatment with antioxidants, chemical chaperone (4-phenylbutyric acid) or Ca^{2+} chelators, but not with the caspase inhibitor benzyloxycarbonyl-VAD-fluoromethyl ketone or the metacaspase inhibitor antipain. In fact, several evidences have demonstrated that trypanosomatids may have features typical of apoptosis, although not having some of the key molecules that contribute to this process in metazoans, such as caspases genes and Bcl-2 family genes. Further, the role of metacaspases as executors of apoptosis in trypanosomatids still remains controversial (Smirlis et al., 2010).

Moreover, Gosline and colleagues (2011) showed that the ER stress response of *Leishmania donovani* may be different from *L. major,* as the first one showed no change in BiP protein levels when treated with TM (50 µg/mL) or DTT (1mM). The DTT-treated cells also exhibited increased eIF2α phosphorylation, which suggests that the PERK-eIF2a associated translational attenuation pathway would be active in this parasite. The authors did not evaluated the induction of PCD but observed that *L. donovani* is more sensitive to DTT than macrophages, which reinforces that the ER stress pathway would be an interesting target for the development of new chemotherapeutic agents.

ER stress in *T. brucei*

T. brucei is the most studied trypanosomatid regarding ER stress and Koumandou et al. (2008) were the first to evaluate possible transcriptional changes due to the ER stress in the bloodstream forms (BSF). Using drug concentrations that invoke UPR in higher eukaryote cells, 5 – 10 µg/mL TM or 1 – 10 mM DTT, they have found that TM treatment resulted in growth arrest within 24 h, while DTT exposure led to rapid cell death. Accordingly, for

transcriptome and BiP expression analysis they treated the cells with 5 µg/mL TM from 1 to 24 h, or 1 mM DTT from 1 to 4 h. However, they have not found significant changes in the transcriptome or in BiP expression by either treatment. Therefore, the authors suggested that *T. brucei* lacks the classical UPR response, which could explain its extreme sensitivity to DTT.

In another study, Goldshmidt and colleagues (2010) evaluated the response of procyclic forms (PCF) treated with 4 mM DTT. In transcriptome analysis many genes involved in the protein folding, lipid metabolism, mitochondrial functions and signal transduction were up-regulated between 1 and 3 h of treatment. They also observed increased mRNA stabilization of DNAJ, PDI, thioredoxin and syntaxin and increased levels of BiP protein. The expansion of the ER, the increased levels of the transcription factor tSNAP42 and the reduction in the transcription of the spliced-leader (SL) RNA led the authors to suggest that there is an ER stress response in trypanosomes, which was named SL silencing (SLS) and is responsible for inhibiting the trans-splicing of all nascent mRNA and consequently inducing PCD. Indeed, typical hallmarks of PCD such as phosphatidylserine (PS) exposure, increase of cytoplasmic Ca^{2+}, depolarization of the $\Delta\Psi m$ and ROS production were observed in treated cells. Some of these features were also found in BSF and the authors proposed that the SLS would not replace the UPR, but trigger PCD under severe ER stress in both stages of the parasite.

In contrast, a more recent research refuted the results of Goldshmidt and colleagues (2010) as the authors affirmed that UPR-like and SLS responses to persistent ER stress do not occur in BSF of *T. brucei* treated with DTT (0.5 mM), TM (200 ng/mL) or TG (5 µM) (Tiengwe et al., 2015). They also did not approve the use of DTT as ER stressor in BSF as it induces a potent redox stress and in their study the DTT was lethal at a concentration of 0.5 mM. However, it is possible that the major differences between the studies may be due to different stage responses, and is still unclear whether African trypanosomes possess a real UPR-like or SLS responses to ER stress.

ER stress in *T. cruzi*

T. cruzi presented different ER stress responses for DTT or TM treatment. According to the data obtained by our research group (Sandes et al., 2016a), DTT treatment (4 – 8 mM) did not elicit an UPR-like response in *T. cruzi*, as the cells maintained steady levels of BiP protein and showed a decrease in the BiP and CRT transcripts. This apparently contradiction may be

due to the induction of chaperones translation to sustain them at basal levels, even at lower mRNA availability, as in trypanosomatids the amount of mRNA is almost always determined by the rate of mRNA degradation and the expression of protein by the rates of translation initiation (Clayton, 2012). The persistent ER stress seems to target mainly the mitochondrion, inducing drastic morphological changes followed by ΔΨm depolarization and a high production of mitochondrial ROS. This suggests that the DTT action mechanism is caused mainly by the redox stress than the ER stress, in accordance to the study of Tiengwe et al. (2015). Some autophagic compartments were also found and may serve as a survival mechanism to try to restore the cell homeostasis. However, as the stress stimulus was persistent the treated parasites evolved to PCD by late apoptosis/necrosis.

The TM treatment had a strong trypanostatic effect in *T. cruzi* and induced an increase in mRNA levels of both BiP and CRT at 2.5 µg/mL, while the BiP protein levels remained unchanged (Sandes et al., 2016b). For the authors, a possible reason for this result is that a small population of nascent BiP would be induced as a response to TM treatment, however it is not enough to be detected by Western blotting. The persistent ER stress also induced the appearance of lipid inclusions and well-developed ER profiles surrounding cytoplasmic structures in degradation process, suggesting that an autophagic process is occurring. Indeed, TM treatment induced depolarization of the ΔΨm without pronounced ROS production and only few cells (≈10 %) presented apoptosis phenotype, which suggests that the autophagy is the major PCD participating in the TM-induced ER stress response.

177 **Table 1. The major findings involving ER stress response in trypanosomatids**

Species	Stage	Compound	Major findings	References
T. brucei	BSF	DTT (0.5 mM)	No alteration in BiP expression	[1]
		DTT (1 mM)	No alteration in BiP expression	[2]
		DTT (4 mM)	Increased levels of BiP protein SLS	[3]
		TM (200 ng/mL)	No alteration in BiP expression	[1]
		TM (5µg/mL)	No alteration in BiP expression	[2]
		TG (5 µM)	No alteration in BiP expression	[1]
	PCF	DTT (4 mM)	Increased mRNA stabilization of DNAJ, PDI, thioredoxin and syntaxin Increased levels of BiP and tSNAP42 protein ER expansion PS exposure Increased cytoplasmic Ca^{2+} ΔΨm depolarization ROS production SLS	[3]
L. major	PRO	TM (20µg/mL)	Increased levels of BiP protein PS exposure DNA fragmentation Increased cytoplasmic Ca^{2+} ΔΨm depolarization ROS production Reduced ATP levels	[4]
L. donovani	PRO	DTT (1 mM)	No alteration in BiP expression Increased eIF2α phosphorylation	[5]
		TM (50 µg/mL)	No alteration in BiP expression No phosphorylation of eIF2a	
	AMA	DTT (1 mM)	More cytotoxic to parasite than macrophages	
T. cruzi	EPI	DTT (4 - 8 mM)	No alteration in BiP protein levels Reduced levels of BiP and CRT mRNAs Mitochondrion swelling ΔΨm depolarization ROS production Autophagosomes PS exposure Loss of PM integrity	[6]
	EPI	TM (2.5 - 20µg/mL)	No alteration in BiP protein levels Increased mRNA levels of BiP and CRT ΔΨm depolarization ROS production Autophagosomes	[7]

178 **Legend:** SLS, spliced leader RNA silencing; ΔΨm, mitochondrial membrane potential; PS,
179 phosphatidylserine; PM, plasma membrane; BSF, bloodstream form; PCF, procyclic form; PRO,
180 promastigote form; AMA, amastigote form; EPI, epimastigote form. [1] = Tiengwe et al., 2015; [2] =
181 Koumandou et al, 2008; [3] = Goldshmidt et al., 2010; [4] = Dolai et al., 2011; [5] = Gosline et al.,
182 2011; [6] = Sandes et al., 2016 a; [7] = Sandes et al., 2016 b.

Conclusions

In recent years the interest in studying the role of ER stress and the existence of an UPR-like response in trypanosomes have increased in attempt to contribute with the knowledge about the basic biology of these protozoans, as well as to provide subsidies for future researches interfere in essential pathways related to these parasites survival, as there are no vaccines for these diseases and available treatments are inefficient.

The different ER stress responses found among the trypanosomatids may be due to the difficulty of achieving the exact concentration and time of treatment that really induces the ER stress as well as the intrinsic susceptibility/resistance to the treatment for each evolutive form/parasite specie. Although more studies are still needed to better evaluate whether or not the UPR occurs in these parasites, this article highlights the importance to standardize the drug concentration and to evaluate different mechanisms of action before ensures that there is an UPR-like pathway in trypanosomatids.

Acknowledgments

This work was supported by CPqAM/FIOCRUZ and FACEPE.

The Author Contributions Statement

JS, DM, AF and RF wrote and reviewed the manuscript text.

205 **References**

206

207 Bartholomeu, D.C., de Paiva, R.M., Mendes, T.A., DaRocha, W.D., Teixeira, S.M. (2014).
208 Unveiling the intracellular survival gene kit of trypanosomatid parasites. *PLoS Pathog.*
209 10(12):e1004399. doi: 10.1371/journal.ppat.1004399

210 Brodsky, J.L., Skach, W.R. (2011). Protein folding and quality control in the endoplasmic
211 reticulum: Recent lessons from yeast and mammalian cell systems. *Curr Opin Cell Biol.*
212 23, 464-475. doi: 10.1016/j.ceb.2011.05.004

213 Clayton, C. (2012). "mRNA turnover in Trypanosomes," in: *Nucleic acids and molecular*
214 *biology*, ed. Albrecht, B. (28, Ch Springer-Verlag Berlin Heidelberg)

215 Diehl, J.A., Fuchs, S.Y. Koumenis, C. (2011). The cell biology of the unfolded protein
216 response. *Gastroenterology*. 141, 38-41. doi: 10.1053/j.gastro.2011.05.018

217 Dolai, S., Swati, P., Yadav, R.K., Adak, S. (2011). Endoplasmic reticulum stress-induced
218 apoptosis in *Leishmania* through Ca2+-dependent and caspase independent mechanism. *J*
219 *Biol Chem.* 286, 13638-13646. doi:10.1074/jbc.M110.201889

220 Goldshmidt, H., Matas, D., Kabi, A., Carmi, S., Hope, R., Michaeli, S. (2010). Persistent ER
221 stress induces the spliced leader RNA silencing pathway (SLS), leading to programmed
222 cell death in *Trypanosoma brucei*. *Plos Pathog.* 6, e1000731. doi:
223 10.1371/journal.ppat.1000731

224 Gosline, S.J., Nascimento, M., Mccall, L.I., Zilberstein, D., Thomas, D.Y., Matlashewski, G.,
225 Hallett, M. (2011). Intracellular eukaryotic parasites have a distinct unfolded protein
226 response. *PLoS One*. 6, e19118. doi: 10.1371/journal.pone.0019118

227 Hope, R., Ben-Mayor, E., Friedman, N., Voloshin, K., Biswas, D., Matas, D., Drori, Y.,
228 Günzl, A., Michaeli, S. (2014). Phosphorylation of the TATA-binding protein activates the
229 spliced leader silencing pathway in *Trypanosoma brucei*. *Sci Signal*. 7(341):ra85. doi:
230 10.1126/scisignal.2005234

231 Iurlaro, R., Muñoz-Pinedo, C. (2015). Cell death induced by endoplasmic reticulum stress.
232 *FEBS J*. doi: 10.1111/febs.13598

233 Koumandou, V.L., Natesan, S.K., Sergeenko, T., Field, M.C. (2008). The trypanosome
234 transcriptome is remodelled during differentiation but displays limited responsiveness
235 within life stages. *BMC Genomics*. 9: 298-326. doi: 10.1186/1471-2164-9-298

236 Lai, E., Teodoro, T., Volchuk, A. (2007). Endoplasmic reticulum stress: signaling the
237 unfolded protein response. *Physiology (Bethesda).* 22: 193-201. doi:
238 10.1152/physiol.00050.2006

239 Liu, Z., Lv, Y., Zhao, N., Guan, G., Wang, J. (2015). Protein kinase R-like ER kinase and its
240 role in endoplasmic reticulum stress-decided cell fate. *Cell Death Dis.* 6:e1822. doi:
241 10.1038/cddis.2015.183
242 Pagliassotti, M.J. (2012). Endoplasmic reticulum stress in nonalcoholic fatty liver disease.
243 *Annu Rev Nutr*. 32: 17-33. doi: 10.1146/annurev-nutr-071811-150644
244 Rashid, H.O., Yadav, R.K., Kim, H.R., Chae, H.J. (2015). ER stress: Autophagy induction,
245 inhibition and selection. *Autophagy*. 11(11):1956-1977.
246 doi:10.1080/15548627.2015.1091141
247 Sandes JM, Moura DMN, Santiago MDS, de Lima GB, Cabral Filho PE, Albuquerque SCG,
248 Cavalcanti MP, Figueiredo RCBQ, Fontes A. The effects of the endoplasmic reticulum
249 stressor agent dithiothreitol (DTT) on *Trypanosoma cruzi*. 2016 a. Unpublished data.
250 Sandes JM, Moura DMN, Santiago MDS, de Lima GB, Cabral Filho PE, Albuquerque SCG,
251 Cavalcanti MP, Figueiredo RCBQ, Fontes A. Endoplasmic Reticulum Stress Induced by
252 Tunicamycin on *Trypanosoma cruzi*. 2016 b. Unpublished data.
253 Schönthal, A.H. (2012). Endoplasmic reticulum stress: its role in disease and novel prospects
254 for therapy. *Scientifica* (Cairo). 2012:857516. doi: 10.6064/2012/857516
255 Smirlis, D., Duszenko, M., Ruiz, A.J., Scoulica, E., Bastien, P., Fasel., N. *et al.* (2010).
256 Targeting essential pathways in trypanosomatids gives insights into protozoan mechanisms
257 of cell death. *Parasit Vectors*. 3:107. doi: 10.1186/1756-3305-3-107
258 Sovolyova, N., Healy, S., Samali, A., Logue, S.E. (2014). Stressed to death - mechanisms of
259 ER stress-induced cell death. *Biol Chem*. 395(1):1-13. doi: 10.1515/hsz-2013-0174
260 Szegezdi, E., Logue, S.E., Gorman, A.M., Samali, A. (2006). Mediators of endoplasmic
261 reticulum stress-induced apoptosis. *EMBO Rep.* 7(9):880-5. doi:
262 10.1038/sj.embor.7400779
263 Tiengwe, C., Brown, A.E., Bangs, J.D. (2015). Unfolded Protein Response Pathways in
264 Bloodstream-Form *Trypanosoma brucei*? *Eukaryot Cell.* 14(11):1094-101. doi:
265 10.1128/EC.00118-15
266 Walter, P., Ron, D. (2011). The unfolded protein response: from stress pathway to
267 homeostatic regulation. *Science*. 334: 1081-1086. doi: 10.1126/science.1209038
268 Zhang, T., Ye, Y. (2014). The final moments of misfolded proteins en route to the
269 proteasome. *DNA Cell Biol*. 33: 477-83. doi:10.1089/dna.2014.2452

5 CONCLUSÕES

- O DTT apresenta atividade tripanostática e tripanocida sobre o *T. cruzi*, como é possível observar pela forte inibição do crescimento de maneira dose-dependente. No entanto, a recuperação do crescimento após a retirada do DTT demonstra que o *T. cruzi* tem uma maior resistência ao tratamento quando comparado com *T. brucei*.

- A TM apresenta uma forte atividade tripanostática sobre o *T. cruzi*, como observado pela inibição do crescimento de maneira independente do tempo ou da concentração, sem recuperação do crescimento após a retirada da droga.

- Os tratamentos com DTT ou TM não são capazes de induzir a resposta clássica da UPR em *T. cruzi* nas condições avaliadas, como observado pela ausência do aumento dos níveis proteicos da chaperona BiP.

- A mitocôndria parece ser o alvo intracelular principal do DTT, como demonstrado pelas drásticas alterações ultraestruturais, pela redução do potencial de membrana mitocondrial e pelo aumento na produção de ROS.

- A persistência do tratamento com o DTT pode induzir vias de MCP características de apoptose tardia/ necrose. No entanto, a presença de autofagossomos sugere que a autofagia possa estar acontecendo em conjunto com as outras vias.

- O tratamento com a TM induz uma resposta específica ao estresse de RE, como observado pelo aumento dos níveis de RNAm de BiP e CRT, por alterar o número de perfis de RE e possivelmente o transporte de proteínas até o complexo de Golgi, culminando na degradação da célula pela autofagia/ER-fagia.

APÊNDICE A – Artigo Publicado

Artigo publicado na revista indexada PLoS One, qualis Capes Ciências Biológicas 1 - A2: "***Trypanosoma cruzi* Cell Death Induced by the Morita-Baylis-Hillman Adduct 3-Hydroxy-2-Methylene-3-(4-Nitrophenylpropanenitrile)**". Este estudo relaciona as ferramentas de microscopia confocal a laser e citometria de fluxo para tentar discriminar os diferentes fenótipos de morte celular programada induzidos pelo composto MBHA 3 em formas epimastigotas de *T. cruzi*.

OPEN ACCESS Freely available online

PLOS ONE

Trypanosoma cruzi Cell Death Induced by the Morita-Baylis-Hillman Adduct 3-Hydroxy-2-Methylene-3-(4-Nitrophenylpropanenitrile)

Jana M. Sandes[1], Adriana Fontes[2], Carlos G. Regis-da-Silva[3], Maria C. A. Brelaz de Castro[4], Claudio G. Lima-Junior[5], Fábio P. L. Silva[5], Mário L. A. A. Vasconcellos[5], Regina C. B. Q. Figueiredo[1]*

1 Departamento de Microbiologia, Centro de Pesquisas Aggeu Magalhães, Recife, PE, Brazil, **2** Departamento de Biofísica e Radiobiologia, Universidade Federal de Pernambuco, Recife, PE, Brazil, **3** Laboratorio de Biologia Parasitaria, Centro Pesquisas Gonçalo Moniz, Salvador, BA, Brazil, **4** Departamento de Imunologia, Centro de Pesquisas Aggeu Magalhães, Recife, PE, Brazil, **5** LASOM-PB, Departamento de Química, Universidade Federal da Paraíba, João Pessoa, PB, Brazil

Abstract

Chagas disease, caused by the protozoan *Trypanosoma cruzi*, remains a serious health concern due to the lack of effective vaccines or satisfactory treatment. In the search for new compounds against this neglected disease, we have previously demonstrated that the compound 3-Hydroxy-2-methylene-3-(4-nitrophenylpropanenitrile) (MBHA3), derived from the Morita-Baylis-Hillman reaction, effectively caused a loss of viability in both the epimastigote and trypomastigote forms. However, the mechanisms of parasite death elicited by MBHA3 remain unknown. The aim of this study was to better understand the morphophysiological changes and the mechanism of cell death induced by MBHA3 treatment on *T. cruzi*. To perform this analysis, we used confocal microscopy and flow cytometry to monitor the fluorescent probes such as annexin-V/propidium iodide (AV/PI), calcein-AM/ethidium homodimer (CA/EH), acridine orange (AO) and rhodamine 123 (Rho 123). Lower concentrations of MBHA3 led to alterations in the mitochondrial membrane potential and AO labeling, but did not decrease the viability of the epimastiogote forms, as determined by the CA/EH and AV/PI assays. Conversely, treatment with higher concentrations of MBHA3 led to extensive plasma membrane damage, loss of mitochondrion membrane potential, DNA fragmentation and acidification of the cytoplasm. Our findings suggest that at higher concentrations, MBHA3 induces *T. cruzi* epimastigote death by necrosis in a mitochondrion-dependent manner.

Citation: Sandes JM, Fontes A, Regis-da-Silva CG, de Castro MCABrelaz, Lima-Junior CG, et al. (2014) *Trypanosoma cruzi* Cell Death Induced by the Morita-Baylis-Hillman Adduct 3-Hydroxy-2-Methylene-3-(4-Nitrophenylpropanenitrile). PLoS ONE 9(4): e93936. doi:10.1371/journal.pone.0093936

Editor: Herbert B. Tanowitz, Albert Einstein College of Medicine, United States of America

Received January 14, 2014; **Accepted** March 9, 2014; **Published** April 8, 2014

Funding: This work was supported by CNPq, FIOCRUZ/CPQAM, PDTIS/FIOCRUZ and FACEPE. The funders had no role in study design, data collection and analysis, decision to publish, or preparation of the manuscript.

Competing Interests: The authors have declared that no competing interest exist.

* E-mail: bressan@cpqam.fiocruz.br

Introduction

Trypanosoma cruzi, the etiological agent of Chagas disease, is one of the most serious infectious pathogens to humans, with 10 million people infected worldwide, mostly in Latin America, and 100 million people at risk of acquiring Chagas disease. Despite their high toxicity, the drugs nifurtimox and benznidazole are the only available treatment for this illness. Although these drugs are effective against acute infections, their efficacy in the chronic phase of the disease remains controversial, and no consensus on the evaluation of a parasitological cure has been achieved [1]. In this regard, the development of more effective, low cost drugs, without significant side effects is still needed for the treatment of Chagas disease.

In a search for new compounds against Chagas disease, we have previously demonstrated that the incubation of parasites with the Morita-Baylis-Hillman adduct, 3-Hydroxy-2-methylene-3-(4-nitrophenylpropanenitrile, MBHA3 (Figure 1), had profound effects on the growth of epimastigotes forms and caused a loss of trypomastigote viability, with IC_{50}/LC_{50} for epi- and trypomastigotes of 28.5 and 25.5 μM respectively. Ultrastructural analysis of *T. cruzi* treated with MBHA3 revealed morphological characteristics of programmed cell death (PCD) [2].

PCD is a genetically regulated active process that plays a central role in the development and homeostasis of multicellular organisms and is associated with a wide variety of human diseases, including immunological and developmental disorders, neurodegeneration and cancer. Cell death involves three major mechanisms: apoptosis, autophagy and necrosis [3]. Apoptosis is an orchestrated process that occurs in both normal and pathological conditions. The morphological hallmarks of apoptosis include chromatin condensation and nuclear fragmentation, which are usually followed by a rounding up of cells. Finally, apoptotic cells give rise to small round bodies that are surrounded by a membrane and contain intact organelles and nuclear fragments [4]. In addition to the morphological changes, three main biochemical events can be observed in cells undergo apoptosis 1) caspase activation, 2) DNA and protein breakdown and 3) phosphatidylserine exposition in the outer layer of plasma membrane [5]. Autophagy is a physiological mechanism that involves the sequestration of excess, old and unneeded cytoplasmic organelles and long-lived macromolecules, into large double-membrane vesicles, called autophagosomes, followed by subsequent delivery of the cargo into lysosomes for degradation,

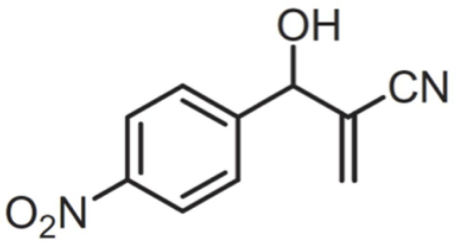

Figure 1. Chemical structure of MBHA3.
doi:10.1371/journal.pone.0093936.g001

with no inflammatory response [6–8]. Necrosis is usually defined as a process of cell collapse that involves an increase in cell volume (oncosis), which ultimately leads to plasma membrane rupture and the unorganized dismantling of swollen organelles [9]. Apart from the presence of plasma membrane permeabilization, necrosis lacks specific biochemical markers.

Essential features of PCD, such as the genes encoding the basic cell death machinery and their morphological and biochemical characteristics, appear to be conserved in nematodes, [10–11], insects [12–13] and vertebrates (mammals) [14]. As in multicellular organisms, it has been demonstrated that various stimuli, such as drugs, oxidative stress, starvation, exposure to human serum, inhibition of signaling molecules, etc., are able to elicit a PCD-like response in an increasing number of unicellular eukaryotic species [15], including kinetoplastid parasites of the genus *Leishmania* [16–17] and *Trypanosoma* [2,18]. Although electron microscopy has proven to be useful for the identification of drug target organelles and the determination of PCD phenotypes [19], in the case of MBHA3-induced cell death, this tool was not sufficiently robust to unequivocally discriminate between different phenotypes of PCD [2]. Therefore, we used the combination of confocal microscopy, flow cytometry, and fluorescent probes to examine the mechanisms involved in *T. cruzi* epimastigote death induced by MBHA3. Understanding the mechanism involved in the drug-induced cell death of this parasite may provide insights into the pathogenesis of Chagas disease and help to better develop therapies against this illness.

Materials and Methods

Drug treatment

The MBHA3 compound (Figure 1) was synthesized and characterized as previously described [20]. The MBHA3 was initially dissolved in dimethyl sulfoxide (DMSO) at a concentration of 250 mM. This solution was diluted into culture medium to obtain a stock solution at 5 mM (stock solution). The stock solution was diluted again in the culture medium to obtain concentrations of 28.5, 57.0 and 114.0 μM, which correspond to the previously determined values of IC_{50}, 2x IC_{50} and 4x IC_{50} after 72 hours of treatment respectively [2]. Throughout the experimental procedures the concentration of DMSO never exceeded 0.05%, which is non-toxic to the protozoa.

Parasites

All experiments were carried out using *T. cruzi* epimastigote forms (Dm28c) from axenic cultures, maintained in liver infusion tryptose (LIT) medium supplemented with 10% fetal bovine serum (FBS) at 28°C and harvested during the exponential phase of growth.

Annexin V and propidium iodide labeling

Parasites, that were non-treated or treated with different concentrations of MBHA3 for 24, 48 and 72 hours, were incubated with an Annexin V-FITC Apoptosis Detection Kit (Sigma-Aldrich, St Louis, USA) following the manufacturer's instructions. Briefly, after drug treatment, the parasites were harvested by centrifugation, washed with PBS and incubated for 15 minutes at 28°C with 5 μg/mL annexin-V-FITC (AV) and 10 μg/mL propidium iodide (PI) diluted in annexin-V binding buffer. Next, the cells were centrifuged, resuspended in phosphate buffered saline (PBS) and immediately analyzed on a laser confocal scanning microscope or flow cytometer. For confocal microscopy, both probes were excited with a 488 nm diode laser and the fluorescence emission was recorded at 510 and 560 nm for AV and PI respectively. The samples were observed under a Leica SPII/AOBS (Mannheim, Germany) scanning confocal microscope. Dual-parameter flow cytometric analysis was performed with the flow cytometer FACS-Calibur (Becton-Dickinson, San Jose, CA, USA), using a 530/30 nm signal detector (FL1-H) for AV-FITC and a 582/42 nm PI emission signal detector (FL2-H). The fluorescence intensity was acquired for 20,000 events, and the data were analyzed using Cell-Quest™ (Becton–Dickinson, San Jose) and expressed as the percentage of cells in each population phenotype (unstained, stained only with PI, stained only with AV or stained with both markers) compared to the total number of cells analyzed.

Live/Dead assay

Cell viability was assessed by a LIVE/DEAD Viability/Cytotoxicity Kit (Molecular Probes, Eugene, Oregon, USA). Control (non treated) and MBHA3-treated parasites were harvested by centrifugation after 72 hours of incubation and resuspended in 0.5 mL PBS containing 0.1 μM of calcein and 8 μM of ethidium homodimer. Samples were incubated for 30 minutes at room temperature and immediately analyzed by flow cytometry with a 530/30 nm filter (FL1-H) for calcein and a 670 nm long pass filter (FL3-H) for the ethidium homodimer. For confocal microcopy, treated and control cells were incubated in PBS with 4 μM of calcein and 4 μM of ethidium homodimer. Cells were observed using a 488 nm laser and, images were acquired and analyzed using the same parameters described for the AV/PI labeled-cells.

Rhodamine 123 (Rho) and acridine orange (AO) assays

Treated and non-treated parasites were washed and resuspended in 0.5 mL PBS with 10 μg/mL Rho 123 (Sigma-Aldrich, St Louis, USA) or 10 μg/mL AO (Sigma-Aldrich, St Louis, USA) for 20 minutes. After loading, the parasites were washed in PBS and immediately analyzed by flow cytometry, and the fluorescence intensities for AO (acid compartments) and Rho 123 (mitochondrial membrane potential) were quantified. A total of 20,000 events were acquired in the region previously established as corresponding to *T. cruzi* epimastigotes, based on the forward (FSC) and side (SSC) scatter. Alterations in the fluorescence intensities of Rho 123 (FL1-H) or AO (FL3-H) were quantified by the index of variation (IV) that was obtained by the equation (TM − CM)/CM, where TM is the median of fluorescence for treated parasites and CM is that of the control (non-treated). AO-labeled parasites were also observed by a confocal microscope using 488 and 543 nm lasers.

Table 1. Flow cytometric analysis of *T. cruzi* epimastigotes treated with MBHA3 and labeled with Annexin V/propidium iodide.

	% cells											
AV/PI	**Control**			**1x IC_{50}**			**2x IC_{50}**			**4xIC_{50}**		
	24 h	**48 h**	**72 h**	**24 h**	**48 h**	**72 h**	**24 h**	**48 h**	**72 h**	**24 h**	**48 h**	**72 h**
AV^-/PI^-	99.18	98.87	98.75	98.7	97.26	95.2	98.77	95.07	90.61	57.66	57.88	28.7
AV^+/PI^-	0.54	0.66	0.85	0.68	1.93	3.21	0.59	1.94	3.42	1.13	2.43	8.84
AV^+/PI^+	0.17	0.33	0.31	0.46	0.58	1.25	0.36	2.24	4.87	31.95	37.39	42.18
AV^-/PI^+	0.11	0.14	0.09	0.16	0.23	0.34	0.28	0.75	1.10	9.76	12.30	20.28

*The values represent the mean of two independent experiments.
doi:10.1371/journal.pone.0093936.t001

DNA fragmentation

After 72 hours of incubation with MBHA3, treated and untreated parasites were harvested by centrifugation, washed in PBS and assayed for DNA fragmentation as previously described [21]. Briefly, the cells pellets (10^7 epimastigotes) were lysed with sarkosyl detergent lysis buffer (50 mM Tris, 10 mM EDTA, 0.5% w/v sodium-N-lauryl sarcosine, pH 7.5) and the supernatant digested with proteinase K (20 mg/mL) for 2 hours at 50°C. The sample was then treated with RNase A (0.3 mg/mL) for 1 hour at 37°C. The lysates were then extracted with phenol/chloroform (25:24), precipitated in cold ethanol and subjected to electrophoresis on 1% agarose gels containing ethidium bromide. DNA fragments were visualized under UV light.

Results

Effects of MBHA3 on the viability of *T. cruzi*

Annexin V is a Ca^{2+}-dependent phospholipid-binding protein with a high affinity for phosphatidylserine, whereas PI is a cell-impermeant fluorescent dye that intercalates DNA and RNA of cells whose plasma membrane integrity has been lost. By using these fluorescent markers, our flow cytometry analysis showed increased cell death in parasites treated with MBHA3, with major differences detected in cells treated with the 4x IC_{50}/72 h. Regardless of the incubation time, at lower concentrations of the drugs (1x and 2x IC_{50}), the percentage of non-apoptotic/intact cells (AV^-/PI^-) was always greater than 90%. Late apoptotic (AV^+/PI^+) and necrotic phenotypes (AV^-/PI^+) were preponderant in cells treated with 4x IC_{50}/72 h, corresponding to approximately 63% of cell population, while 8.84% of the epimastigote population was AV^+/PI^-, and 28.7% of cells were negative for both markers (AV^-/PI^-) (Table 1). Because the effects of MBHA3 were more noticeable at 72 hours, we used this incubation time for all further analysis. Confocal microscopy assays of cells labeled with AV/PI corroborated the data obtained by flow cytometry. Incubation of epimastigotes with 28.5 μM of MBHA3 (1x IC_{50}) (Figure 2) did not yield a substantial labeling for either markers compared to the control, for which most of the cells were unstained (AV^-/PI^-) after treatment. Conversely, at drug concentrations corresponding to the 2x and the 4x IC_{50} values, an increase of AV^+/PI^-, AV^+/PI^+ and AV^-/PI^+ phenotypes, which are indicative of intense cell death, could be observed. Morphological changes associated with apoptosis, such as nuclear material trapped in plasma membrane blebs, were also observed in AV^+/PI^+ positive cells treated with the 2x IC_{50} (Figure 2, inset). A large number of cells undergoing necrosis cell death without the translocation of phosphatidylserine (AV^-/PI^+) were mostly detected at the 4x IC_{50}.

In an attempt to clarify whether non-apoptotic/intact parasites presenting an AV^-/PI^- phenotype, undoubtedly corresponded to viable cells, the Calcein-AM (CA) and ethidium homodimer-1 (EH) live/dead viability test was performed. Flow cytometric analysis showed a dose-dependent decrease of CA^+/EH^- cells, followed by a corresponding increase in CA^+/EH^+ and CA^-/EH^+ cells (Figure 3). It is important to note that even in those cells stained only with CA, a considerable decrease in the fluorescence intensity for this marker could be observed at the 2x IC_{50} of MBHA3 (Figure 3C). In all concentrations, the double-negative cells (CA^-/EH^-) did not reach rates higher than 10% of the total of cell population.

The confocal images showed that most untreated cells exhibited homogeneous, bright calcein green fluorescence in the cytoplasm, nucleus and kinetoplast, while few cells were stained red (CA^+/EH^-) (Figure 4). No considerable difference in this profile could be

detected in cells incubated with IC_{50} of MBHA3. However, in cells treated at the 2x IC_{50} of MBHA3, the labeling pattern of CA was affected, and a punctuated and heterogeneous labeling became evident, indicating a gradual loss of esterase activity. A considerable decrease in the CA^+/EH^- population and increase in the CA^+/EH^+ population could be observed in cells treated with the 4x IC_{50}.

Consistent with the findings above, the treatment of cells with the 2x IC_{50} and the 4x IC_{50} of MBHA3 or 4 mM of H_2O_2 (used as a positive control for inducing cells death) led to an increased DNA smearing, a characteristic of autolytic DNA breakdown, compared to the IC_{50}-treated cells and the control (Figure 5).

Effects of MBHA3 on the acidic compartments of *T. cruzi*

The treatment of epimastigotes with the IC_{50} and 2x IC_{50} of MBHA3 led to an increase in the AO red fluorescence intensity, as observed by flow cytometry (Figure 6A). This result was confirmed by positive IV values of +2.01 and +1.9 for the IC_{50} and the 2x IC_{50} MBHA3, respectively. However, at the higher drug concentration, a striking decrease of AO red fluorescence could be observed (IV = −0.9). To test whether the increase of red fluorescence at lower drug concentrations was due to an increase in the number of acidic compartments or to general cytoplasm acidification, control and treated cells were observed by confocal microscopy. Control cells stained with AO presented a well-preserved morphology with bright green labeling in the nucleus and kinetoplast and a pale green fluorescence in the cytoplasm (Figure 6B). Red fluorescence was detected mainly within large organelles located at the posterior end of the cells, which correspond to the reservosome, a pre-lysosomal compartment in epimastigote forms. Small red vesicles were observed randomly distributed throughout the cytoplasm. In the IC_{50}-treated cells, we observed a discrete increase in the number of red-labeled compartments and a few cells already presenting nuclear alterations (Figure 6C). Treatment with the 2x IC_{50} of MBHA3 caused a decrease in the green fluorescence and acidification of the cytoplasm (Figure 6D). At this concentration, the effects of the drug on the parasite nucleus became more pronounced, with intense nuclear pyknosis and karyorrhexis (Figure 6D, inset). Dramatic morphological changes, including cell body swelling and a completely loss of red labeling could be observed in most of cells at the higher MBHA3 concentration (Figure 6E).

Effects of MBHA3 on the mitochondrial membrane potential of *T. cruzi*

To determine whether MBHA3-induced PCD of parasites was related to an alteration of the mitochondrial membrane potential ($\Delta\psi m$), we performed flow cytometry using Rho 123 staining. Incubation of the parasites with the IC_{50} of MBHA3 had no drastic impact on Rho 123 fluorescence intensity, as demonstrated by flow cytometry. The IV value at this concentration was −0.02. Conversely, at higher concentrations of MBHA3, gradual mitochondrion depolarization could be observed (Figure 7), with IV values of −0.64 and −0.87 at 2x IC_{50} and 4x IC_{50} of MBHA3, respectively.

Discussion

Chagas disease, caused by the protozoa *Trypanosoma cruzi*, remains a serious health concern due a lack of effective vaccines and treatments. Efforts to control this endemic illness are based on therapeutic drugs, which have serious side effects and low efficacy during the chronic phase of disease. In addition, drug resistance has increased, and the cost of treatment is extremely expensive for most affected people. Thus, a search for new anti-parasitic agents for Chagas disease that have low patient toxicity and low cost is needed [22].

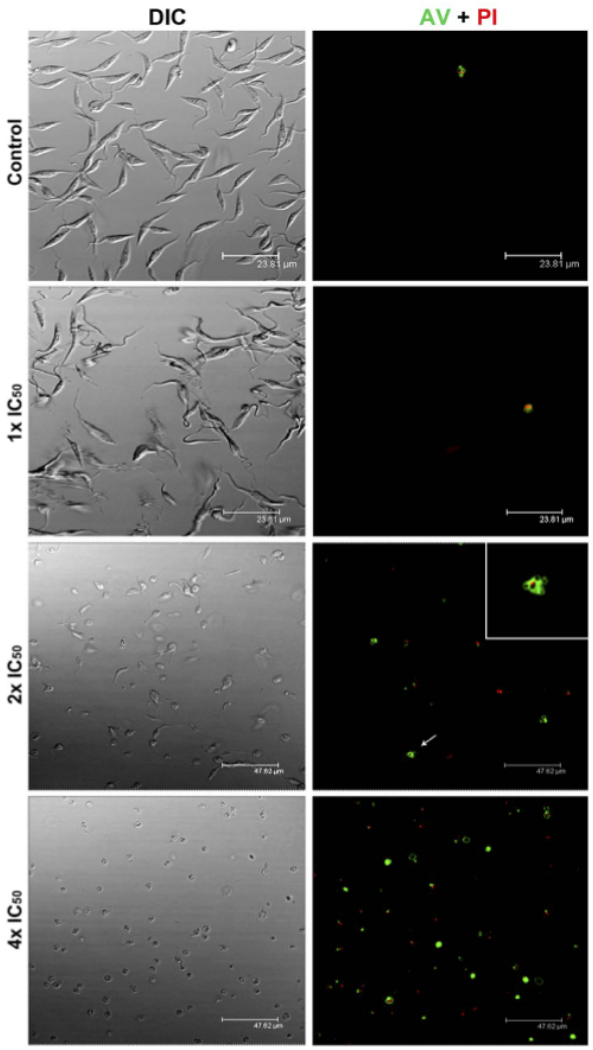

Figure 2. Effects of BMHA3 treatment on Anexin V/PI labeling. Confocal microcopy analysis of control and MBHA3-treated parasites labeled with AV/PI, after 72 hours of incubation. Note the presence of AV and PI double positive cells presenting membrane blebs at the 2x IC_{50} of MBHA3 (arrow and inset). Drastic morphological changes could be observed by differential interference contrast (DIC, left column) at the 2x and the 4x IC_{50} of MBHA3.
doi:10.1371/journal.pone.0093936.g002

The Morita–Baylis–Hillman (MBH) reaction is a low cost, atom-efficient condensation method that provides easy access to highly functionalized carbonyl derivatives [20,23]. MBH adducts are extensively used in the synthesis as versatile starting materials for many natural products and drugs. Previous work carried out by our group showed that at low concentrations, the compound 3-Hydroxy-2-methylene-3-(4-nitrophenylpropanenitrile), derived from the Morita-Baylis-Hillman reaction, effectively inhibited epimastigote growth and led to a decrease in trypomastigote viability. Ultrastructural analysis of treated-cells showed morphological characteristic that are associated with programmed cell

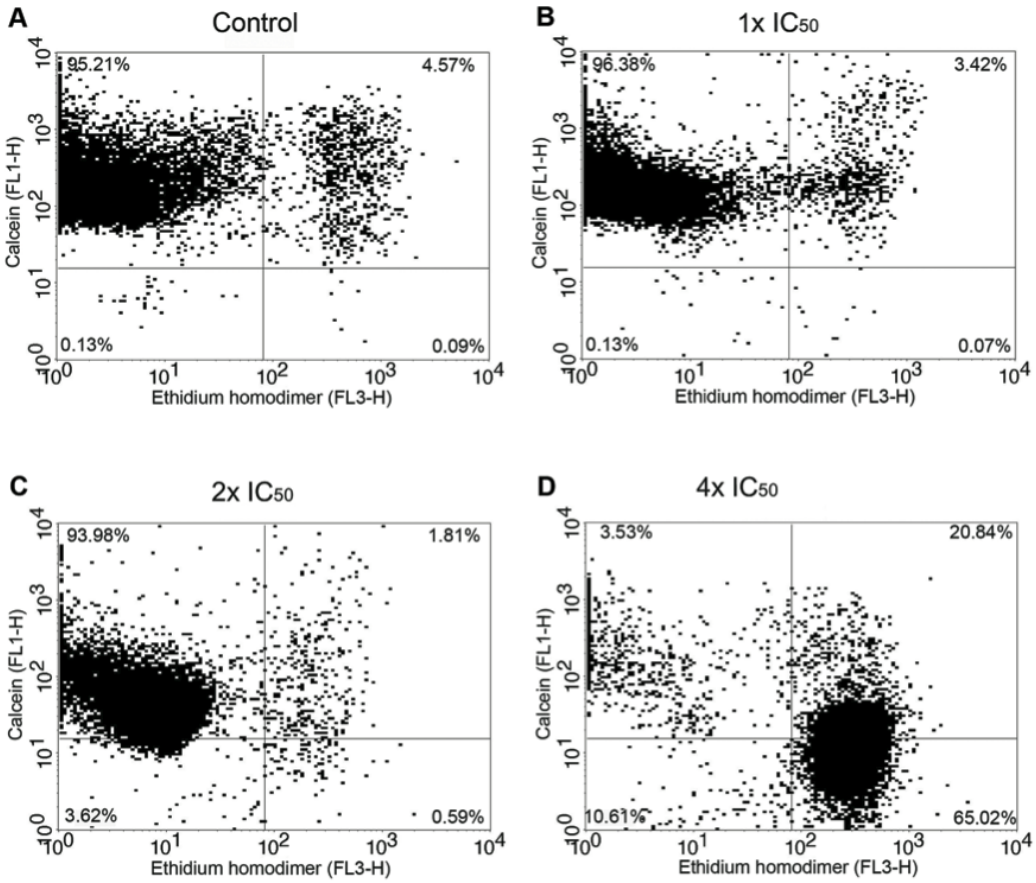

Figure 3. Cytometry analysis of the effects of MBHA3 on Calcein AM/EH. Flow cytometric dot plots of control (A) and MBHA3-treated cells (B – D) labelled with CA/EH. Cells in the upper left quadrant were positive only for calcein. Cells in the lower right quadrant were positive only for ethidium heterodimer. Events in the upper right quadrant were double positive for both markers, whereas the lower left quadrant corresponds to the cells negative for the both dyes. The dot plots are representative of duplicate experiments with similar results. There were 20,000 recorded events/experimental condition.
doi:10.1371/journal.pone.0093936.g003

death. However, the mechanisms of cell death elicited by MBHA3 treatment remain unknown [2].

In this work, we examined the effects of MBHA3 on the epimastigote form of *T. cruzi*. By using fluorescent markers, we attempted to better characterize the morphophysiological changes and the mechanism of cell death induced by MBHA3. Although this evolutive stage of the parasite is non-infective, epimastigotes are easily analyzed under confocal microscopy and flow cytometry; therefore, they are more suitable than trypomastigotes in physiological studies. Although there is experimental evidence that the mechanisms of cell death found in multicellular organisms are also present in unicellular organisms, including trypanosomatids, the evaluation of cell death in these parasites remains challenging [24]. For example, genes encoding caspases and death receptors, which are involved in cell death by apoptosis, are absent in trypanosomatids [25]. Thus, most studies on cell death in these microorganisms are still based on morphological parameters, mainly examined by transmission and scanning electron microscopy [26]. Although these techniques can provide valuable clues related to PCD in parasites, the ability to follow this process by direct live cell imaging is critical to better understanding the entire process [24,27].

The evaluation of apoptosis and necrosis by both fluorescence microscopy and flow cytometry is usually accomplished by the combined use of annexin V-FITC, which accesses phosphatidylserine that is exposed on the external membrane in the early stage of apoptosis, and PI, which allows for the identification of nuclear alterations in the late stages of apoptosis or necrosis as a consequence of the increase in membrane permeability [9,28–29]. Our results showed that the incubation of cells with MBHA3 at concentrations corresponding to once and twice the IC_{50} values did not yield significant losses in cell viability, although some morphological changes could be already identified. These results have been confirmed by other experiments, suggesting that MBHA3 has a more cytostatic than cytotoxic effect at the IC_{50} concentration. Most cells positive for AV were also PI positive, suggesting that apoptotic cells evolved into a secondary necrosis. However, we cannot rule out the possibility that annexin might also bind to the inner phosphatidylserine residues after the membrane integrity has been lost. It is usually assumed that annexin- and PI-negative cells (AV^-/PI^-) correspond to viable cells. However, this supposition should be considered carefully. It is possible that cell death mechanisms other than apoptosis or necrosis are operating in AV^-/PI^- cells. To confirm this

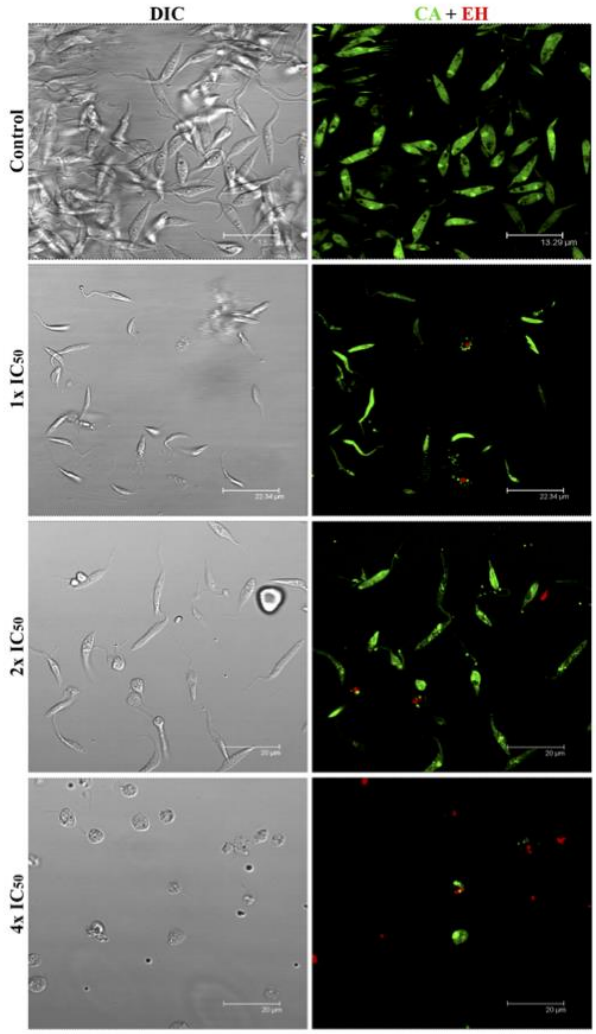

Figure 4. Confocal microscopy of control and MBHA3-treated parasites submitted to CA/EH labelling. Control cells presenting normal morphology as observed by DIC (left column) and CA bright green fluorescence indicative of intense esterase activity. Few control cells were labeled with EH (red). However, a dose-dependent loss of green fluorescence with corresponding increase in red fluorescence could be observed in the treated cells. Note in the 4x IC_{50} treated-cells the presence of swollen parasites.
doi:10.1371/journal.pone.0093936.g004

hypothesis, we used a CA/EH viability test to check whether the AV^-/PI^- phenotype corresponds to live cells. According to the CA/EH viability test, we found that the viability was considerably lower than that reported from the AV/PI assay. The differences found between these methodologies were more pronounced in cell treated with 4x IC_{50} of the drug. Although both probes allowed for the detection of apoptotic and necrotic cells, annexin might be less effective than calcein in discriminating viable from dead cells. Thus, the use of the AV/PI assay alone could lead to an overestimate of live cells in culture [30].

AO is a nucleic acid-selective dye that emits green fluorescence upon DNA intercalation. AO also enters and becomes trapped in acidic vesicular organelles (AVOs), such as lysosomes [31]. In a low pH environment this dye emits red florescence. Thus, AO has

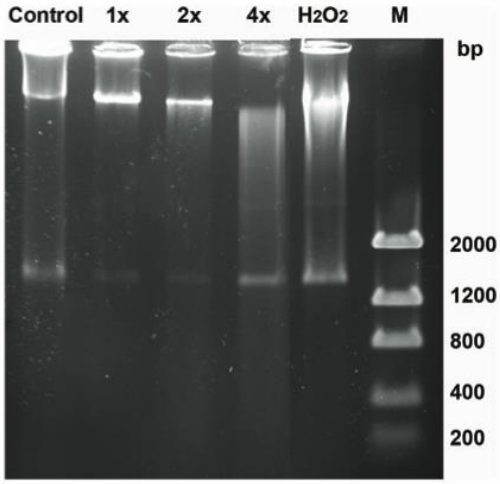

Figure 5. DNA fragmentation induced by MBHA3 on *T. cruzi* epimastigote forms. Electrophoresis of total DNA of the control and MBHA3-treated epimastigote forms. Non-specific DNA fragmentation could be observed in cells treated with the 2x IC_{50} and the 4x IC_{50} MBHA3. H_2O_2 was used as a positive control of parasite death. M = Low DNA Mass Ladder.
doi:10.1371/journal.pone.0093936.g005

been used, among other applications, to monitor major morphological changes induced by different stimuli and drug treatment [32–33]. We have found an increase in the red fluorescence intensity in cells treated with low concentrations of MBHA3. The increasing number of acidic compartments observed in the IC_{50}-treated cells might be due to autophagy. Conversely, the diffuse red labeling observed throughout the cytoplasm in cells treated with 2x IC_{50} could be due to the deterioration of lysosomal membranes and acidification of the cytoplasm, leading to a loss of cell viability. The considerable decrease in green fluorescence found in cells treated with 4x IC_{50} MBHA3 could be due to damage or conformational alterations to nucleic acids, impairing AO-DNA intercalation. Consistent with this idea, we showed that MBHA3 induced a nonspecific DNA degradation at higher concentrations, resulting in a 'smear' of randomly degraded DNA, a feature commonly attributed to cell necrosis.

The mechanism of action by which MBHA3 induces cell death remains unsolved, but our previous molecular docking analyses have suggested that MBHA3 is a putative inhibitor of a *T. cruzi* farnesyl pyrophosphate synthase [2] a key enzyme in the mevalonate pathway in trypanosomes [34–36]. Furthermore, it has been proposed that the nitro groups present in MBHA3 might undergo a reduction leading to the oxidation of cellular constituents, such as nucleic acids and mitochondria, which are highly dependent on redox reactions [2,37–38]. To test the latter hypothesis and investigate whether the MBHA3-induced apoptosis and necrosis of *T. cruzi* were related to alterations in the parasite mitochondrion we used Rho 123 to detect changes in the mitochondrial membrane potential. It has been shown that mitochondria play a pivotal role in cell death decisions [39]. In normal cells, the electrochemical gradient is maintained by active pumping of H^+ during the transfer of electron throughout the respiratory chain. In this regard, the membrane potential maintains the integrity and function of mitochondria. Perturbations in this potential could lead to a decrease in ATP production and a reduction in the translation and transcription of mitochondrial genes, which ultimately results in apoptosis and/or necrosis

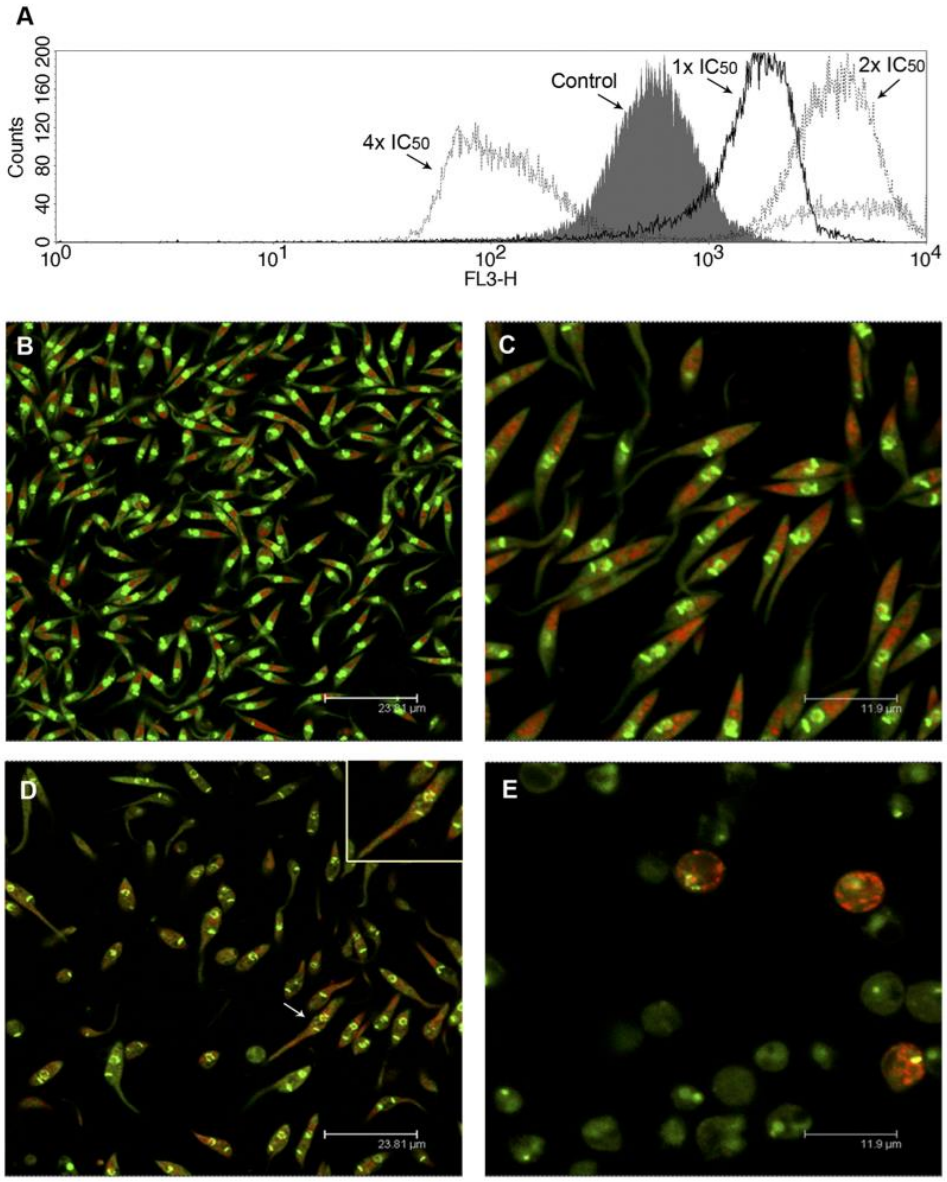

Figure 6. Effects of MBHA3 treatment on the acidic compartments of T. cruzi. (A) Overlay flow cytometric histograms of the control and treated-cells labeled with AO, after 72 hours of drug incubation. A gradual shift of the red fluorescence could be observed in the cells treated with the IC_{50} and the 2x IC_{50} of MBHA3. Nevertheless, in cells treated with the 4x IC_{50} of MBHA3, a striking decrease of the fluorescent signal from red channel was observed. (B–E). Confocal microscopy images of the control (B) and treated-cells (C–E). Control cells presented a normal morphology with a bright green nucleus, pale green cytoplasm and large red-labeled compartments at the posterior end of cells (B). Detail of the IC_{50}-treated culture showing slight changes in the parasite nucleus. (C). Aspect of parasite culture treated with the 2x IC_{50} of MBHA3 showing severe acidification of the parasite cytoplasm (D). Note the presence of the pyknotic nucleus (white arrow, inset). Parasites treated with the 4x IC_{50} of MBHA3 showed a round-shape body and a decrease in both green and red AO fluorescent signals (E).
doi:10.1371/journal.pone.0093936.g006

[40]. Flow cytometry analysis of MBHA3-treated cells labeled with Rho 123 indicated a considerable loss of the mitochondrial membrane potential, even at low concentrations. Drug concentrations corresponding to IC_{50} and 2x IC_{50} led to a decrease of the Rho 123 fluorescence intensity, which cannot be attributed to plasma membrane permeabilization, because, at these concentrations no substantial labeling with PI could be detected. Our results showed that the alterations in mitochondria membrane potential, induced by MBHA3 treatment, preceded the *T. cruzi* cell death. As previously stated, the nitro groups of the MBHA3 molecules can induce the production of free radicals and reactive oxygen species, resulting in the decrease of mitochondrial membrane potential and cell death.

In conclusion our finds suggest that MBHA3, at higher concentrations, induces *Trypanosoma cruzi* cell death by necrosis in mitochondrion-dependent manner.

37. Tonin LT, Barbosa VA, Bocca CC, Ramos ER, Nakamura CV, et al. (2009) Comparative study of the trypanocidal activity of the methyl 1-nitrophenyl-1,2,3,4-9H-tetrahydro-beta-carboline-3-carboxylate derivatives and benznidazole using theoretical calculations and cyclic voltammetry. Eur J Med Chem 44:1745–1750.
38. Souza RO de, Pereira VL, Muzitano MF, Falcão CA, Rossi-Bergmann B, et al. (2007) High selective leishmanicidal activity of 3-hydroxy-2-methylene-3-(4-bromophenyl) propanenitrile and analogous compounds. Eur J Med Chem 42:99–102.
39. Lee WK, Thévenod F (2006) A role for mitochondrial aquaporins in cellular life-and-death decisions? Am J Physiol Cell Physiol 291:C195–202.
40. Shang XJ, Yao G, Ge JP, Sun Y, Teng WH, et al. (2009) Procyanidin induces apoptosis and necrosis of prostate cancer cell line PC-3 in a mitochondrion-dependent manner. J Androl 30:122–126.

ANEXO A – Normas de submissão dos artigos

- **Artigo 1 –** ***Scientific Reports***
  ISSN 2045-2322 (online)
  Impact factor: 5.578

Preparing a manuscript for submission to Scientific Reports:

Accepted file types:
For article text: txt, doc, docx, tex
For figures: eps, tiff, jpg

A submission template is available in the Overleaf template gallery to help you prepare a LaTeX manuscript within the Scientific Reports formatting criteria.

Cover letter All submissions must be accompanied by a cover letter.

Scientific Reports sections and ordering of manuscripts We recommend that your manuscript is structured as follows.

Title The title must be no longer than 20 words.

Author list and affiliations The corresponding author should be identified with an asterisk.

Abstract (heading not used) The abstract must be no longer than 200 words, and must not have a heading. The Abstract should serve both as a general introduction to the topic and as a brief, non-technical summary of the main results and their implications. Abstracts must not contain references or subheadings.

Main body Scientific Reports has no explicit requirements for section organization. According to the authors' preferences, the main body of the text can be organized as best suits the research. In some cases, it may be appropriate to combine relevant sections. As a guideline, we recommend that your manuscript contains the following sections:

Introduction The introduction section of the main text expands on the background of the work (some overlap with the Abstract is acceptable). The background should put your paper into context and must be clear so that readers are able to understand the aims, purpose and significance of your research.

Results With topical subheadings

Discussion The Discussion should be succinct and may not contain subheadings.

Methods Subheadings are recommended. We recommend that authors limit their Methods section to 1,500 words

The recommended maximum length for the main body of your manuscript is 4,500 words.

References We recommend that references are limited to 60. References should be numbered sequentially, first throughout the text, then in tables, followed by figures. Scientific Reports uses the standard Nature referencing style, for example:

Published papers:
Schott, D. H., Collins, R. N. & Bretscher, A. Secretory vesicle transport velocity in living cells depends on the myosin V lever arm length. J. Cell Biol. 156, 35-39 (2002).

For papers with more than five authors include only the first author's name followed by 'et al.'.

Books:
Smith, J. Syntax of referencing in How to reference books (ed. Smith, S.) 180-181 (Macmillan, 2013).

Website:
Buckley, M. and Reid, A., Global food safety - keeping food safe from farm to table. Technical report. (2010) Available at: insert website here. (Accessed: 4th November 2012)

Acknowledgements Acknowledgements should be brief, and should not include effusive comments. Grant or contribution numbers may be acknowledged.

Author Contributions Statement All manuscripts must include an Author Contributions Statement detailing the contribution of each author. Author names must be listed as initials. For example, "A.B and C.D wrote the main manuscript text and E.F prepared figures 1-3. All authors reviewed the manuscript."

Additional Information To include, in this order: Accession codes (where applicable); Competing financial interests (mandatory statement).

The corresponding author is responsible for submitting a competing financial interests statement on behalf of all authors of the paper. This statement must be included in the submitted article file.

Figure Legends Each figure legend must be no longer than 350 words. Text for figure legends should be provided in numerical order after the references.

Display Items We suggest that articles contain no more than 8 display items (figures and/or tables). In addition, a limited number of uncaptioned molecular structure graphics and numbered mathematical equations may be included if necessary. To enable typesetting of papers, the number of display items should be commensurate with the word length — we suggest that for articles with word counts less than 2,000, no more than 4 figures/tables should be included. Please note that schemes are not used; these should be presented as figures.

Tables Please submit tables at the end of your text document (in Word or TeX/LaTeX, as appropriate).

Figures Figures should be uploaded upon submission via our online submission system, in one of our accepted formats (eps, tiff, jpg). For first submissions (i.e. not revised manuscripts), authors may choose to incorporate the manuscript text and figures into a single file up to 3 MB in size - the figures may be inserted within the text at the appropriate positions, or grouped at the end.

Authors submitting revised manuscripts, or final version figures should see our figure guidelines.

Supplementary Information Any supplementary information must be uploaded as a separate file, preferably as a single PDF, clearly labelled with the manuscript title and author list.

- **Artigo 2 –** ***Cell death & disease***

  ISSN (online): 2041-4889

  Impact factor: 5.014

Preparation of articles

Title Page: The title page should bear the title of the paper, the full names of all the authors and their affiliations, together with the name, full postal address, telephone and e-mail address of the author to whom correspondence and offprint requests are to be sent (this information is also asked for on the electronic submission form).
 The title should be brief, informative, of 150 characters or less.
 The running title should consist of no more than 50 letters and spaces. It should be as brief as possible, convey the essential message of the paper and contain no abbreviations.
 Authors should disclose in the Acknowledgements the sources of funding, grants and/or equipment and drugs.
 If authors regard it as essential to indicate that two or more co-authors are equal in status, they may be identified by an asterisk symbol with the caption 'These authors contributed equally to this work' immediately under the address list.

Abstract: Original Articles must be prepared with an abstract that summarises the essential features of the paper in a logical and concise sequence.

Introduction: The Introduction should assume that the reader is knowledgeable in the field and should therefore be as brief as possible but can include a short historical review where desirable.

Results and Discussion: The Results section should present the experimental data in text, tables or figures. Data in tables and figures should not be repeated extensively in the text. The discussion should focus on the interpretation and the significance of the findings with concise objective comments that describe their relation to other work in the area. If there are several models consistent with data, all plausible models should be mentioned. It should not repeat information in the results. The final paragraph should highlight the main conclusion(s), and provide some indication of the direction future research should take.

Materials/Subjects and Methods: This section should contain sufficient detail, so that all experimental procedures can be reproduced. Methods, that have been published in detail elsewhere do not have to be repeated, but must be fully referenced. Authors should provide the name of the manufacturer and their location for any specifically named medical equipment and instruments, and all drugs should be identified by their pharmaceutical names, and by their trade name if relevant.

Acknowledgements: These should be brief, and should include all sources of support including sponsorship (e.g. university, charity, government, commercial organisation) and sources of material (e.g. novel drugs) not available commercially.

Conflict of Interest: Authors must declare whether or not there are any competing financial interests in relation to the work described. This information must be included at submission and will be published as part of the paper. Conflict of interest should also be included in the online submission form. Please see the Conflict of Interest documentation in the Editorial Policy section for detailed information.

References: Only papers directly relevant to the article should be cited. References should follow the Vancouver format. In the text they should appear as numbers starting at one and at the end of the paper they should be listed (double-spaced) in numerical order corresponding to the order of citation in the

text. Where a reference is to appear next to a number in the text, for example following an equation, chemical formula or biological acronym, citations should be written as (ref. X) and not as superscript.
Example. "detectable levels of endogenous Bcl-2 (ref. 3), as confirmed by western blot"
All authors should be listed for papers with up to six authors; for papers with more than six authors, the first six only should be listed, followed by *et al.* Abbreviations for titles of medical periodicals should conform to those used in the latest edition of Index Medicus. The first and last page numbers for each reference should be provided. Meeting abstracts and correspondence must be identified as such. Papers in press may be included in the list of references. Personal communications must be allocated a number and included in the list of references in the usual way or simply referred to in the text; the authors may choose which method to use. In either case authors must obtain permission from the individual concerned to quote his/her unpublished work.

Examples:
Journal article, up to six authors:
Belkaid Y, Rouse BT. Natural regulatory T cells in infectious disease. *Nat Immunol* 2005; **6**: 353–360.

Journal article, e-pub ahead of print:
Bonin M, Pursche S, Bergeman T, Leopold T, Illmer T, Ehninger G *et al*. F-ara-A pharmacokinetics during reduced-intensity conditioning therapy with fludarabine and busulfan. *Bone Marrow Transplant* 2007; e-pub ahead of print 8 January 2007; doi:10.1038/sj.bmt.1705565

Journal article, in press:
Gallardo RL, Juneja HS, Gardner FH. Normal human marrow stromal cells induce clonal growth of human malignant Tlymphoblasts. *Int J Cell Cloning* (in press).

Complete book:
Atkinson K, Champlin R, Ritz J, Fibbe W, Ljungman P, Brenner MK (eds). *Clinical Bone Marrow* and *Blood Stem Cell Transplantation*, 3rd edn. Cambridge University Press: Cambridge, UK, 2004.

Chapter in book:
Coccia PF. Hematopoietic cell transplantation for osteopetrosis. In: Blume KG, Forman SJ, Appelbaum FR (eds). *Thomas' Hematopoietic Cell Transplantation*, 3rd edn. Blackwell Publishing Ltd: Malden, MA, USA, 2004, pp 1443–1454.

Abstract:
Syrjala KL, Abrams JR, Storer B, Heiman JR. Prospective risk factors for five-year sexuality late effects in men and women after haematopoietic cell transplantation. *Bone Marrow Transplant* 2006; **37**(Suppl 1): S4 (abstract 107).

Correspondence:
Caocci G, Pisu S. Overcoming scientific barriers and human prudence [letter]. *Bone Marrow Transplant* 2006; **38**: 829–830.

Figure Legends: These should be brief, specific and appear on a separate manuscript page after the References section. See Editorial Policies.

Tables: It is imperative that any tables used are computer readable, for example presented in Excel. Each must be uploaded as a separate workbook with a title or caption and be clearly labelled, sequentially. Reference to table footnotes should be made by means of Arabic numerals. Tables should consist of at least two columns; columns should always have headings. Each must be uploaded as a separate workbook with a title or caption and be clearly labelled, sequentially. Please make sure each table is cited within the text and in the correct order, e.g. (Table 3).
Please save the files with extensions .xls / .xlsx / .ods / or .doc or .docx. Please ensure that you provide a 'flat' file, with single values in each cell with no macros or links to other workbooks or worksheets and no calculations or functions.

Figures: Figures and images should be labelled sequentially and cited in the text. Figures should not be embedded within the text but rather uploaded as separate files. Detailed guidelines for submitting artwork can be found by downloading our Artwork Guidelines. The use of three-dimensional histograms is strongly discouraged when the addition of the third dimension gives no extra information.

Graphs, Histograms and Statistics:
 Plotting individual data points is preferred to just showing means, especially when N<10
 If error bars are shown, they must be described in the figure legend
 Axes on graphs should extend to zero, except for log axes
 Statistical analyses (including error bars and p values) should only be shown for independently repeated experiments, and must not be shown for replicates of a single experiment
 The number of times an experiment was repeated (N) must be stated in the legend

Supplementary Information: Supplementary information (SI) is peer-reviewed material directly relevant to the conclusion of an article that cannot be included in the printed version owing to space or format constraints. The article must be complete and self-explanatory without the SI, which is posted on the journal's website and linked to the article. SI may consist of data files, graphics, movies or extensive tables. Please see our Artwork Guidelines for information on accepted file types.
Authors should submit supplementary information files in the FINAL format as they are not edited, typeset or changed, and will appear online exactly as submitted. When submitting SI, authors are required to:
 Include a text summary (no more than 50 words) to describe the contents of each file.
 Identify the types of files (file formats) submitted.
 Include the text "Supplementary information is available at (journal name)'s website" at the end of the article and before the references.

Availability of Data and Materials: Please see our Editorial Policies for information regarding data, protocols, sequences, or structures.

House Style
 Text should be double spaced with a wide margin.
 All pages and lines are to be numbered. To add page numbers in MS Word, go to Insert then Page Numbers. To add line numbers go to File, Page Setup, then click the Layout tab. In the Apply to box, select Whole document, click Line Numbers then select the Add line numbering check box, followed by Continuous.
 Do not make rules thinner than 1pt (0.36mm).
 Use a coarse hatching pattern rather than shading for tints in graphs.
 Colour should be distinct when being used as an identifying tool.
 Spaces, not commas should be used to separate thousands.
 At first mention of a manufacturer, the town (and state if USA) and country should be provided.
 Statistical methods: N must be stated. Where N <10 individual data values should be plotted. If summary statistics (e.g. SD, SEM, CI) are used, their nature must be described. Relative risks should be expressed as odds ratios with 95% confidence interval. To compare two methods for measuring a variable the method of Bland & Altman (1986, Lancet 1, 307–310) should be used; for this, calculation of P only is not appropriate.
 Units**:** Use metric units (SI units) as fully as possible.
Preferably give measurements of energy in kiloJoules or MegaJoules with kilocalories in parentheses (1 kcal = 4.186kJ). Use % throughout.
 Abbreviations: On first using an abbreviation place it in parentheses after the full item. Note these abbreviations: gram **g**; litre **l**; milligram **mg**; kilogram **kg**; kilojoule **kJ**; megajoule **MJ**; weight **wt**; seconds **s**; minutes **min**; hours **h**. Do not add s for plural units.

- **Artigo 3 – *Frontiers in Microbiology* (online)**
  ISSN: 1664-302X

  Impact factor: 4.0

Manuscript Guidelines

Opinion articles allow researchers to contribute viewpoints on the interpretation of facts, value of methods used, weaknesses and strengths of any scientific theory or on any topic relevant to the field of research. Opinion Articles allow maximum freedom of expression for researchers, encourage constructive discussion and are peer-reviewed. Emotionally-charged argumentation is not appropriate.
Opinion Articles should be supported by evidence (whether factual or anecdotal) and promote dialogue; however they should not contain unpublished or original data. Opinion Articles should be properly substantiated, with typically at least five references, have a maximum word count of 2,000 and may contain no more than 1 Figure/Table.

Manuscript Length The manuscript length includes only the main body of the text, footnotes and all citations within it, and excludes abstract, section titles, figure and table captions, funding statements, acknowledgements and references in the bibliography. Please indicate the number of words and the number of figures included in your manuscript on the first page.

Language Style Authors are requested to follow American English spelling. For any questions regarding style Frontiers recommends authors to consult the Chicago Manual of Style.

Title The title is written in title case, centered, and in 16 point bold Times New Roman font at the top of page. The title should be concise, omitting terms that are implicit and, where possible, be a statement of the main result or conclusion presented in the manuscript. Abbreviations should be avoided within the title. For article types requiring it, the running title should be a maximum of 5 words in length.

Authors and Affiliations All names are listed together and separated by commas. Provide exact and correct author names as these will be indexed in official archives. Affiliations should be keyed to the author's name with superscript numbers and be listed as follows: Laboratory, Institute, Department, Organization, City, State abbreviation (USA, Canada, Australia), and Country (without detailed address information such as city zip codes or street names).

The Corresponding Author(s) should be marked with an asterisk. Provide the exact contact email address of the corresponding author(s) in a separate section.

Headings and Sub-headings Except for special names (e.g. GABAergic), capitalize only the first letter of headings and subheadings. Headings and subheadings need to be defined in Times New Roman, 12, bold. You may insert up to 5 heading levels into your manuscript (not more than for example: 3.2.2.1.2 Heading title).

Keywords All article types: you may provide up to 8 keywords; at least 5 are mandatory.

Text The body text is in 12 point normal Times New Roman. New paragraphs will be separated with a single empty line. The entire document should be single-spaced and should contain page and line numbers in order to facilitate the review process. Your manuscript should be written using either LaTeX or MS-Word.

Nomenclature The use of abbreviations should be kept to a minimum. Non-standard abbreviations should be avoided unless they appear at least four times, and defined upon first use in the main text. Consider also giving a list of non-standard abbreviations at the end, immediately before the Acknowledgments.

Sections Your manuscript is organized by headings and subheadings. For Original Research Articles, Clinical Trial Articles, and Technology Reports the section headings should be those appropriate for your field and the research itself.

Conflict of Interest Statement Frontiers follows the recommendations by the International Committee of Medical Journal Editors (http://www.icmje.org/recommendations/browse/roles-and-responsibilities/author-responsibilities--conflicts-of-interest.html) which require that all financial, commercial or other relationships that might be perceived by the academic community as representing a potential conflict of interest must be disclosed. If no such relationship exists, authors will be asked to declare that the research was conducted in the absence of any commercial or financial relationships that could be construed as a potential conflict of interest.

Author and Contributors The statement about the authors and contributors can be up to several sentences long, describing the tasks of individual authors. Please list only 2 initials for each author, without periods, but separated by commas (e.g. JC, JS). In the case of two authors with the same initials, please use their middle initial to differentiate between them (e.g. REW, RSW). The Author Contributions section should be included at the end of the manuscript before the References.

Funding Details of all funding sources should be provided, including grant numbers if applicable. Please ensure to add all necessary funding information, as after publication this is no longer possible.

Acknowledgments This is a short text to acknowledge the contributions of specific colleagues, institutions, or agencies that aided the efforts of the authors.

References All citations in the text, figures or tables must be in the reference list and vice-versa. The references should only include articles that are published or accepted. Data sets that have been deposited to an online repository should be included in the reference list, include the version and unique identifier when available. For accepted but unpublished works use "in press" instead of page numbers. Unpublished data, submitted manuscripts, or personal communications should be cited within the text only, for the article types that allow such inclusions. Personal communications should be documented by a letter of permission. Website urls should be included as footnotes. Any inclusion of verbatim text must be contained in quotation marks and clearly reference the original source.

Reference list: provide the names of the first six authors followed by et al and doi when available.
In-text citations should be called according to the surname of the first author, followed by the year. For works by 2 authors include both surnames, followed by the year. For works by more than 2 authors include only the surname of the first author, followed by et al., followed by the year. For Humanities and Social Sciences articles please include page numbers in the in-text citations.

Article in a print journal:
Sondheimer, N., and Lindquist, S. (2000). Rnq1: an epigenetic modifier of protein function in yeast. Mol. Cell. 5, 163-172.

Article in an online journal:
Tahimic, C.G.T., Wang, Y., Bikle, D.D. (2013). Anabolic effects of IGF-1 signaling on the skeleton. Front. Endocrinol. 4:6. doi: 10.3389/fendo.2013.00006

Article or chapter in a book:
Sorenson, P. W., and Caprio, J. C. (1998). "Chemoreception," in The Physiology of Fishes, ed. D. H. Evans (Boca Raton, FL: CRC Press), 375-405.

Book:
Cowan, W. M., Jessell, T. M., and Zipursky, S. L. (1997). Molecular and Cellular Approaches to Neural Development. New York: Oxford University Press.

Abstract:
Hendricks, J., Applebaum, R., and Kunkel, S. (2010). A world apart? Bridging the gap between theory and applied social gerontology. Gerontologist 50, 284-293. Abstract retrieved from Abstracts in Social Gerontology database. (Accession No. 50360869)

Patent:
Marshall, S. P. (2000). Method and apparatus for eye tracking and monitoring pupil dilation to evaluate cognitive activity. U.S. Patent No 6,090,051. Washington, DC: U.S. Patent and Trademark Office.

Data:
Perdiguero P, Venturas M, Cervera MT, Gil L, Collada C. Data from: Massive sequencing of Ulms minor's transcriptome provides new molecular tools for a genus under the constant threat of Dutch elm disease. Dryad Digital Repository. (2015) http://dx.doi.org/10.5061/dryad.ps837

Disclaimer
Any necessary disclaimers which must be included in the published article should be clearly indicated in the manuscript.

Supplementary Material Frontiers journals do not support pushing important results and information into supplementary sections. However, data that are not of primary importance to the text, or which cannot be included in the article because it is too large or the current format does not permit it (such as movies, raw data traces, power point presentations, etc.) can be uploaded during the submission procedure and will be displayed along with the published article.

Figure and Table Guidelines
General Style Guidelines for Figures Frontiers requires figures to be submitted individually, in the same order as they are referred to in the manuscript, the figures will then be automatically embedded at the end of the submitted manuscript. Kindly ensure that each table and figure is mentioned in the text and in numerical order.

General Style Guidelines for Tables Tables should be inserted at the end of the manuscript. If you use a word processor, build your table in word. If you use a LaTeX processor, build your table in LaTeX. An empty line should be left before and after the table.

Please note that large tables covering several pages cannot be included in the final PDF for formatting reasons. These tables will be published as supplementary material on the online article abstract page at the time of acceptance. The author will notified during the typesetting of the final article if this is the case. A link in the final PDF will direct to the online material.

Figure and Table Legends Figure and table legends are required to have the same font as the main text (12 point normal Times New Roman, single spaced). Legends should be preceded by the appropriate label, for example "Figure 1" or "Table 4". Figure legends should be placed at the end of the manuscript (for supplementary images you must include the caption with the figure, uploaded as a separate file). Table legends must be placed immediately before the table. Please use only a single paragraph for the legend. Figure panels are referred to by bold capital letters in brackets: (A), (B), (C), (D), etc.

Image Size Figure images should be prepared with the PDF layout in mind, individual figures should not be longer than one page and with a width that corresponds to 1 column or 2 columns. All articles are prepared using the 2 column layout: 2 column articles can contain images 85 mm or 180 mm wide.